bioRxiv preprint doi: https://doi.org/10.1101/2021.12.13.472401; this version posted December 13, 2021. The copyright holder for this preprint (which was not certified by peer review) is the author/funder, who has granted bioRxiv a license to display the preprint in perpetuity. It is made available under aCC-BY 4.0 International license.

Pentoxifylline-induced Protein Expression Change in RAW 264.7 Cells as Determined by Immunoprecipitation-based High Performance Liquid Chromatography

Mi Hyun Seo[1], Dae Won Kim[2], Yeon Sook Kim[3], Suk Keun Lee[4]*

[1] Department of Oral and Maxillofacial Surgery, College of Dentistry, Seoul National University, Seoul, South Korea; tjalgus@snu.ac.kr

[2] Department of Oral Biochemistry, College of Dentistry, Gangneung-Wonju National University, Gangneung, Korea; kimdw@gwnu.ac.kr

[3] Department of Dental Hygiene, College of Health & Medical Sciences, Cheongju University, Cheongju, South Korea; yeonsookkim1@naver.com

[4] Department of Oral Pathology, College of Dentistry, Gangneung-Wonju National University, Gangneung; and Institute of Hydrogen Magnetic Reaction Gene Regulation, Dae Jeon, South Korea; sukkeunlee2@naver.com

* Correspondence: ¶SKL: sukkeunlee2@naver.com

bioRxiv preprint doi: https://doi.org/10.1101/2021.12.13.472401; this version posted December 13, 2021. The copyright holder for this preprint (which was not certified by peer review) is the author/funder, who has granted bioRxiv a license to display the preprint in perpetuity. It is made available under aCC-BY 4.0 International license.

Abstract

Although pentoxifylline (PTX) was identified as a competitive non-selective phosphodiesterase inhibitor, its pharmacological effect has not been clearly elucidated. The present study explored the effect of low dose 10 μg/mL PTX (therapeutic dose) compared to high dose 300 μg/mL PTX (experimental dose) in RAW 264.7 cells through immunoprecipitation-based high performance liquid chromatography (IP-HPLC), immunohistochemistry, and western blot. 10 μg/mL PTX increased the expression of proliferation (Ki-67, PCNA, cyclin D2, cdc25A), epigenetic modification (KDM4D, PCAF), protein translation (DOHH, DHPS, eIF5A1), RAS signaling (KRAS, pAKT1/2/3, PI3K), NFkB signaling (NFkB, GADD45, p38), protection (HSP70, SOD1, GSTO1/2), neuromuscular differentiation (NSEγ, myosin-1a, desmin), osteoblastic differentiation (BMP2, RUNX2, osterix), acute inflammation (TNFα, IL-1, CXCR4), innate immunity (β-defensin 1, lactoferrin, TLR-3, -4), cell-mediated immunity (CD4, CD8, CD80), while decreased the expression of ER stress (eIF2α, eIF2AK3, ATF6α), fibrosis (FGF2, CTGF, collagen 3A1), and chronic inflammation (CD68, MMP-2, -3, COX2) versus the untreated controls. The activation of proliferation by 10 μg/mL PTX was also supported by the increase of cMyc-MAX heterodimer and β-catenin-TCF1 complex in double IP-HPLC. 10 μg/mL PTX enhanced FAS-mediated apoptosis but diminished p53-mediated apoptosis, and downregulated many angiogenesis proteins (angiogenin, VEGF-A, and FLT4), but upregulated HIF1α, VEGFR2, and CMG2 reactively. Whereas, 300 μg/mL PTX consistently decreased proliferation, epigenetic modification, RAS and NFkB signaling, neuromuscular and osteoblastic differentiation, but increased apoptosis, ER stress, and fibrosis compared to 10 μg/mL PTX. These data suggest PTX has different biological effect on RWA 264.7 cells depending on the concentration of 10 μg/mL and 300 μg/mL PTX. The low dose 10 μg/mL PTX enhanced RAS/NFkB signaling, proliferation, differentiation, and inflammation, particularly, it stimulated neuromuscular and osteoblastic differentiation, innate immunity, and cell-mediated

bioRxiv preprint doi: https://doi.org/10.1101/2021.12.13.472401; this version posted December 13, 2021. The copyright holder for this preprint (which was not certified by peer review) is the author/funder, who has granted bioRxiv a license to display the preprint in perpetuity. It is made available under aCC-BY 4.0 International license.

immunity, but attenuated ER stress, fibrosis, angiogenesis, and chronic inflammation, while the high dose 300 μg/mL PTX was found to alleviate the 10 μg/mL PTX-induced biological effects, resulted in the suppression of RAS/NFkB signaling, proliferation, neuromuscular and osteoblastic differentiation, and inflammation.

Keywords: 10 μg/mL or 300 μg/mL Pentoxifylline; Protein Expressions; IP-HPLC; RAW 264.7 Cells

Introduction

Pentoxifylline (PTX), a xanthine derivative, is primarily used as an antiproteolytic agent to treat muscle pain in people with peripheral artery disease [1, 2] by activating cAMP/EPAC/AKT signaling [3, 4]. It has been frequently reported that PTX remarkably suppressed the secretions of pro-inflammatory cytokines and the nuclear factor-kappaB (NFkB) activation [5-7], and reduced chronic inflammation [5, 8]. PTX appeared to have anti-fibrotic effect on radiation-induced lung fibrosis by modulation of PKA and PAI-1 expression as possible anti-fibrotic mechanisms [9], and PTX therapy with vitamin E showed prevention of radiation-induced fibrosis in breast cancer patients [10]. PTX is suggested as an oral osteogenic drug for the treatment of post-menopausal osteoporosis [11]. As PTX given before tooth extraction is prophylactic, it might affect healing in a positive way by optimizing the inflammatory response [12]. Many authors suggest that PTX may increase the anticancer potential of anticancer drugs such as cisplatin or doxorubicin as well as reduce side effects of these drugs [13-16].

As RAW 264.7 cells are immortalized macrophages which are mainly involved with wound healing and tumor progression, the present study utilized RAW 264.7 cells for *in vitro* protein expression experiment.

bioRxiv preprint doi: https://doi.org/10.1101/2021.12.13.472401; this version posted December 13, 2021. The copyright holder for this preprint (which was not certified by peer review) is the author/funder, who has granted bioRxiv a license to display the preprint in perpetuity. It is made available under aCC-BY 4.0 International license.

Although PTX has short half-life (0.39–0.84 h for the various doses and 0.96–1.61 h for the metabolites), its therapeutic dose for adult human is usually 400 mg (Trental), three times a day [17, 18]. Therefore, in this study, RAW 264.7 cells were primarily treated with 10 μg/mL PTX, which is similar to human therapeutic dose (6.7 mg/kg, Trental). However, in the pilot study to know the trends of protein expressions by PTX, 10 μg/mL PTX increased the expression of some proliferation-related proteins, RAS and NFkB signaling proteins, and even some inflammatory proteins in RAW 264.7 cells. These results were contrary to many reports insisting the anti-proliferative and anti-inflammatory effect of PTX. However, it was found that many experiments for PTX-induced effects on cells and animals were frequently performed by using higher dose of PTX, 100 – 500 μg/mL [5, 8, 19-22], than therapeutic dose of PTX, about 10 μg/mL. In order to elucidate the different pharmacological effect depending on the dose of PTX, the present study was performed to compare 10 μg/mL PTX-induced protein expressions with 300 μg/mL PTX-induced protein expression in RAW 264.7 cells.

As the essential protein signalings are intimately correlated and cross-talked with each other to maintain cellular homeostasis during proliferation, differentiation, inflammation, apoptosis, and senescence, it is necessary to know the global protein expression involving multiple signaling pathways in order to explain or predict the fate of cells involved with diseases or drug therapy. The present study examined PTX-induced global protein expression changes in RAW 264.7 cells through IP-HPLC, immunocytochemistry (ICC), and western blot. Particularly, IP-HPLC analysis is available to determine protein expression levels in different biological fluids, such as blood plasma, urine, saliva [23, 24], inflammatory exudates [25-27], cancer tissues [28, 29], cell culture extract [30-34], and blood plasma [32, 35]. Contrary to enzyme-linked immunosorbent assay (ELISA). IP-HPLC uses protein A/G agarose beads in chaotic buffer solution and micro-sensitive UV spectroscopy to determine protein expression level (%) compared to the control. It can rapidly analyze multiple

bioRxiv preprint doi: https://doi.org/10.1101/2021.12.13.472401; this version posted December 13, 2021. The copyright holder for this preprint (which was not certified by peer review) is the author/funder, who has granted bioRxiv a license to display the preprint in perpetuity. It is made available under aCC-BY 4.0 International license.

proteins samples. Furthermore, multiple repeats of same protein IP-HPLC showed accurate results (±5% standard deviation) reproducibly [33, 34]. Therefore, 10 µg/mL PTX-induced global protein expression changes in RAW 264.7 cells were extensively examined through IP-HPLC partly with immunocytochemistry (ICC) and western blot methods in this study.

Materials and Methods

RAW 264.7 cell culture in the presence of PTX

RAW 264.7 cells (an immortalized murine macrophage cell line; ATCC, USA) were cultured in Dulbecco's modified Eagle's medium (WelGene Inc. Korea) supplemented with 10% (vol/vol) heat-inactivated fetal bovine serum (WelGene Inc. Korea), 100 unit/mL penicillin, 100µg/mL streptomycin, and 250ng/mL amphotericin B (WelGene Inc. Korea), in 5% CO_2 chamber at 37.5°C. The cells from passage no. 10-12 were used in this study [36]. Antigen free media was utilized in order to detect native protein expressional changes induced by PTX.

About 70% confluent RAW 264.7 cells grown on Petri dish surfaces were treated with 10 µg/mL PTX or 300 µg/mL PTX (safe single dose in dogs 100-300 mg/kg according to WHO food additives Series 35, 835) for 12, 24, or 48 h; control cells were treated with 1 mL of normal saline. Cultured cells were harvested with protein lysis buffer (PRO-PREP™, iNtRON Biotechnology INC, Korea) cooled on ice, and immediately preserved at -70°C until required.

Cytological cell counting for the proliferation index

RAW 264.7 cells were cultured on the surfaces of two-well culture slide dishes (SPL, Korea) until they reached 50% confluence, and then treated with 10 µg/mL PTX for 12, 24, or 48 h. The control was treated with

bioRxiv preprint doi: https://doi.org/10.1101/2021.12.13.472401; this version posted December 13, 2021. The copyright holder for this preprint (which was not certified by peer review) is the author/funder, who has granted bioRxiv a license to display the preprint in perpetuity. It is made available under aCC-BY 4.0 International license.

normal saline only. The cells on the culture slides were fixed with 10 % buffered formalin solution for 1 hour, stained with hematoxylin, and observed by optical microscope (CX43, Olympus, Japan) at x400 magnification. Thirty representative images were digitally captured in each group (DP-73, Olympus Co., Japan), followed by a cell counting using the IMT i-solution program (version 21.1; Martin Microscope, Vancouver, Canada). The results were plotted on a graph.

Immunocytochemical staining analysis

When approximately 70% confluent RAW 264.7 cells were spread over the surfaces of two-well culture slide dishes, the cells were treated with 10 μg/mL PTX for 12, 24, or 48 h, while the control cells were treated with 100 μL of normal saline. The cells on the culture slides were fixed with 4% paraformaldehyde solution for 20 min, permeabilized with cooled methanol for 10 min at -20°C, and applied for immunohistochemistry using selected antisera (the same ones used in IP-HPLC, Table 1); Ki-67 for cellular proliferation, KMD4D and PCAF for epigenetic modification, TNFα, IL-6, TLR3, and TLR4 for inflammation, GSTO1/2, LC3, and GADD153 (CHOP) for endoplasmic reticulum stress, PARP-1 and caspase 3 for apoptosis, NSEγ for neural differentiation, MYH2 for muscular differentiation, TGF-β1, RUNX2, OPG, and BMPR2 for osteoblastic differentiation.

Immunocytochemical (ICC) staining was performed using the indirect triple sandwich method on the Vectastatin system (Vector Laboratories, USA), and visualized using a 3-amino-9-ethylcarbazole solution (Santa Cruz Biotechnology, USA) with no counter staining. The results were observed by optical microscope, and their characteristic images were captured (DP-73, Olympus Co., Japan) and illustrated.

Western blot analysis

Some representative antisera were utilized for western blot analysis to assess the 10 μg/mL or 300 μg/mL PTX-induced protein expression in RAW 264.7 cells. Ki-67 was selected for cellular proliferation, p53, Rb1, and E2F1 for p53/Rb/E2F signaling, β-catenin, E-cadherin, VE-cadherin, Wnt1, and TCF1 for Wnt/β-catenin signaling, cMyc, MAX, and MAD1 for cMyc/MAX/MAD network, KDM4D and HDAC10 for epigenetic modification, KRAS, HRAS, NRAS, ERK1, and p-ERK1 for RAS signaling, TNFα, TLR2, and TLR4 for inflammation, eIF2AK3, p-eIF2AK3, ATF4, LC3β, and c-caspase 3 for endoplasmic reticulum stress, TGF-β1,

bioRxiv preprint doi: https://doi.org/10.1101/2021.12.13.472401; this version posted December 13, 2021. The copyright holder for this preprint (which was not certified by peer review) is the author/funder, who has granted bioRxiv a license to display the preprint in perpetuity. It is made available under aCC-BY 4.0 International license.

BMP2, RUNX2 for osteogenesis, NSEγ and NF1 for neural differentiation, and MYH2 and desmin for muscular differentiation. These antisera were the same ones used in IP-HPLC (Table 1).

The cells treated with 10 μg/mL and 300 μg/mL PTX for 0, 12, 24, and 48 h were collected with phosphate-buffered saline (PBS) separately, treated with trypsin-ethylene-diamine-tetra-acetic acid (trypsin-EDTA) for one minute, and washed with PBS, and followed by cell lysis with ice-cold RIPA buffer (Sigma Aldrich, USA). The lysates were centrifuged at 12,000 g for 20 min at 4° C. The protein concentration of the supernatant was quantified using a Bradford assay (BioRad, USA). Equal amounts (30 μg/lane) of the sample proteins were separated by 8, 10, 15, or 20% sodium dodecyl sulfate-polyacrylamide gel electrophoresis (SDS-PAGE) in Tris-glycine SDS running buffer (25 mM Tris, 0.1% SDS, and 0.2M glycine), and transferred to a nitrocellulose membrane. The membranes were blocked with 5% nonfat dry milk in TBST buffer (25 mM Tris-HCl, 150 mM NaCl, 0.1% Tween 20, pH 7.5) for 1 h. After washing three times with TBST buffer, the membrane was incubated with each primary antibody (dilution ratio = 1:1000, the same antibody used in IP-HPLC) and horseradish peroxidase-conjugated secondary antibody for 1 h separately. The protein bands were then detected using an enhanced chemiluminescence system (Amersham Pharmacia Biotech, Piscataway, NJ, USA) and digitally imaged using a ChemiDoc XRS system (Bio-Rad Laboratories, Hercules, CA, USA). The level of β-actin expression was used as an internal control to normalize the expression of the target proteins. The size and intensity of protein bands from the cells treated with 10 μg/mL PTX for 0, 12, 24, and 48 h were demonstrated, and the protein bands from 10 μg/mL PTX-treated cells were compared with those from 300 μg/mL PTX-treated cells.

Immunoprecipitation-based high performance liquid chromatography (IP-HPLC)

bioRxiv preprint doi: https://doi.org/10.1101/2021.12.13.472401; this version posted December 13, 2021. The copyright holder for this preprint (which was not certified by peer review) is the author/funder, who has granted bioRxiv a license to display the preprint in perpetuity. It is made available under aCC-BY 4.0 International license.

159 Protein A/G agarose columns were separately pre-incubated with each 1 μg antibody for
160 proliferation-related proteins (n=13), cMyc/MAX/MAD network proteins (n=6(3)), p53/Rb/E2F signaling
161 proteins (n=7(3)), Wnt/β-catenin signaling proteins (n=9), epigenetic modification proteins (n=8), protein
162 translation proteins (n=8), growth factors (n=23), RAS signaling proteins (n=25), NFkB signaling proteins
163 (n=23(10)), upregulated inflammatory proteins (n=34), downregulated inflammatory proteins (n=30),
164 p53-mediated apoptosis proteins (n=15(1)), FAS-mediated apoptosis proteins (n=10), protection and survival
165 proteins (n=27(7)), endoplasmic reticulum stress proteins (n=19(11)), SHH and Notch signaling proteins
166 (11(3)), differentiation proteins (n=27(9)), neuromuscular differentiation proteins (19(10)), fibrosis proteins
167 (19(16)), oncogenesis proteins (n=18(5)), angiogenesis proteins (n=26(11)), osteogenesis proteins (n=23(7)),
168 and control housekeeping proteins (n=3) (numbers in parenthesis indicate number of overlapping antibodies,
169 Table 1). Although the immunoprecipitation is unable to define the size-dependent expression of target protein
170 compared to western blot, it collects every protein containing a specific epitope against antibody. Therefore,
171 the IP-HPLC can detect whole target proteins, precursor and modified ones, similar to enzyme-linked
172 immunosorbent assay (ELISA).
173

bioRxiv preprint doi: https://doi.org/10.1101/2021.12.13.472401; this version posted December 13, 2021. The copyright holder for this preprint (which was not certified by peer review) is the author/funder, who has granted bioRxiv a license to display the preprint in perpetuity. It is made available under aCC-BY 4.0 International license.

174 Table 1. Antibodies used in the study.

175

Proteins	No.	Antibodies
Proliferation-related proteins	13	Ki-67*, PCNA*, PLK4*, MPM2*, CDK4*, cyclin D2*, cdc25A*, BRG1*, p14*, p15/16*, p21*, p27*, lamin A/C*
cMyc/MAX/MAD network	6 (3)	cMyc*, MAX*, MAD1*, (p27, CDK4, cyclin D2)
p53/Rb/E2F signaling	7 (3)	p53, E2F1*, Rb1#, p-Rb1*, (cyclin D2, CDK4, p21)
Wnt/β-catenin signaling	9	Wnt1*, APC*, β-catenin*, snail*, TCF1*, E-cadherin*, MMP9, vimentin*, VE-cadherin&,
Epigenetic modification	8	histone H1*, KDM4D$, HDAC10$, MBD4*, DMAP1*, DNMT1*, PCAF*, EZH2
Protein translation	8	DOHH!, DHSP!, eIF5A1!, eIF5A2!, eIF2AK3 (PERK)*, p-eIF2AK3 (Thr981, p-PERK)*, eIF2α^, p-eIF2α (Ser51)^
Growth factor	23	TGF-α, TGF-β1#, TGF-β2*, TGF-β3*, SMAD2/3, SMAD4*, p-SMAD4, HGFα*, Met*, FGF1*, FGF2*, FGF7*, GH*, GHRH*, IGF-1*, IGF2R*, HER1*, HER2*, PDGF-A*, CTGF*, ERβ*, ALK1, EGF
RAS signaling proteins	25	NRAS$, KRAS$, HRAS*, STAT3*, p-STAT3 (p727), pAKT1/2/3, PI3K, Rab1*, RAF-B*, MEKK1, ERK1 (MAPK3)*, p-ERK1 (T202, Y204)$, JNK1 (MAPK8)*, p-JNK1, PKC*, p-PKC1α (Thr514)@, mTOR@, p-mTOR, PTEN, p38 (MAPK14), p-p38 (Thr180, Tyr182), AKAP13, JAK2$, TYK2*, (Thr308), SOS1*
NFkB signaling proteins	23 (10)	NFkB*, IKK*, GADD45*, GADD153* (CHOP)*, p-GADD153, NRF2*, PGC-1α*, AMPKα@, NFAT5, MDR*, SRC1*, NFAT5*, NFATC1*, (p38 (MAPK14), p-p38 (Thr180, Tyr182)*, mTOR@, p-mTOR*, PKC*, p-PKC1α@, JAK2*, RAF-B, MEKK1, AKAP13*)
Upregulated inflammatory proteins	34	TNFα@, IL-1*, IL-6*, IL-10*, CD4*, CD8*, CD28*, CD31 (PECAM1)*, CD34, CD44 (HCAM)*, CD80 (B7-1) *, MMP1*, MMP1/8*, MMP12$, TIMP1*, TIMP2*, M-CSF*, CXCR4*, CTLA4*, granzyme B, β-defensin-1, MCP-1, HLA-DR, lactoferrin, kininogen*, TLR2*, TLR3*, TLR4*, TLR7*, integrin α2*, integrin α5*, versican*, CRP*, perforin*
Downregulated inflammatory proteins	30	IL-8*, IL-12*, IL-28*, CD3*, CD20*, CD40*, CD54 (ICAM1)*, CD56 (NCAM) *, CD68*, CD99 (MIC2) *, CD106 (VCAM1) *, MMP2*, MMP3$, MMP9$, MMP10, cathepsin C*, cathepsin G*, cathepsin K*, lysozyme*, hepcidin, α1-antitrypsin&, β-defensin-2, β-defensin-3, COX1*, COX2*, LTA4H&, elafin, integrin β1, LL-37, PD-1 (CD279)
p53-mediated apoptosis	15 (1)	(p53*), p73, MDM2*, BAD*, BAK*, NOXA*, PUMA*, BAX*, BCL2*, APAF1*, caspase 9*, c-caspase 9*, AIF*, PARP-1*, c-PARP*
FAS-mediated apoptosis	10	FASL*, FAS*, FADD*, FLIP*, BID*, caspase 3*, c-caspase 3*, caspase 7, c-caspase 8*, c-caspase 10*,

bioRxiv preprint doi: https://doi.org/10.1101/2021.12.13.472401; this version posted December 13, 2021. The copyright holder for this preprint (which was not certified by peer review) is the author/funder, who has granted bioRxiv a license to display the preprint in perpetuity. It is made available under aCC-BY 4.0 International license.

Protection- and survival proteins	27 (7)	HO-1*, HSP27*, HSP70*, HSP90α/β*, SOD1*, GSTO1/2*, NOS1$, TERT*, LC3β, SVCT2&, SP1@, SP3@, leptin*, SIRT1*, SIRT3*, SIRT6*, SIRT7*, FOXP3*, FOXP4*, PLC-β2*, (AMPKα, pAKT1/2/3, mTOR, PKC, p-PKC1α, NRF2, PGC-1α)
Endoplasmic reticulum stress proteins	19 (11)	ATF4*, ATF6α*, BIP*, IRE1α, AP1M1, calnexin, caveolin-1, endothelin-1, (HSP-27, HSP-70, eIF2AK3* (PERK), p-eIF2AK3 (p-PERK), eIF2α^, p-eIF2α (Ser51)^, GADD153 (CHOP)*, p-GADD153*, PGC-1α*, LC3β*, AIF*)
SHH and Notch signaling proteins	11 (3)	SHH*, PTCH1*, GLI1*, EpCAM*, Notch1*, Jagged2*, HIF1α*, VEGF-A*, (CD44 (HCAM), BCL2, Wnt1)
Cytodifferentiation proteins	27 (9)	α-actin*, p63$, vimentin*, TGase 2+, TGase 4+, HK2*, FAK*, CaM*, CRIP1*, cystatin A*, SOX9, AP1M1*, Krox-25, DLX2, TBX22, laminin α5*, pancreatic lipase, PSA, (caveolin-1*, PKC, p-PKC1α, AKAP13, calnexin, PLC-β2, EpCAM, E-cadherin, VE-cadherin)
Neuro-muscular differentiation-	19 (10)	NSEγ*, NK1R*, GFAP*, S-100*, myosin 1a, MYH2*, desmin*, NF1*, α-SMA*, (CaM, calnexin, CRIP1*, cystatin A, AP1M1*, FAK, SHH, β-catenin, Wnt1, TGase 2)
Fibrosis proteins	19 (16)	(FGF1, FGF2, FGF7, TGF-β1, CTGF, PDGF-A, collagen 3A1, collagen 4, collagen 5A, laminin α5, integrin α2, integrin α5, integrin β1, α1-antitrypsin&, elafin, endothelin-1*), CMG2, PAI-1*, plasminogen*
Oncogenesis proteins	18 (5)	PTEN&, BRCA1&, BRCA2&, ATM*, maspin*, DMBT1*, PIM-1*, CEA$, 14-3-3θ*, survivin@, mucin 1*, mucin 4*, YAP1*, (NF1*, PTCH-1, MBD4, p53, Rb1)
Angiogenesis proteins	26 (12)	HIF1α&, angiogenin$, VEGF-A*, VEGF-C*, VEGF-D, VEGFR2*, p-VEGFR2 (Y951), vWF$, CMG2$, FLT4$, LYVE1*, fibrinogen*, kininogen-1, TEM8, (plasminogen*, FGF2, PDGF-A, CD31 (PECAM1)*, CD44 (HCAM)*, CD54 (ICAM-1)*, CD56 (NCAM), CD106 (VCAM1), MMP2, MMP10, PAI-1*, endothelin-1*)
Osteogenesis proteins	23 (7)	BMP2*, BMP3*, BMP4*, BMPR1B, BMPR2, osteocalcin*, osteopontin*, osteonectin*, RUNX2*, osterix*, ALP*, aggrecan*, OPG*, RANKL*, DMP1*, SOSTDC1*, (versican*, TGF-β1, CTGF*, cathepsin K*, HSP-90α/β*, SMAD4, ATF4)
Control housekeeping proteins	3	α-tubulin*, β-actin*, GAPDH*
Total	403 (97)	

* Santa Cruz Biotechnology, USA; # DAKO, Denmark; $ Neomarkers, CA, USA; @ ZYMED, CA, USA; &Abcam, Cambridge, UK; ^Cell signaling technology, USA; ! kindly donated from M. H. Park in NIH, USA [37]; + kindly donated from S. I. Chung in NIH, USA [38, 39]; the number of antibodies overlapped; ( ).

Abbreviations: AIF: apoptosis inducing factor, AKAP13: A-kinase anchoring proteins 13, ALK1: activin receptor-like kinase 1, ALP: alkaline phosphatase, AMPK: AMP-activated protein kinase, pAKT: v-akt murine thymoma viral oncogene homolog, p-Akt1/2/3

bioRxiv preprint doi: https://doi.org/10.1101/2021.12.13.472401; this version posted December 13, 2021. The copyright holder for this preprint (which was not certified by peer review) is the author/funder, who has granted bioRxiv a license to display the preprint in perpetuity. It is made available under aCC-BY 4.0 International license.

phosphorylated (p-Akt, Thr 308), APAF1: apoptotic protease-activating factor 1, APC: adenomatous polyposis coli, ATF4: activating transcription factor 4, ATM: ataxia telangiectasia caused by mutations, BAD: BCL2 associated death promoter, BAK: BCL2 antagonist/killer, BAX: BCL2 associated X, BCL2: B-cell leukemia/lymphoma-2, BID: BH3 interacting-domain death agonist, BIP (GRP 78): binding immunoglobulin protein, BMP2: bone morphogenesis protein 2, BMPR1B: Bone morphogenetic protein receptor type-1B, BRCA1: breast cancer type 1 susceptibility protein, BRG1 (SMARCA4): transcription activator, c-caspase 3: cleaved-caspase 3, CaM: calmodulin, CD3: cluster of differentiation 3, cdc25A: cell division cycle 25A, CDK4: cyclin dependent kinase 4, CEA: carcinoembryonic antigen, CHOP: C/EBP homologous protein, CMG2: capillary morphogenesis protein 2 (anthrax toxin receptor 2), COX1: cyclooxygenase-2, CRP: C-reactive protein, CTGF: connective tissue growth factor, CTLA4: cytotoxic T lymphocyte-associatedprotein-4, CXCR4: C-X-C chemokine receptor type 4, DHS: deoxyhypusine synthase, DLX2, homeobox protein Distal-less (Dlx) family, DMAP1: DNA methyltransferase 1 associated protein, DMBT1: deleted in malignant brain tumors 1, DNMT1: DNA 5-cytosine methyltransferase 1, DOHH: deoxyhypusine hydroxylase, E2F1: transcription factor, eIF2AK3 (PERK): protein kinase R (PKR)-like endoplasmic reticulum kinase (PERK), elF5A1: eukaryotic translation initiation factor 5A-1, EpCAM: Epithelial cell adhesion molecule, ERβ: estrogen receptor beta, EZH2 (ENX-1): enhancer of zeste homolog 2, FADD: FAS associated via death domain, FAK: focal adhesion kinase, FAS: CD95/Apo1, FASL: FAS ligand, FGF1: fibroblast growth factor 1, FLIP: FLICE-like inhibitory protein, FLT4: Fms-related tyrosine kinase 4, FOXP3: forkhead box P3, GADD45: growth arrest and DNA-damage-inducible 45, GAPDH: glyceraldehyde 3-phosphate dehydrogenase, GFAP: glial fibrillary acidic protein, GH: growth hormone, GHRH: growth hormone-releasing hormone, GSTO1/2: glutathione S-transferase ω 1/2, HCAM (CD44): homing cell adhesion molecule, HDAC10: histone deacetylase 10, HER1: human epidermal growth factor receptor 1, HGFα: hepatocyte growth factor α, HIF1α: hypoxia inducible factor-1α, HO-1: heme oxygenase 1, HRAS: GTPase HRas, HSP70: heat shock protein 70, ICAM-1 (CD54): intercellular adhesion molecule 1, IGF-1: insulin-like growth factor 1, IGFIIR: insulin-like growth factor 2 receptor, IKK: ikappaB kinase, IL-1: interleukin-1, IRE1α (ERN1): inositol-requiring enzyme 1 α, JAK2: Janus kinase 2, JNK1: Jun N-terminal protein kinase 1, KDM4D: Lysine-specific demethylase 4D, KRAS: V-Ki-ras2 Kirsten rat sarcoma viral oncogene homolog, LC3β: microtubule-associated protein 1A/1B-light chain 3β, LTA4H: leukotriene A4 hydrolase, LYVE1: lymphatic vessel endothelial hyaluronan receptor 1, MAD1: mitotic arrest deficient 1, ERK1 (extracellular signal-regulated protein kinase 1, MAPK3 (mitogen-activated protein kinase 3)), maspin: mammary serine protease inhibitor, MAX: myc-associated factor X, MBD4: methyl-CpG-binding domain protein 4, MCP1: monocyte chemotactic protein 1, M-CSF: macrophage colony-stimulating factor, MDM2: mouse double minute 2 homolog, MDR: multiple drug resistance, MEKK1, MMP1: matrix metalloprotease 1, MPM2: mitotic protein monoclonal 2, mTOR: mammalian target of rapamycin, cMyc: V-myc myelocytomatosis viral oncogene homolog, MYH2: myosin-2, NFkB: nuclear factor kappa-light-chain-enhancer of activated B cells, NCAM (CD56): neural cell adhesion molecule 1, NF1: neurofibromin 1, NFAT5: nuclear factor of activated T cells 5, NFATC1: nuclear factor of activated T-cells, cytoplasmic 1, NFkB: nuclear factor kappa-light-chain-enhancer of activated B cells, NOS1: nitric oxide synthase 1, NOXA: Phorbol-12-myristate-13-acetate-induced protein 1, NRAS: neuroblastoma RAS Viral Oncogene homolog, NRF2: nuclear factor (erythroid-derived)-like 2, OPG: osteoprotegerin, PAI-1: plasminogen activator inhibitor-1, PARP-1: poly-ADP ribose polymerase 1, c-PARP-1: cleaved-PARP-1, PCAF: p300/CBP-associated factor, PCNA: proliferating cell nuclear antigen, PD-1 (CD279): programmed cell death protein 1, PDGF-A: platelet-derived growth factor-A, PECAM-1 (CD31): platelet endothelial cell adhesion molecule-1, PERK: protein-like endoplasmic reticulum kinase, PGC-1α: peroxisome proliferator-activated receptor gamma coactivator 1α, PI3K: phosphatidylinositol-3-kinase, PIM-1: Proto-oncogene serine/threonine-protein kinase 1, PKC: protein kinase C, PLC-β2: 1-phosphatidylinositol-4,5-bisphosphate phosphodiesterse β-2, PLK4: polo like kinase 4 or serine/threonine-protein kinase, PSA: prostate-specific antigen, PTEN: phosphatase and tensin homolog, PUMA: p53 upregulated modulator of apoptosis, Rab1: RAS-related protein, Rab GTPases, RAF-B: v-Raf murine sarcoma viral oncogene homolog B, RANKL: receptor activator of nuclear factor kappa-B ligand, Rb-1: retinoblastoma-1, RUNX2: Runt-related transcription factor-2, SHH: sonic hedgehog, SIRT3: sirtuin (silent mating type information regulation 2 homolog) 3, NAD-dependent deacetylase, α-SMA: alpha-smooth muscle actin, SMAD4: mothers against decapentaplegic, drosophila homolog 4, SOD1: superoxide dismutase-1, SOS1: son of sevenless homolog 1, SOSTDC1: sclerostin domain-containing protein 1**,** SOX9: SRY (sex-determining region Y)-related HMG-box transcription factor 9, SP1: specificity protein

bioRxiv preprint doi: https://doi.org/10.1101/2021.12.13.472401; this version posted December 13, 2021. The copyright holder for this preprint (which was not certified by peer review) is the author/funder, who has granted bioRxiv a license to display the preprint in perpetuity. It is made available under aCC-BY 4.0 International license.

225 1, SRC1: steroid receptor coactivator-1, STAT3: signal transducer and activator of transcription-3, SVCT2: sodium-dependent vitamin
226 C transporter 2, TBX22: T-box transcription factor 22, TEM8: tumor-specific endothelial marker 8 (anthrax toxin receptor 1), TERT:
227 human telomerase reverse transcriptase, TGase 2: transglutaminase 2, TGF-β1: transforming growth factor-β1, TNFα: tumor necrosis
228 factor-α, VCAM-1: vascular cell adhesion molecule-1, VE-cadherin: vascular endothelial cadherin, VEGF-A vascular endothelial
229 growth factor A, VEGFR2: vascular endothelial growth factor receptor 2, p-VEGFR2: phosphorylated vascular endothelial growth
230 factor receptor 2 (Y951), vWF: von Willebrand factor, Wnt1: proto-oncogene protein Wnt1, YAP1: Yes-associated protein 1.

231

bioRxiv preprint doi: https://doi.org/10.1101/2021.12.13.472401; this version posted December 13, 2021. The copyright holder for this preprint (which was not certified by peer review) is the author/funder, who has granted bioRxiv a license to display the preprint in perpetuity. It is made available under aCC-BY 4.0 International license.

The supernatant of the antibody-incubated column was removed, and followed by immunoprecipitation-based IP-HPLC. Briefly, each protein sample was mixed with 5 mL of binding buffer (150mM NaCl, 10mM Tris pH 7.4, 1mM EDTA, 1mM EGTA, 0.2mM sodium vanadate, 0.2mM PMSF and 0.5% NP-40) and incubated in the antibody-bound protein A/G agarose bead column on a rotating stirrer at room temperature for 1 h. After multiple washing of the columns with Tris-NaCl buffer, pH 7.5, in a graded NaCl concentration (0.15 – 0.3M), the target proteins were eluted with 300μL of IgG elution buffer (Pierce, USA). The immunoprecipitated proteins were analyzed using a precision HPLC unit (1100 series, Agilent, Santa Clara, CA, USA) equipped with a reverse-phase column and a micro-analytical UV detector system (SG Highteco, Hanam, Korea). Column elution was performed using 0.15M NaCl/20% acetonitrile solution at 0.5 mL/min for 15 min, 40°C, and the proteins were detected using a UV spectrometer at 280 nm. The control and experimental samples were run sequentially to allow comparisons. For IP-HPLC, the whole protein peak areas (mAU*s) were obtained and calculated mathematically using an analytical algorithm (see supplementary data 1) by subtracting the negative control antibody peak areas, and protein expression levels were compared and normalized using the square roots of protein peak areas. The ratios of the protein levels between the experimental and control groups were plotted into line and star graphs. Protein expressional changes of less than ±5%, ±5-10%, ±10-20%, or over ±20% changes were described as minimal, slight, significant, or marked, respectively [30-33, 40]. The housekeeping proteins including *β*-actin, *α*-tubulin, and glyceraldehyde 3-phosphate dehydrogenase (GAPDH) were simultaneously used as internal controls.

In the previous study, the IP-HPLC results were compared with western blot data using cytoplasmic housekeeping protein (β-actin), the former showed minute error ranges less than ± 5% which were appropriate for statistical analysis, while the latter showed a large error range of more than 20% which were impossible to be analyzed statistically [40] (see Supplementary data 2). Therefore, the present study mainly performed

bioRxiv preprint doi: https://doi.org/10.1101/2021.12.13.472401; this version posted December 13, 2021. The copyright holder for this preprint (which was not certified by peer review) is the author/funder, who has granted bioRxiv a license to display the preprint in perpetuity. It is made available under aCC-BY 4.0 International license.

IP-HPLC, and its results were compared to representative findings of ICC and western blot performed with some selected antisera, even though ICC and western blot are usually involved with great error range (≥20%).

Double IP-HPLC

The double IP-HPLC was designed to detect a protein complex or a binding body contained two different proteins. The first IP-HPLC was performed using the first antibody against one protein of complex as the above procedures to get 300 μL protein elute, which was applied as a protein sample in the second IP-HPLC. Subsequently, the second IP-HPLC was performed using the second column containing protein A/G beads bound with the second antibody against the other protein of complex. The protein elute sample was incubated with the protein A/G beads in the second column, and followed the same procedures of IP-HPLC described above.

Global protein expression indexes

As the overexpression and under-expression of essential 150 proteins observed in this study showed characteristics of 21 cellular functions affected by 10 μg/mL PTX. The maximum expression value (%) of upregulated proteins and the minimum protein expression values (%) of downregulated proteins at 12, 24, 48 h after 10 μg/mL PTX treatment were selected and plotted into a star graph.

Statistical analysis

Proportional data (%) of the experimental and control groups were plotted on line graphs and star plots. Their analyses were repeated two to six times until the standard deviations reached ≤±5%. The line graphs

bioRxiv preprint doi: https://doi.org/10.1101/2021.12.13.472401; this version posted December 13, 2021. The copyright holder for this preprint (which was not certified by peer review) is the author/funder, who has granted bioRxiv a license to display the preprint in perpetuity. It is made available under aCC-BY 4.0 International license.

revealed time-dependent expression changes between the relevant proteins, and the star plots revealed the different expression levels of all proteins examined. The results were analyzed by measuring the standard error ($s = \pm \sqrt{\frac{\sigma^2}{n}}$). The expression of the control housekeeping proteins, i.e., β-actin, α-tubulin, and glyceraldehyde 3-phosphate dehydrogenase (GAPDH) was non-responsive (≤5%) to 12, 24, or 48 h of PTX treatment [40, 41] (see Supplementary data 3).

Results

Proliferation by cytological cell counting assay

10 μg/mL PTX-treated RAW 264.7 cells were evenly spread on two-well culture slide dishes and cultured for 48 h. Their monotonous small round nuclei were stained with hematoxylin, and then well distinguishable under microscope. They were increased in cell number depending on time, at 0, 12, 24, and 48 h (Fig. 1). The number of RAW 264.7 cells observed at x400 magnification was 1273.2±72.48 at 0 h, as a control, 1317.1±71.42 at 12 h, 1358±61.16 at 24 h, and 1415±89.41 at 48 h after PTX treatment. 10 μg/mL PTX increased the proliferation index of RW 264.7 cells by 3.5%, 6.7%, and 11.2% compared to the untreated controls at 12, 24, and 48 h, respectively (Figs 1 A-D and E).

Figure 1. Proliferation of RAW 264.7 cells by direct cell counting with hematoxylin staining. 10 μg/mL PTX-treated RAW 264.7 cells showed the increase of proliferation by 3.5% at 12 h, 6.7% at 24 h, and 11.2% at 48 h compared to the non-treated controls. A-D: Histological observation at x400 magnification, E: Statistical analysis plotted into a rod graph, cell number versus culture time (0, 12, 24, and 48 h).

bioRxiv preprint doi: https://doi.org/10.1101/2021.12.13.472401; this version posted December 13, 2021. The copyright holder for this preprint (which was not certified by peer review) is the author/funder, who has granted bioRxiv a license to display the preprint in perpetuity. It is made available under aCC-BY 4.0 International license.

Immunocytochemical observation

The characteristic protein expressions were observed in RAW 264.7 cells through immunocytochemical (ICC) staining, that is, Ki-67, a marker of proliferation was strongly positive in 10 μg/mL PTX-treated cells at 12, 24, and 48 h compared to the untreated controls, and KDM4D and PCAF, markers of histone demethylation and acetylation, respectively, were strongly positive at 12 and 24 h. For the immunoreaction of inflammatory proteins, 10 μg/mL PTX-treated cells showed stronger positivity of TNFα, TLR3, and TLR4 at 24 and 48 h compared to the untreated controls, and increased positivity of IL-6 at 12, 24, and 48 h (Fig. 3).

Figure 2. Immunocytochemical staining of Ki-67 (A), KMD4D (B), PCAF (C), TNFα (D), IL-6 (E), TLR3 (F), and TLR4 (G) in RAW 264.7 cells after 10 μg/mL PTX treatment for 0, 12, 24, and 48 hours. Noted the cytoplasmic (arrow heads) and nuclear (arrows) localization of different immunoreactions in monocytic round cells. No counter stain.

bioRxiv preprint doi: https://doi.org/10.1101/2021.12.13.472401; this version posted December 13, 2021. The copyright holder for this preprint (which was not certified by peer review) is the author/funder, who has granted bioRxiv a license to display the preprint in perpetuity. It is made available under aCC-BY 4.0 International license.

10 μg/mL PTX-treated cells showed slight increase of immunoreaction for GSTO1/2 (a marker of antioxidant and cellular stress) and LC3β (a marker of autophagosome biogenesis), compared to the untreated controls. Caspase 3, a marker of apoptosis executor was markedly positive in 10 μg/mL PTX-treated cells at 12, 24, and 48 h, while the immunoreaction of GADD153 (CHOP, a marker of endoplasmic reticulum stress) and PARP-1 (a marker of DNA damage) was almost similar in the experimental and control cells.

Figure 3. Immunocytochemical staining of GSTO1/2 (A), LC3β (B), GADD153 (C), PARP-1(D), and caspase-3 (E) in RAW 264.7 cells after 10 μg/mL PTX treatment for 0, 12, 24, and 48 hours. Noted the cytoplasmic (arrow heads) and nuclear (arrows) localization of different immunoreactions in monocytic round cells. No counter stain.

10 μg/mL PTX-treated cells showed slight increase of NSEγ immunoreaction at 24 and 48 h compared to the untreated controls, and marked increase of MYH2 (a marker of muscular differentiation) immunoreaction at 12, 24, and 48 h. Regarding the markers of osteoblastic differentiation, RUNX2, OPG, BMPR2, and TGF-β1 were markedly positive in 10 μg/mL PTX-treated cells at 12, 24, and 48 h. These results indicate 10 μg/mL PTX affect RAW 264.7 cells to have a potential for neuro-muscular and osteogenic differentiation.

Figure 4. Immunocytochemical staining of NSEγ (A), MYH2 (B), TGF-β1 (C), RUNX2 (D), OPG (E), and BMPR2 (F) in RAW 264.7 cells after 10 μg/mL PTX treatment for 0, 12, 24, and 48 hours. Noted the cytoplasmic (arrow heads) and nuclear (arrows) localization of different immunoreactions in monocytic round cells. No counter stain.

bioRxiv preprint doi: https://doi.org/10.1101/2021.12.13.472401; this version posted December 13, 2021. The copyright holder for this preprint (which was not certified by peer review) is the author/funder, who has granted bioRxiv a license to display the preprint in perpetuity. It is made available under aCC-BY 4.0 International license.

Western blot detection for selected proteins

For the proteins relevant to proliferation, 10 μg/mL PTX-treated cells showed stronger bands for markers of cell proliferation (Ki-67), p53/Rb signaling (p53, Rb1, and E2F1), Wnt/β-catenin signaling (Wnt1, β-catenin, TCF1), and guided cell migration (E-cadherin and VE-cadherin) at 12, 24, and 48 h than the untreated controls. Among the cMyc/MAX/MAD network proteins, the bands of cMyc and MAX were gradually attenuated at 12, 24, and 48 h, while the bands of MAD1 were increased. The proteins relevant to epigenetic modification, KDM4D and HDAC10 were increased in 10 μg/mL PTX-treated cells at 12, 24, and 48 h versus the untreated controls. RAS signaling proteins, KRAS, HRAS, NRAS, ERK1, and p-ERK1 were also increased at 12, 24, and 48 h (Fig. 5).

Figure 5. Western blot analysis for 10 μg/mL PTX-induced protein expression in RAW 264.7 cells regarding the proliferation (Ki-67), p53/Rb/E2F signaling (p53, Rb1, and E2F1), Wnt/β-catenin signaling (Wnt1, β-catenin, and TCF1), guided cell migration (E-cadherin and VE-cadherin), cMyc/MAX/MAD network (cMyc, MAX, and MAD1), epigenetic modification (KDM4D and HDAC10), and RAS signaling (KRAS, HRAS, NRAS, ERK1, and p-ERK1). The level of β-actin expression was used as an internal control.

TNFα, an inflammatory cytokine, TLR2 and TLR4, markers of innate immunity were increased in 10 μg/mL PTX-treated cells at 12, 24, and 48 h compared to the untreated controls. ER stress proteins, eIF2AK3 and p-eIF2AK3, a marker for autophagy formation, LC3β, and an apoptosis executing protein, caspase 3 were coincidently increased at 24 and 48 h. 10 μg/mL PTX-treated cell showed stronger bands of osteoblastic differentiation proteins, TGF-β1, BMP2, RUNX2, and ATF4 than the untreated controls, and slightly strong bands of nerve differentiation proteins, NSEγ and NF1, and muscle differentiation proteins, MYH2 and desmin at 12, 24, and 48 h compared to the untreated controls (Fig. 6).

bioRxiv preprint doi: https://doi.org/10.1101/2021.12.13.472401; this version posted December 13, 2021. The copyright holder for this preprint (which was not certified by peer review) is the author/funder, who has granted bioRxiv a license to display the preprint in perpetuity. It is made available under aCC-BY 4.0 International license.

Figure 6. Western blot analysis for 10 μg/mL PTX-induced protein expression in RAW 264.7 cells regarding the inflammation (TNFα, TLR2, and TLR4), ER stresses (eIF2AK3, p-eIF2AK3, ATF4, LC3β, and caspase 3), osteoblastic differentiation (TGF-β1, BMP2, and RUNX2), neurogenic differentiation (NSEγ and NF1), and muscular differentiation (MYH2 and desmin). The level of β-actin expression was used as an internal control.

Additionally, 300 μg/mL PTX-induced protein expressions in RAW 264.7 cells were also explored by western blot, and compared with 10 μg/mL PTX-induced protein expressions. 300 μg/mL PTX slightly decreased the expression of Ki-67, cMyc, MAX, E2F1, Wnt1, and TCF1 at 12, 24, and 48 h versus the untreated controls, while 10 μg/mL PTX increased the protein expressions of Ki-67, E2F1, Wnt1, and TCF1, and decreased the protein expressions of cMyc and MAX. The expression of HDAC10 was gradually decreased by 300 μg/mL PTX at 12, 24, and 48 h, while slightly increased by 10 μg/mL PTX.

Regarding RAS signaling, KRAS, ERK1, and pERK1 were slightly downregulated by 300 μg/mL PTX at 12, 24, and 48 h, while upregulated by 10 μg/mL PTX. Apoptosis proteins, p53 and c-caspase 3 were rarely affected by 300 μg/mL PTX, while 10 μg/mL PTX slightly decreased the p53 expression at 12, 24, and 48 h but increased the c-caspase 3 expression at 12, 24, and 48 h. The ER stress proteins, eIF2AK3 and p-eIF2AK3 were slightly upregulated by 300 μg/mL PTX, while eIF2AK3 and p-eIF2AK3 were slightly downregulated but ATF4 was upregulated by 10 μg/mL PTX.

The expressions of inflammatory proteins, TNFα and TLR2 were rarely affected by 300 μg/mL PTX compared to the untreated controls, while increased by 10 μg/mL PTX at 12, 24, and 48 h. And the expressions of osteogenesis proteins, BMP2, RUNX2, and ATF4 were slightly decreased by 300 μg/mL PTX, while increased by 10 μg/mL PTX at 12, 24, and 48 h. On the other hand, the TGF-β1 expression was rarely affected by 300 μg/mL PTX, while slightly increased by 10 μg/mL PTX at 12 and 24 h. And the expression of house-keeping protein, β-actin was almost not affected by 10 μg/mL and 300 μg/mL PTX at 12, 24, and 48 h.

Figure 7. Western blot comparison between 10 μg/mL and 300 μg/mL PTX-induced protein expressions in RAW 264.7 cells regarding the proliferation (Ki-67, cMyx, MAX, E2F1, Wnt1, and TCF1), epigenetic modification (HDAC10), RAS signaling (KRAS, ERK1, and pERK1), apoptosis (p53 and c-caspase 3), ER

bioRxiv preprint doi: https://doi.org/10.1101/2021.12.13.472401; this version posted December 13, 2021. The copyright holder for this preprint (which was not certified by peer review) is the author/funder, who has granted bioRxiv a license to display the preprint in perpetuity. It is made available under aCC-BY 4.0 International license.

stresses (eIF2AK3, p-eIF2AK3, and ATF4), inflammation (TNFα and TLR2), and osteogenesis (BMP2, and RUNX2). The level of β-actin expression was used as an internal control.

Immunoprecipitation-based high performance liquid chromatography (IP-HPLC) analysis

10 μg/mL PTX-treated RAW 264.7 cells were extensively explored for different protein expression by IP-HPLC using 403 antisera, and 300 μg/mL PTX-treated cells were simply done using 61 antisera. The results of 10 μg/mL PTX-induced protein expression were compared with the results of 300 μg/mL PTX-induced protein expression. The IP-HPLC data were statistically analyzed and illustrated in line and star graphs as follows.

Effects of 10 μg/mL PTX on the expression of proliferation-related proteins

RAW 264.7 cells treated with 10 μg/mL PTX for 12, 24, or 48 h showed significant increases in the expression of proliferation-activating proteins including Ki-67 (by 7.7% at 48h), proliferating cell nuclear antigen (PCNA, 7.3% at 48 h), polo-like kinase 4 (PLK4, a regulator of centriole duplication, 12.1% at 48h), CDK4 (4.2% at 12h), cyclin D2 (a regulator of cyclin-dependent kinase, 10.1% at 12 h), cell division cycle 25A (cdc25A, 6.2% at 12h), transcription factor BRG1 (ATP-dependent chromatin remodeler SMARCA4, 4% at 24h), and reactive increase in the expression of p14ARF (an alternate reading frame (ARF) protein product of the CDKN2A locus, 17.2% at 24 h), p15/16INK (inhibitors of cyclin-dependent kinases (INK), 13% at 48 h), and p21CIP1 (a CDK-interacting protein 1 (CIP1), 5.2% at 48 h) versus the untreated controls. On the other hand, the expressions of mitosis phase promoting factor (MPF) recognized by a mitosis-specific monoclonal antibody 2 (MPM2) and lamin A/C involved in nuclear stability, chromatin structure and gene expression were

bioRxiv preprint doi: https://doi.org/10.1101/2021.12.13.472401; this version posted December 13, 2021. The copyright holder for this preprint (which was not certified by peer review) is the author/funder, who has granted bioRxiv a license to display the preprint in perpetuity. It is made available under aCC-BY 4.0 International license.

406 decreased by 6.7% and 12.1% at 12 h, respectively, and the expression of p27KIP1 (a cyclin dependent kinase
407 inhibitor protein 1 (KIP1), was minimally affected by PTX (≤5%) (Figs. 8 A and B).
408

409 Effects of 10 µg/mL PTX on the expression of cMyc/MAX/MAD network
410 proteins

411 The expression of cMyc (regulator genes and proto-oncogenes that code for transcription factors) was
412 increased by 8.2% at 12h after 10 µg/mL PTX treatment but gradually decreased to the untreated control level
413 at 48 h, the expression of MAX (bHLH-Zip protein forming heterodimer with cMyc) was decreased by 3% at
414 48 h, while the expression of MAD-1 (bHLH-Zip protein forming heterodimer with MAX which can oppose
415 functions of Myc-MAX heterodimers) was increased by 4.8% at 48 h versus the untreated controls (Figs. 8 C
416 and D). Whereas the double IP-HPLC using first antibody of cMyc and second antibody of MAX or MAD-1
417 showed that the heterodimers of cMyc and MAX were increased by 11% at 24 h and 11.9% at 48 h, while the
418 heterodimer of cMyc and MAD-1 was decreased by 4.2% at 12 h and 2.1% at 24 h compared to the untreated
419 controls (Figs. 8 E and F). On the other hand, the expressions of cMyc/MAX/MAD network interacting
420 proteins, CDK4 and cyclin D2 were increased by 4.2% at 12 h and 10.1% at 12 h, respectively, but the
421 expression of p27 (cyclin-dependent kinase inhibitor 1B) was minimally affected by PTX (≤5%) (Figs. 8 C
422 and D).

423 In the double IP-HPLC using antisera of cMyc/MAX and cMyc/MAD1, the cMyc-MAX heterodimer
424 was increased by 11% at 24 h and 11.9% at 48 H, while the cMyc-MAD heterodimer was decreased by 4.2%
425 at 12 h and 2.1% at 24 h compared to the untreated controls. On the other hand, CDK4-p27 complex was
426 consistently reduced by 4.6%, at 12 h, 4.1% at 24 h, and 4.7% at 48h in the double IP-HPLC using CDK4 and
427 p27 antisera (Figs. 8 E and F).

bioRxiv preprint doi: https://doi.org/10.1101/2021.12.13.472401; this version posted December 13, 2021. The copyright holder for this preprint (which was not certified by peer review) is the author/funder, who has granted bioRxiv a license to display the preprint in perpetuity. It is made available under aCC-BY 4.0 International license.

Figure 8. Expression of proliferation-related proteins (A and B), cMyc/MAX/MAD network proteins (C and D), and double IP-HPLC for cMyc/MAX/MAD network protein complexes (E and F) in 10 μg/mL PTX-treated RAW 264.7 cells as determined by IP-HPLC. Line graphs, A, C, and E show protein expression on the same scale (%) versus culture time (12, 24, or 48 h), whereas the star plots (B, D, and F) show the differential expression levels of the proteins at 12, 24, or 48 h after PTX treatment on the appropriate scales (%). The thick black line, untreated controls (100%); the blue, yellow, and red dots show differential protein levels after PTX administration for 12, 24, or 48 h, respectively.

Effects of 10 μg/mL PTX on the expression of p53/Rb/E2F signaling proteins

10 μg/mL PTX decreased the expression of tumor suppressor proteins, that is, p53 by 17.5% at 24 h, Rb1 by 9.8% at 48 h, and phosphorylated Rb1 (p-Rb1) at 5.5% in RAW 264.7 cells versus the untreated controls, while the expression of objective transcription factor, E2F-1 was increased by 10.6% at 12 h. And the Ser/Thr-kinase components of cyclin D2 and CDK4 were upregulated by 10.1% and 4.2% at 12 h, respectively, and a cyclin-dependent kinase inhibitor protein, p21CIP1 was also upregulated by 5.2% at 48 h (Figs. 9 A and B).

In the double IP-HPLC using antisera of E2F1/Rb1, CDK4/p21, and E2F1/VE-cadherin, the E2F1-Rb1 and CDK4-p21 complexes were increased by 8.4% and 12.9% at 24 H, respectively, but E2F1-VE-cadherin complex was minimally affected by 10 μg/mL PTX. On the other hand, CDK4-p27 complex was consistently reduced by 4.6% at 12 h, 4.1% at 24 h, and 4.7% at 48h in the double IP-HPLC using CDK4 and p27 antisera (Figs. 8 E and F).

bioRxiv preprint doi: https://doi.org/10.1101/2021.12.13.472401; this version posted December 13, 2021. The copyright holder for this preprint (which was not certified by peer review) is the author/funder, who has granted bioRxiv a license to display the preprint in perpetuity. It is made available under aCC-BY 4.0 International license.

Effects of 10 μg/mL PTX on the expression of Wnt/β-catenin signaling proteins

10 μg/mL PTX increased the protein expressions of Wnt1 (by 14.9% at 24 h), β-catenin (by 16% at 24 h), adenomatous polyposis coli (APC, by 16.8% at 48 h), snail (by 13.1% at 48 h), and T-cell factor 1 (TCF1, a transcription factor, by 15.9% at 12 h) versus the untreated controls. On the other hand, E-cadherin (a type-I transmembrane protein stabilized by β-catenin) and VE-cadherin (vascular endothelial cadherin) were increased by 17.4% at 48 h and 22.1% at 12 h, respectively, while the expressions of Wnt signaling cofactors, MMP9 and vimentin which are necessary in the process of epithelial-mesenchymal transition, were decreased by 10.4% and 12.9% at 24 h, respectively (Figs. 2 A1 and A2).

These results indicate Wnt/β-catenin signaling was enhanced with concomitant upregulation of Wnt1, β-catenin, APC, snail, and TCF1 by 10 μg/mL PTX, but the activation of Wnt/β-catenin signaling was not followed by overexpressions of MMP9 and vimentin, but led to the overexpression of E-cadherin and VE-cadherin.

Figure 9. Expression of p53/Rb/E2F signaling proteins (A and B), double IP-HPLC for p53/Rb/E2F signaling protein complexes (C and D), Wnt/β-catenin signaling proteins (E and F), and double IP-HPLC for Wnt/β-catenin signaling protein complexes (G and H) in 10 μg/mL PTX-treated RAW 264.7 cells as determined by IP-HPLC. Line graphs, A, C, and E show protein expression on the same scale (%) versus culture time (12, 24, or 48 h), whereas the star plots (B, D, and F) show the differential expression levels of the proteins at 12, 24, or 48 h after PTX treatment on the appropriate scales (%). The thick black line, untreated controls (100%); the blue, yellow, and red dots show differential protein levels after PTX administration for 12, 24, or 48 h, respectively.

bioRxiv preprint doi: https://doi.org/10.1101/2021.12.13.472401; this version posted December 13, 2021. The copyright holder for this preprint (which was not certified by peer review) is the author/funder, who has granted bioRxiv a license to display the preprint in perpetuity. It is made available under aCC-BY 4.0 International license.

Effects of 10 μg/mL PTX on the expression of epigenetic modification proteins

10 μg/mL PTX increased the expression of histone H1 (by 10.6% at 24 h), lysine-specific demethylase 4D (KDM4D, 12% at 48 h), and p300/CBP-associated factor K (lysine) acetyltransferase 2B which has histone acetyl transferase activity (PCAF, by 14% at 12 h) versus the untreated controls, while decreased the expression of histone deacetylase 10 (HDAC10, 9.6% at 24 h), DNA (cytosine-5)-methyltransferase 1 (DNMT1: 23.5% at 48 h), DNA methyltransferase 1-associated protein 1 (DMAP1: 17.7% at 48 h), histone-lysine N-methyltransferase enzyme (enhancer of zeste homolog 2 (EZH2), 6.6% at 24 h), and methyl-CpG binding domain 4 (MBD4: 6.7% at 12 h) (Figs. 10 A and B).

Effects of 10 μg/mL PTX on the expression of protein translation proteins

RAW 264.7 cells treated with 10 μg/mL PTX showed increase in the expression of protein translation protein: deoxyhypusine hydroxylase (DOHH, by 7.6% at 12 h), deoxyhypusine protein synthase (DHPS, 17.1% at 24 h), eukaryotic translation initiation factor 5A-1 (eIF5A1, 6.5% at 12 h), and eIF5A2 (7.5% at 24 h) versus the untreated controls. On the other hand, the essential factor for protein synthesis to form a ternary complex (TC)with GTP andtheinitiator Met-tRNA, that is, eIF2α and p-eIF2α were decreased by 8.7% at 12 h and 5.7% at 48 h, respectively, and eukaryotic translation initiation factor 2-α kinase 3 (eIF2AK3, a protein kinase R (PKR)-like endoplasmic reticulum kinase (PERK)) was decreased by 9.3% at 12 h, but p-eIF2AK3 was reactively increased by 6.7% at 48 h (Figs. 10 C and D).

Effects of 10 μg/mL PTX on the expression of growth factor

bioRxiv preprint doi: https://doi.org/10.1101/2021.12.13.472401; this version posted December 13, 2021. The copyright holder for this preprint (which was not certified by peer review) is the author/funder, who has granted bioRxiv a license to display the preprint in perpetuity. It is made available under aCC-BY 4.0 International license.

RAW 264.7 cells after 10 μg/mL PTX administration showed marked decrease in the expression of HGFα (by 17.5% at 24 h), Met (9.9% at 48 h), fibroblast growth factor-1 (FGF1, 5.5% at 12 h), FGF2 (10.3% at 12 h), FGF7 (2% at 48 h), connective tissue growth factor (CTGF, 17.7% at 24 h), and estrogen receptor-β (ERβ, 14.1% at 24 h) versus the untreated controls. Particularly, PTX decreased the expression of TGF-α (by 21% at 48 h), TGF-β1 (12.5% at 12 h), TGF-β2 (18.5% at 48 h), TGF-β3 (16.4% at 24 h), activin receptor-like kinase 1 (ALK1, 14.6% at 12 h), SMAD2/3 (15.8% at 12 h), and HER1 (epidermal growth factor receptor, 13.4%), while compensatory increased the expression of SMAD4 (14.9% at 48 h), p-SMAD4 (7.1% at 24 h), growth hormone (GH, 11.4% at 48 h), growth hormone releasing hormone (GHRH, 16.9% at48 h), insulin-like growth factor 2 receptor (IGF2R, 11.4% at 48 h), HER2 (EGF receptor tyrosine-protein kinase erbB-2, 9.6% at 24 h), and epidermal growth factor (EGF, 18.8% at 24 h). On the other hand, the expressions of FGF7, IGF1, and PDGF-A were affected minimally by PTX (≤5%) (Figs. 10 E and F).

Figure 10. Expression of epigenetic modification proteins (A and B), protein translation proteins (C and D), and growth factors (E and F) in 10 μg/mL PTX-treated RAW 264.7 cells as determined by IP-HPLC. Line graphs, A, C, and E show protein expression on the same scale (%) versus culture time (12, 24, or 48 h), whereas the star plots (B, D, and F) show the differential expression levels of the proteins at 12, 24, or 48 h after PTX treatment on the appropriate scales (%). The thick black line, untreated controls (100%); the blue, yellow, and red dots show differential protein levels after PTX administration for 12, 24, or 48 h, respectively.

bioRxiv preprint doi: https://doi.org/10.1101/2021.12.13.472401; this version posted December 13, 2021. The copyright holder for this preprint (which was not certified by peer review) is the author/funder, who has granted bioRxiv a license to display the preprint in perpetuity. It is made available under aCC-BY 4.0 International license.

Effects of 10 μg/mL PTX on the protein expressions of RAS signaling proteins

10 μg/mL PTX affected RAS signaling protein expressions of RAW 264.7 cells positively or negatively. The RAS signaling proteins were initially upregulated at 12 and 24 h and subsequently became similar to control level or downregulated at 48 h by 10 μg/mL PTX, that is, Kirsten Rat Sarcoma virus oncogene (KRAS) to 121% at 12 h and 103.3% at 48 h, neuroblastoma RAS viral oncogene homolog (NRAS) to 102.7% at 24 h and 95.9% at 48 h, GTPase HRAS also known as transforming protein p21 (HRAS) to 110.3% at 12 h and 106.5% at 48 h, signal transducer and activator of transcription 3 (STAT3) to 106.8% at 12 h and 99.1% 48 h, p-STAT3 to 106.7% at 24 h and 99.4% at 48 h, phosphorylated AKT1/2/3 (pAKT1/2/3: Thr 308, a critical mediator of growth factor-induced signals) to 106.5% at 24 h and 102.2% at 48 h, phosphatidylinositol 3-kinase (PI3K) to 113.6% at 24 h and 108% at 48 h, GTPases Rab to 110.2% at 12 h and 101.6% at 48 h, serine/threonine-protein kinase RAF-B to 107.6% at 12 h and 99.3% at 48 h, non-receptor tyrosine-protein kinase (TYK2, the first member of JAK family) to 122.9% at 12 h and 104.7% at 48 h, protein kinase C (PKC) to 108.6% at 24 h and 99.3% at 48 h, p-PKC1α to 111.5% at 24 h and 103% at 48 h, and A-kinase anchoring proteins (AKAP13) to 116.4% at 24 h and 102.2% at 48 h versus the untreated controls. However, some downstream effector proteins of RAS signaling were consistently upregulated by 10 μg/mL PTX, that is, extracellular signal-regulated kinase 1 (a.k.a. mitogen-activated protein kinase 3, ERK1) by 8.6% at 24 h, pERK-1 by 9.3% at 24 h, p38 by 13.1% at 48 h, and p-p38 by 12.3% at 48 h.

Whereas the expressions of other RAS signaling proteins were decreased, that is, c-Jun N-terminal kinase-1 (JNK1) by 5.6% at 24 h, phosphorylated JNK1 (p-JNK1, Thr 183/Tyr 185) by 11.1% at 24 h, MEK kinase 1 (also designated MAP kinase kinase kinase 1, MKKK1, MAP3K1 or MEKK1) by 11.7% at 12 h, mammalian target of rapamycin (mTOR) by 19.5% at 24 h, phosphorylated mTOR (p-mTOR) by 15.7% at 48

bioRxiv preprint doi: https://doi.org/10.1101/2021.12.13.472401; this version posted December 13, 2021. The copyright holder for this preprint (which was not certified by peer review) is the author/funder, who has granted bioRxiv a license to display the preprint in perpetuity. It is made available under aCC-BY 4.0 International license.

h, Janus kinase 2 (JAK2, non-receptor tyrosine kinase) by 14.8% at 48 h, and son of sevenless homolog 1 (SOS1) by 22.3% at 12 h. On the other hand, the expression of phosphatase and tensin homolog (PTEN) was affected minimally by PTX (≤5%) (Figs. 11 A and B).

Effects of 10 µg/mL PTX on the expression of NFkB signaling proteins

10 µg/mL PTX had different effects on the expression of NFkB signaling proteins in RAW 264.7 cells. PTX markedly upregulated nuclear factor kappa-light-chain-enhancer of activated B cells (NFkB) by 20.7% at 24 h but slightly downregulated ikappaB kinase (IKK) by 6.8% at 12 h versus the untreated controls, and subsequently increased the expression of downstream effector proteins of NFkB signaling, that is, p38 mitogen-activated protein kinase (p38) by 13.1% at 48 h, phosphorylated p38 (p-p38) by 12.3% at 48 h, growth arrest and DNA damage 45 (GADD45) by 18.7% at 48 h, multiple drug resistance (MDR) by 12.5% at 48 h, protein kinase C (PKC) by 8.6% at 24 h, p-PKC1α by 11.5% at 24 h, steroid receptor co-activator-1 (SRC1) by 12.3% at 48 h, and A-kinase anchoring proteins (AKAP13) by 16.4% at 24 h.

On the other hand, the expressions of some downstream regulating proteins of NFkB signaling were decreased, that is, mTOR by 19.5% at 24 h, p-mTOR by 15.7% at 48 h, and peroxisome proliferator-activated receptor gamma coactivator 1-α (PGC1α) by 12.1% at 24 h, MEKK1 by 11.7% at 12 h, JAK2 by 14.8% at 48 h, and nuclear factor of activated T-cells 1 (NFATC1) by 7.3% at 24 h. The expressions of GADD153, nuclear factor (erythroid-derived 2)-like 2 (NRF2), 5' AMP-activated protein kinase α (AMPKα), and nuclear factor of activated T cells (NFAT5) were only minimally affected by PTX (≤ 5%) (Figs. 11 C and D).

Inflammatory proteins upregulated by 10 µg/mL PTX

bioRxiv preprint doi: https://doi.org/10.1101/2021.12.13.472401; this version posted December 13, 2021. The copyright holder for this preprint (which was not certified by peer review) is the author/funder, who has granted bioRxiv a license to display the preprint in perpetuity. It is made available under aCC-BY 4.0 International license.

Among the inflammatory proteins, some proteins were upregulated by 10 μg/mL PTX in RAW 264.7 cells as follows, that is, tumor necrosis factor α (TNFα) by 10.6% at 24 h, interleukin-1 (IL-1) by 5.7% at 48 h, IL-6 by 15.2% at 24 h, IL-10 by 10.9% at 24 h, CD4 by 25.3% at 48 h, CD8 by 7.3% at 24 h, CD31 by 4.6% at 48 h, CD34 by 22.2% at 24 h, CD44 (homing cell adhesion molecule (HCAM)) by 9.8% at 48 h, CD80 by 13.3% at 24 h, matrix metalloproteinase 1 (MMP1) by 18.1% at 24 h, MMP1/8 by 10.8% at 48 h, tissue inhibitor of metalloproteinase 1 (TIMP1) by 14.7% at 48 h, TIMP-2 by 5.2% at 48 h, macrophage colony-stimulating factor (M-CSF) by 14%% at 48 h, C-X-C chemokine receptor type 4 (CXCR4, a.k.a. CD184) by 13.5% at 48 h, cytotoxic T lymphocyte-associated protein-4 (CTLA4) by 8.4% at 24 h, granzyme B by 9.1% at 12 h but decreased by 10.2% at 12 h, β-defensin-1 by 11.4% at 12 h, monocyte chemotactic protein-1 (MCP1) by 10.1% at 48 h, human leukocyte antigen - DR isotype (HLA-DR) by 13.3% at 48 h, lactoferrin by 16% at 24 h, kininogen by 6.5% at 12 h, toll-like receptor 3 (TLR3) by 10.9% at 48 h, TLR4 by 11.7% at 48 h, integrin α2 by 16% at 24 h, integrin α5 by 12.2% at 48 h, chondroitin sulfate proteoglycan versican by 16.9% at 24 h, and perforin by 14.7% at 24 h. On the other hand, the expression of MMP12, TLR2, TLR7, and C-reactive protein (CRP) showed a trend of increase but were only minimally affected by PTX (≤ 5%) (Figs. 11 E and F).

Figure 11. Expression of RAS signaling proteins (A and B), NFkB signaling proteins (C and D), and upregulated inflammatory proteins (E and F) in 10 μg/mL PTX-treated RAW 264.7 cells as determined by IP-HPLC. Line graphs, A, C, and E show protein expression on the same scale (%) versus culture time (12, 24, or 48 h), whereas the star plots (B, D, and F) show the differential expression levels of the proteins at 12, 24, or 48 h after PTX treatment on the appropriate scales (%). The thick black line, untreated controls (100%); the blue, yellow, and red dots show differential protein levels after PTX administration for 12, 24, or 48 h, respectively.

bioRxiv preprint doi: https://doi.org/10.1101/2021.12.13.472401; this version posted December 13, 2021. The copyright holder for this preprint (which was not certified by peer review) is the author/funder, who has granted bioRxiv a license to display the preprint in perpetuity. It is made available under aCC-BY 4.0 International license.

Inflammatory proteins downregulated by 10 µg/mL PTX

Among the inflammatory proteins, some proteins were downregulated by 10 µg/mL PTX in RAW 264.7 cells as follows: IL-8 by 7.5% at 12 h, IL-12 by 5.4% at 48 h, IL-28 by 17.9% at 48 h, CD3 by 14% at 12 h, CD20 by 18.3% at 12 h, CD28 by 10.2% at 12 h, CD54 (Intercellular Adhesion Molecule 1 (ICAM-1)) by 12.6% at 12 h, CD56 (Neural Cell Adhesion Molecule (NCAM)) by 18.8% at 24 h, CD99 by 15.3% at 12 h, CD106 (Vascular Cell Adhesion Molecule-1 (VCAM-1)) by 15.5% at 12 h, MMP-2 by 16.3% at 24 h, MMP3 by 12.7% at 12 h, MMP9 by 10.5% at 24 h, MMP10 by 9.4% at 12 h, cathepsin C by 10.8% at 24 h, cathepsin G by 23% at 24 h, cathepsin K by 9.2% at 48 h, lysozyme by 10.9% at 24 h, hepcidin by 17.4% at 24 h, α1-antitrypsin by 17% at 24 h, β-defensin 2 by 6.9% at 48 h, β-defensin 3 by 11.4% at 12 h, cyclooxygenase 1 (COX1) by 20.3% at 24 h, COX2 by 12.4% at 48 h, leukotriene A4 hydrolase (LTA4H) by 10.6% at 48 h, elafin by 5.2% at 48 h, integrin β1 by 8.7% at 12 h, and LL-37 by 19.5% at 24 h. On the other hand, the expression of CD40 and programmed cell death protein 1/1 (PD-1, CD279) showed a trend of decrease but were only minimally affected by PTX (≤ 5%) (Figs. 12 A and B).

Effects of 10 µg/mL PTX on the expression of p53-mediated apoptosis proteins

10 µg/mL PTX significantly reduced the expression of p53-mediated pro-apoptotic proteins, that is, p53 by 17.5% at 24 h, BCL2 homologous antagonist/killer (BAK) by 5.5% at 48 h, p73 by 23.9% at 12 h, NOXA (a pro-apoptotic member of the BCL2 protein family) by 7.8% at 24 h, p53 upregulated modulator of apoptosis (PUMA, mitochondria pro-apoptotic BCL-2 homolog) by 6.1% at 24 h, apoptosis regulator BAX by 24% at 48 h, apoptotic protease activating factor 1 (APAF1) by 10.9% at 48 h, caspase 9 by 14.4% at 12 h, and c-caspase 9 by 15.7% at 24 h, apoptosis inducing factor (AIF) by 10.9% at 48 h, poly [ADP-ribose] polymerase 1

bioRxiv preprint doi: https://doi.org/10.1101/2021.12.13.472401; this version posted December 13, 2021. The copyright holder for this preprint (which was not certified by peer review) is the author/funder, who has granted bioRxiv a license to display the preprint in perpetuity. It is made available under aCC-BY 4.0 International license.

(PARP1) by 13.1% at 12 h, and cleaved PARP (c-PARP) by 21.5% at 12 h versus the untreated controls, while it increased the expression of murine double minute-2 homolog (MDM2, negative regulator of p53) by 8.9% at 12 h and minimally affected the expression of B cell lymphoma 2 (BCL2, anti-apoptotic protein) (≤ 5%) (Figs. 12 C and D).

Effects of 10 µg/mL PTX on the expression of FAS-mediated apoptosis proteins

RAW 264.7 cells treated with 10 µg/mL PTX showed increases in the expression of FAS-mediated apoptosis proteins, that is, FAS ligand (FASL) by 20.5% at 48 h, FAS (CD95) by 10.1% at 12 h, FAS-associated protein with death domain (FADD) by 15.3% at 12 h, BH3 interacting-domain death agonist (BID) by 8.5% at 24 h, caspase 3 by 19.2% at 48 h, c-caspase 3 by 16.1% at 48 h, caspase 7 by 24.8% at 48 h, c-caspase 8 by 14% at 24 h, c-caspase 10 by 21.4% at 24 h versus the untreated controls, while the expression of FLICE-like inhibitory protein (FLIP) was decreased by 9.3% at 48 h (Figs. 12 E and F).

Figure 12. Expression of downregulated inflammatory proteins (A and B), p53-mediated apoptosis proteins (C and D), and FAS-mediated apoptosis proteins (E and F) in 10 µg/mL PTX-treated RAW 264.7 cells as determined by IP-HPLC. Line graphs, A, C, and E show protein expression on the same scale (%) versus culture time (12, 24, or 48 h), whereas the star plots (B, D, and F) show the differential expression levels of the proteins at 12, 24, or 48 h after PTX treatment on the appropriate scales (%). The thick black line, untreated controls (100%); the blue, yellow, and red dots show differential protein levels after PTX administration for 12, 24, or 48 h, respectively.

Effects of 10 µg/mL PTX on the expression of cell protection proteins

bioRxiv preprint doi: https://doi.org/10.1101/2021.12.13.472401; this version posted December 13, 2021. The copyright holder for this preprint (which was not certified by peer review) is the author/funder, who has granted bioRxiv a license to display the preprint in perpetuity. It is made available under aCC-BY 4.0 International license.

10 µg/mL PTX-treated RAW 264.7 cells showed increases in the expression of cellular stress protection-, antioxidant-, and cell survival proteins versus the untreated controls, as follows: heat shock protein-70 (HSP70) by 17.2% at 12 h, Cu-Zn superoxide dismutase-1 (SOD1) by 28.2 % at 48 h, glutathione S-transferase ω 1/2 (GSTO1/2, a detoxifying enzyme) by 30.3% at 48 h, nitric oxide synthases-1 (NOS1) by 6.4% at 12 h, pAKT1/2/3 by 6.5% at 24 h, PKC by 8.6% at 24 h, p-PKC1α by 11.5% at 24 h, LC3β by 11.6% at 48 h, sodium-dependent vitamin C transporter 2 (SVCT2) by 6.6% at 48 h, SP-1 by 8.3% at 48 h, a transcription factor regulating the expression of antioxidant proteins NRF2 by 4.1% at 24 h, energy expenditure hormone leptin by 13.1% at 24 h, a stress responsive protein deacetylase sirtuin 6 by 5.8% at 24 h, FOXP3 by 7.4% at 12 h, and PLC-β2 by 13.1% at 48 h versus the untreated controls. Whereas PTX decreased the expression of cellular maintenance proteins: heme oxygenase-1 (HO1) by 12.1% at 48 h, small heat shock protein HSP-27 by 14.2% at 48 h, HSP-90α/β by 15.8% at 24 h, telomerase reverse transcriptase (TERT) by 10.4% at 12 h, mTOR by 19.5% at 24 h, SP-3 by 16.4% at 48 h, and peroxisome proliferator-activated receptor gamma coactivator 1-alpha (PGC1α) by 12.1% at 24 h, sirtuin 1 by 9% at 24 h, sirtuin 3 by 7.1% at 24 h, and FOXP4 by 11% at 48 h. The expressions of 5' AMP-activated protein kinase α (AMPKα, an enzyme that regulates cellular energy homeostasis) and sirtuin 7 were only minimally affected by PTX (≤ 5%) (Figs. 13 A and B).

Effects of 10 µg/mL PTX on the expression of endoplasmic reticulum stress proteins

10 µg/mL PTX had different effects on the expression of endoplasmic reticulum stress proteins in RAW 264.7 cells. PTX downregulated the proteins contributing to ER stress signaling; eIF2AK3, (PERK, which functions as an ER kinase) by 9.3% at 12 h, eIF2α and p-eIF2α (essential factors for protein synthesis also

bioRxiv preprint doi: https://doi.org/10.1101/2021.12.13.472401; this version posted December 13, 2021. The copyright holder for this preprint (which was not certified by peer review) is the author/funder, who has granted bioRxiv a license to display the preprint in perpetuity. It is made available under aCC-BY 4.0 International license.

649 responsible for ER stresses) by 8.7% at 12 h and 5.7% at 48 h, respectively, activating transcription factor 6α
650 (ATF6α) by 9% at 12 h, binding immunoglobulin protein (BIP, a HSP70 molecular chaperone) by 8.4% at 12
651 h, serine/threonine-protein kinase/endoribonuclease inositol-requiring enzyme 1 α (IRE1α) by 8.2% at 24 h,
652 PGC-1α by 12.1% at 24 h, caveolin-1 by 8.3% at 48 h, and AIF by 10.9% at 48 h compared to the untreated
653 controls. On the other hand, PTX upregulated the proteins contributing to ER-stress environment in cells;
654 HSP-70 by 17.2% at 12 h, p-eIF2AK3 by 6.7% at 48 h, ATF4 (cAMP-response element binding protein 2) by
655 8% at 24 h, AP1M1 (the medium chain of the trans-Golgi network clathrin-associated protein complex AP-1)
656 by 12.9% at 48 h, calnexin (a chaperone for the protein folding in the membrane of the ER) by 8.5% at 12 h,
657 LC3β (microtubule-associated proteins 1A/1B light chain 3B contributing to autophagosome biogenesis) by
658 11.6% at 48 h, and endothelin-1 (inducing Ca^{2+} release from ER) by 17.8% at 24 h. The expressions of
659 GADD153 (C/EBP homologous protein (CHOP)) and p-GADD153 were only minimally affected by PTX (≤
660 5%) (Figs. 13 C and D).
661

662 **Effects of 10 μg/mL PTX on the expression of SHH/PTCH/GLI and**
663 **Notch/Jagged signaling proteins**

664 10 μg/mL PTX was found to influence the expression of SHH/PTCH/GLI signaling proteins positively or
665 negatively in RAW 264.7 cells. PTX upregulated the upstream proteins of SHH/PTCH/GLI signaling; sonic
666 hedgehog (SHH) by 14.6% at 24 h, patched homolog 1 (PTCH1, the receptor for sonic hedgehog) by 8.8% at
667 48 h, and CD44 (HCAM, the activator of SHH signaling) by 9.8% at 48 h versus the untreated controls, while
668 downregulated the downstream proteins of SHH/PTCH/GLI signaling; GLI1(Glioma-associated oncogene,
669 the effectors of SHH signaling) by 12.9% at 24 h, EpCAM (epithelial cell adhesion molecule, involved in

bioRxiv preprint doi: https://doi.org/10.1101/2021.12.13.472401; this version posted December 13, 2021. The copyright holder for this preprint (which was not certified by peer review) is the author/funder, who has granted bioRxiv a license to display the preprint in perpetuity. It is made available under aCC-BY 4.0 International license.

SHH signaling) by 3.1% at 48 h, and BCL2 (GLI binding site in BCL2 promoter, upregulated by GLI1) by 4.6% at 12 h.

On the other hand, PTX downregulated Notch/Jagged signaling proteins; Notch1 (Notch homolog 1, translocation-associated (Drosophila)) by 5.3% at 48 h, Jagged2 (ligand for Notch) by 6.1% at 24 h, and VEGF-A (crosstalk between VEGF and Notch signaling) by 6.7% at 48 h. The expressions of Notch upstream signaling proteins, HIF1α (hypoxia-inducible factors 1α) and Wnt1 were compensatory increased by 13% and 13% at 24 h, respectively (Figs. 13 E and F).

Figure 13. Expression of protection proteins (A and B), endoplasmic reticulum stress proteins (C and D), and SHH/PTCH/GLI and Notch/Jagged signaling in 10 μg/mL PTX-treated RAW 264.7 cells as determined by IP-HPLC. Line graphs, A, C, and E show protein expression on the same scale (%) versus culture time (12, 24, or 48 h), whereas the star plots (B, D, and F) show the differential expression levels of the proteins at 12, 24, or 48 h after PTX treatment on the appropriate scales (%). The thick black line, untreated controls (100%); the blue, yellow, and red dots show differential protein levels after PTX administration for 12, 24, or 48 h, respectively.

Effects of 10 μg/mL PTX on the expression of cytodifferentiation proteins

10 μg/mL PTX was found to influence the expression of cytodifferentiation proteins positively or negatively in RAW 264.7 cells. PTX upregulated some cytodifferentiation proteins, that is, α-actin by 12% at 24 h, transglutaminase 2 (TGase 2) by 15.3% at 48 h, protein kinase C (PKC, serine/threonine protein kinase, 8.6% at 24 h), p-PKC1α(11.5% at 24 h), focal adhesion kinase (FAK, 6.3% at 48 h), A-kinase anchoring proteins 13 (AKAP13, 7.8% at 48 h), calmodulin (CaM, the universal calcium sensor) by 8.2% at 48 h, calnexin by 8.5% at 12 h, cystatin A (a thiol protease inhibitor) by 6.9% at 12 h, SOX9 (SRY-related HMG-box) by 9.6%

bioRxiv preprint doi: https://doi.org/10.1101/2021.12.13.472401; this version posted December 13, 2021. The copyright holder for this preprint (which was not certified by peer review) is the author/funder, who has granted bioRxiv a license to display the preprint in perpetuity. It is made available under aCC-BY 4.0 International license.

693 at 48 h, AP-1 complex subunit mu-1 (AP1M1, localized at Golgi vesicles for endocytosis and Golgi processing)
694 by 12.9% at 48 h), phosphoinositide-specific phospholipase C β2 (PLCβ2) by 13.1% at 48 h, E-cadherin by
695 17.4% at 48 h, and VE-cadherin (vascular endothelial cadherin) by 12.9%at 12 h, while downregulated other
696 cytodifferentiation proteins, that is, p63 by 9% at 24 h, vimentin by 14.5% at 24 h, TGase 4 by 11% at 24 h,
697 hexokinases 2 (HK2) by 10.9% at 12 h, Krox-25 by 7.1% at 24 h, DLX2 (homeobox protein from distal-less
698 (Dll) gene expressed in the head and limbs of the developing fruit fly) by 17.3% at 24 h, laminin α5 by 14.2%
699 at 48 h, pancreatic lipase by 5.4% at 48 h, and prostate-specific antigen (PSA, gamma-seminoprotein or
700 kallikrein-3 (KLK3)) by 16.9% at 48 h. On the other hand, the expressions of cysteine-rich protein that
701 participates in cytoskeletal remodeling (CRIP1) by 16.3% at 12 h), TBX22 (T-box transcription factor), and
702 epithelial cell adhesion molecule (EpCAM) were only minimally affected by PTX (≤ 5%) (Figs. 14 A and B).
703

704 Effects of 10 μg/mL PTX on the expression of neuromuscular
705 differentiation proteins

706 10 μg/mL PTX was found to have positive influence on the expression of neuromuscular differentiation
707 proteins in RAW 264.7 cells. PTX upregulated some neuromuscular differentiation proteins, that is, neuron
708 specific γ enolase (NSEγ) by 13.6% at 24 h, glial fibrillary acidic protein (GFAP) by 9.5% at 12h, myosin
709 heavy chain 2 (MYH2) by 28.6% at 24 h, desmin by 12.2% at 12h, calmodulin (CaM) by 8.2% at 48 h,
710 calnexin by 8.5% at 12 h, cystatin A by 6.9% at 12 h, AP-1 complex subunit mu-1 (AP1M1) by 12.9% at 48 h,
711 focal adhesion kinase (FAK), substrate for tyrosin kinase of Src) by 6.3% at 48 h, SHH by 14.6 at 24 h,
712 β-catenin by 18.5% at 24 h, Wnt1 by 13% at 24 h, TGase 2 by 15.3% at 48 h, and α-smooth muscle actin
713 (α-SMA) by 30.3% at 12 h, while downregulated other neuromuscular differentiation proteins, that is, S-100
714 by 13.8% at 48 h, unconventional myosin-1a (membrane binding class I myosin), 10.9% at 12 h,

bioRxiv preprint doi: https://doi.org/10.1101/2021.12.13.472401; this version posted December 13, 2021. The copyright holder for this preprint (which was not certified by peer review) is the author/funder, who has granted bioRxiv a license to display the preprint in perpetuity. It is made available under aCC-BY 4.0 International license.

715 neurofibromin 1 (NF1) by 6.3% at 12 h. The expressions of neurokinin 1 receptor (NK1R, substance P
716 receptor) and cysteine-rich protein 1 (CRIP1) were only minimally affected by PTX (≤ 5%) (Figs. 14 C and D).
717

718 ## Effects of 10 μg/mL PTX on the expression of fibrosis proteins

719 10 μg/mL PTX was found to decrease the expression of fibrosis-inducing proteins; FGF1 by 5.5% at 12 h,
720 FGF2 by 10.3% at 12 h, TGF-β1 by 12.5% at 12 h, CTGF by 17.7% at 12 h, collagen 3A1 by 13.7% at 48 h,
721 collagen 4 by 14.6% at 24 h, collagen 5A by 6.9% at 24 h, laminin α5 by 14.2% at 48 h, integrin β1 by 8.7%
722 at 12 h, plasminogen activator inhibitor-1 (PAI1) by 8.7% at 12 h, α1-antitrypsin by 7% at 24 h, elafin
723 (peptidase inhibitor 3, elastase-specific protease inhibitor) by 5.2% at 48 h, and also to increase anti-fibrosis
724 proteins; plasminogen by 15.6% at 48 h, integrin α2 by 16% at 24 h, integrin α5 by 12.2% at 48 h, and
725 capillary morphogenesis gene 2 (CMG2) by 13.5% at 12 h. On the other hand, the expression of endothelin-1,
726 a key role of vascular homeostasis, was reactively upregulated by 17.8% at 24 h. And the expressions of
727 FGF7 and platelet-derived growth factor A (PDGF-A) were only minimally affected by PTX (≤ 5%) (Figs. 14
728 E and F).
729

730 **Figure 14**. Expression of cytodifferentiation proteins (A and B), neuromuscular differentiation proteins (C
731 and D), and fibrosis proteins (E and F) in 10 μg/mL PTX-treated RAW 264.7 cells as determined by IP-HPLC.
732 Line graphs, A, C, and E show protein expression on the same scale (%) versus culture time (12, 24, or 48 h),
733 whereas the star plots (B, D, and F) show the differential expression levels of the proteins at 12, 24, or 48 h after
734 PTX treatment on the appropriate scales (%). The thick black line, untreated controls (100%); the blue, yellow,
735 and red dots show differential protein levels after PTX administration for 12, 24, or 48 h, respectively.
736

bioRxiv preprint doi: https://doi.org/10.1101/2021.12.13.472401; this version posted December 13, 2021. The copyright holder for this preprint (which was not certified by peer review) is the author/funder, who has granted bioRxiv a license to display the preprint in perpetuity. It is made available under aCC-BY 4.0 International license.

Effects of 10 µg/mL PTX on the expression of oncogenesis proteins

10 µg/mL PTX was found to influence the expression of oncogenesis proteins positively or negatively in RAW 264.7 cells. PTX decreased the expression of tumor suppressor proteins; breast cancer type 1 susceptibility protein (BRCA1) by 8.4% at 12 h, breast cancer type 2 susceptibility protein (BRCA2) by 18.6% at 24 h, neurofibromin 1 (NF1, a GTPase-activating protein that negatively regulates RAS/MAPK pathway activity) by 6.3% at 12 h, ataxia telangiectasia caused by mutations (ATM, a serine/threonine protein kinase recruited and activated by DNA double-strand breaks) by 13.9% at 24 h, maspin (a mammary serine protease inhibitor, serpin superfamily) by 9.5% at 24 h, deleted in malignant brain tumors 1 protein (DMBT1, a glycoprotein that interacts between tumor cells and the immune system) by 18% at 24 h, methyl-CpG-binding domain protein 4 (MBD4, a DNA repair enzyme that removes mismatched U or T) by 6.7% at 12 h, p53 by 17.5% at 24 h, retinoblastoma protein (Rb1) by 9.8% at 48 h, but increased the expression of PTCH1 (Protein patched homolog 1, a suppressor of smoothened release, which signals cell proliferation) by 10.1% at 24 h. On the other hand, PTX increased the expression of oncogenic proteins; carcinoembryonic antigen (CEA) by 9.6% at 12 h, 14-3-3 θ proteins (a phosphoserine binding protein that regulates Cdc25C) by 10.9% at 48 h, survivin (a negative regulator of apoptosis) by 11.9% at 48 h, mucin 4 (an anti-adhesive glycoprotein that contributes to tumor development and metastasis) by 15.6% at 24 h, Yes-associated protein 1 (YAP1, a potent oncogene that binds to 14-3-3) by 10.3% at 12 h, but decreased the expression of mucin 1 (a glycoprotein with extensive O-linked glycosylation of its extracellular domain, oncogenic epithelial membrane antigen) by 21.2% at 48 h. the expression of phosphatase and tensin homolog (PTEN, tumor suppressor protein) and PIM1 (proto-oncogene serine/threonine-protein kinase) were only minimally affected by PTX (≤ 5%) (Figs. 15 A and B).

bioRxiv preprint doi: https://doi.org/10.1101/2021.12.13.472401; this version posted December 13, 2021. The copyright holder for this preprint (which was not certified by peer review) is the author/funder, who has granted bioRxiv a license to display the preprint in perpetuity. It is made available under aCC-BY 4.0 International license.

Effects of 10 µg/mL PTX on the expression of angiogenesis proteins

10 µg/mL PTX reduced the expression of major angiogenesis proteins in RAW 264.7 cells; angiogenin by 5.3% at 12 h, vascular endothelial growth factor A (VEGF-A) by 6.7% at 48 h), VEGF-D by 15.6% at 24 h, von Willebrand factor (vWF) by 7.7% at 12 h, Fms-related tyrosine kinase 4 (FLT4) by 12.4% at 48 h, lymphatic vessel endothelial hyaluronan receptor 1 (LYVE1) by 10.9% at 48 h, fibroblast growth factor-2 (FGF2) by 10.3% at 12 h, CD106 (vascular cell adhesion molecule-1 (VCAM-1) by 15.5% at 12 h, matrix metalloprotease-2 (MMP2), 14.9% at 24 h, MMP-10 (9.4% at 12 h), plasminogen activator inhibitor-1 (PAI1) by 8.7% at 12 h, tumor-specific endothelial marker 8 (TEM8) by 12.3% at 12 h, CD54 (intercellular adhesion molecule 1 (ICAM-1)) by 12.6% at 12 h, and CD56 (neural cell adhesion molecule (NCAM) versus the untreated controls, while it compensatory elevated the expression of wound healing-related proteins, VEGF-C [42] by 10.7% at 12 h, VEGFR2 [43] by 15.1% at 24 h, capillary morphogenesis protein 2 (CMG2) [44] by 13.5% at 12 h, plasminogen (cleavage of the serine proteinase plasminogen to form plasmin, proangiogenic proteinase) by 15.6% at 48 h, endothelin-1 (21-amino acid vasoconstricting peptides) [45] by 17.8% at 24 h, and CD44 (homing cell adhesion molecule (HCAM)) by 9.8% at 24 h. The expression of PDGF-A and CD31 (platelet endothelial cell adhesion molecule (PECAM-1)) were only minimally affected by PTX (≤ 5%) (Figs. 15 C and D).

Effects of 10 µg/mL PTX on the expression of osteogenesis proteins

10 µg/mL PTX-treated RAW 264.7 cells showed increase in the expression of osteogenesis proteins, that is, bone morphogenetic protein-2 (BMP2, 16.6% at 24 h), BMP3 (a negative regulator for bone density by antagonizing other BMPs) by 7.9% at 24 h, BMP4 by 21.3% at 24 h, BMPR1B (bone morphogenetic protein receptor type-1B) by 15.6% at 12 h, BMPR2 (bone morphogenetic protein receptor type 2) by 24.4% at 48 h,

bioRxiv preprint doi: https://doi.org/10.1101/2021.12.13.472401; this version posted December 13, 2021. The copyright holder for this preprint (which was not certified by peer review) is the author/funder, who has granted bioRxiv a license to display the preprint in perpetuity. It is made available under aCC-BY 4.0 International license.

781 osteocalcin by 8.2% at 24 h, osteopontin by 18.4% at 48 h, osteonectin by 14.3% at 12 h, mammalian
782 Runt-related transcription factor 2 (RUNX2, a key transcription factor associated with osteoblast
783 differentiation) by 21.3% at 24 h, osterix (a zinc finger-containing transcriptional activator for osteoblastic
784 differentiation) by 13.3% at 48 h, alkaline phosphatase (ALP) by 13.1% at 48 h, osteoprotegerin (OPG) by 16%
785 at 24 h, versican (abundant in the woven bone matrix) by 16.9% at 24 h, DMP1 by 19% at 24 h, SMAD4 by
786 14.9% AT 48 H, and activating transcription factor 4 (ATF4) by 8% at 24 h, while decreased the expression
787 of aggrecan (a large chondroitin sulfate proteoglycan) by 7.4% at 12 h, receptor activator of nuclear factor
788 kappa-B ligand (RANKL, a binding partner of OPG) by 6.6% at 12 h, TGF-β1 by 12.5% at 12 h, connective
789 tissue growth factor (CTGF, CCN2, a role in chondrogenesis and angiogenesis) by 17.7% at 12 h, cathepsin K
790 (a lysosomal cysteine protease involved in bone remodeling and resorption [46]) by 9.2% at 48 h, HSP90α/β
791 (a crucial regulator of vesicular transport of cellular proteins in osteoclasts [47]) by 16.1% at 24 h, and
792 sclerostin domain-containing protein 1 (SOSTDC1, a bone morphogenetic protein antagonist) by 7% at 24 h
793 (Figs. 15 E and F).
794
795 **Figure 15**. Expression of oncogenesis proteins (A and B), angiogenesis proteins (C and D), and osteogenesis
796 proteins (E and F) in 10 μg/mL PTX-treated RAW 264.7 cells as determined by IP-HPLC. Line graphs, A, C,
797 and E show protein expression on the same scale (%) versus culture time (12, 24, or 48 h), whereas the star plots
798 (B, D, and F) show the differential expression levels of the proteins at 12, 24, or 48 h after PTX treatment on the
799 appropriate scales (%). The thick black line, untreated controls (100%); the blue, yellow, and red dots show
800 differential protein levels after PTX administration for 12, 24, or 48 h, respectively.
801

802 **Global protein expressions in 10 μg/mL PTX-treated RAW 264.7 cells**
803

bioRxiv preprint doi: https://doi.org/10.1101/2021.12.13.472401; this version posted December 13, 2021. The copyright holder for this preprint (which was not certified by peer review) is the author/funder, who has granted bioRxiv a license to display the preprint in perpetuity. It is made available under aCC-BY 4.0 International license.

Fig. 16 presents the global protein expression changes in 150 representative proteins of 21 different protein signaling pathways as a star plot. 10 μg/mL PTX was found to affect the expression of proteins in different signaling pathways of RAW 264.7 cells, and regulated characteristic cellular functions. PTX increased cell proliferation by upregulating proliferation-activating proteins, Ki-67, PCNA, cyclin D2, and CDK4, and enhancing proliferation-related pathways; that is, cMyc/MAX/MAD network by upregulating cMyc and MAX, p53/Rb/E2F by upregulating E2F1 and downregulating p-Rb1, and Wnt/β-catenin signaling by upregulating Wnt1, APC, β-catenin, TCF1 and by downregulating snail. PTX decreased histone/DNA methylation by downregulating EZH2, DNMT1, and DMAP1 and upregulating KDM4D, increased histone acetylation by upregulating PCAF and downregulating HDAC-10, and also enhanced protein translation by upregulating DOHH, DHS, and eIF5A1.

PTX was found to downregulate TGF-β1, TGF-β2, TGF-β3, SMAD2/3, HGFα, Met, but reactively upregulate SMAD4, while it stimulated RAS signaling by upregulating KRAS, HRAS, pAKT1/2/3, PI3K, Rab1, ERK1, and pERK1 and by downregulating JAK2, p-JNK1, and MEKK1, and simultaneously elevated NFkB signaling by upregulating NFkB, GADD45, p38, p-p38, and MDR, and downregulating p-mTOR and PGC1α.

PTX increased the expression of acute inflammatory proteins (TNFα, IL-1, IL-6, granzyme B, MCP1, CXCR4, CTLA4, M-CSF, and MMP1), cell-mediated immunity proteins (CD4, CD8, CD80, HLA-DR, and perforin), and innate immunity proteins (lactoferrin, versican [48], TLR3, and TLR4).

PTX diminished p53-mediated apoptosis by downregulating p53, BAD, NOXA, APAF1, caspase 9, c-caspase 9, and c-PARP in RAW 264.7 cells, whereas it enhanced FAS-mediated apoptosis by upregulating FAS, FADD, caspase 7, c-caspase 8, c-caspase 10, caspase 3, and c-caspase 3. On the other hand, PTX activated cell protection by increasing the expression of HSP70, SOD1, GSTO1/2, SVCT2, NRF2, and NOS1 [49], and stimulated cell survival and homeostasis by upregulating PLCβ2, SP1, and downregulating TERT, SIRT1, SP3, AMPKα, and PGC1α. Particularly, PTX attenuated ER-stress by downregulating HSP27, IRE1α, eIF2AK3, p-eIF2α, ATF6α, p-GADD153, caveolin-1, AIF, BIP, and upregulating LC3β.

PTX stimulated SHH/PTCH signaling by upregulating SHH and PTCH1, but reduced the expression of GLI1, and subsequently attenuated Notch/Jagged signaling by downregulating Notch1 and Jagged2. PTX-treated RAW 264.7 cells appeared to be differentiated into mature macrophages by upregulation of α-actin, VE-cadherin, CaM, TGase 2, PKC, p-PKC1α, AP1M1, FAK, AND AKAP13, and showed a characteristics of neuromuscular differentiation by upregulating NSE-γ, GFAP, MYH2, and desmin.

bioRxiv preprint doi: https://doi.org/10.1101/2021.12.13.472401; this version posted December 13, 2021. The copyright holder for this preprint (which was not certified by peer review) is the author/funder, who has granted bioRxiv a license to display the preprint in perpetuity. It is made available under aCC-BY 4.0 International license.

834 PTX was found to have anti-fibrosis effect on RAW 264.7 cells by downregulating FGF2, CTGF,
835 collagen 3A1, laminin α5, and α1-antitrypsin. And PTX-treated cells showed a state of oncogenic stress by
836 upregulating surviving, YAP1, CEA, and 14-3-3θ, and downregulating ATM, BRCA2, MBD4, and DMBT1.
837 PTX affected the expression of angiogenesis proteins in RAW 264.7 cells positively or negatively, that is,
838 angiogenin, VEGF-A, vWF, and CD106 (VCAM-1) were downregulated by 10 μg/mL PTX, while HIF1α,
839 CMG2, VEGF-C, VEGFR2, and p-VEGFR2 were upregulated. On the other hand, PTX consistently
840 increased the expression of osteogenesis proteins, BMP-2, BMPR1B, osterix, RUNX2, osteocalcin,
841 osteonectin, versican, and ALP, but decreased RANKL expression (Fig. 16).
842

843 **Figure 16.** Star plot of global protein expression in RAW 264.7 cells treated with 10 μg/mL PTX. The
844 representative proteins (n=150) were selected and their maximum or minimum expression levels (%) were
845 plotted in a circular manner. 21 major signaling pathways showed different levels of protein expression. 10
846 μg/mL PTX activated the growth factors, epigenetic modification, protein translation, RAS and NFkB
847 signaling, protection, neuromuscular ad osteoblastic differentiation, acute inflammation associated with innate
848 immunity and cell-mediated immunity, but inactivated ER stress, fibrosis, and chronic inflammation.
849 FAS-mediated apoptosis was enhanced contrary to p53-mediated apoptosis. Also noted that the upregulation
850 of oncogenic proteins and the downregulation of tumor suppressor proteins. Red circle: maximum expression
851 of upregulated proteins. Blue circle: minimum expression of downregulated proteins

852

853 Comparison between 10 μg/mL and 300 μg/mL PTX application
854 in RWA 264.7 cells

855

856 Proliferation-related protein expression by 10 μg/mL and 300 μg/mL PTX

857 300 μg/mL PTX reduced the expression of proliferation-related proteins in RAW 264.7 cells compared
858 to 10 μg/mL PTX, that is, Ki-67 by 8.5% at 48 h, CDK4 by 9.9% at 12 h, cyclin D2 by 16.6% at 12 h, E2F1
859 by 14.8% at 24 h, cMyc by 6.4% at 12 h, MAX by 5.1% at 12 h, and MAD1 by 8.6% at 48 h, but increased
860 the expression of p-Rb1 by 2.7% at 24 h. 10 μg/mL PTX stimulated the proliferation of RAW 264.7 cells by

bioRxiv preprint doi: https://doi.org/10.1101/2021.12.13.472401; this version posted December 13, 2021. The copyright holder for this preprint (which was not certified by peer review) is the author/funder, who has granted bioRxiv a license to display the preprint in perpetuity. It is made available under aCC-BY 4.0 International license.

upregulating Ki-67, CDK4, cyclin D2, E2F1, cMyc, MAX, and downregulating p-Rb1, while 10 µg/mL PTX showed anti-proliferative effect on RAW 264.7 cells by downregulating Ki-67, cyclin D2, E2F1, and MAX compared to the untreated controls (Figs. 17 A and B).

RAS/NFkB signaling protein expression by 10 µg/mL and 300 µg/mL PTX

300 µg/mL PTX reduced the expression of RAS/NFkB signaling proteins in RAW 264.7 cells compared to 10 µg/mL PTX, that is, KRAS by 11.3% at 12 h, pAKT1/2/3 by 11.3% at 12 h, p-ERK1 by 14.7% at 24 h, NFkB by 15.4% at 24 h, p-p38 by 6.9% at 24 h, GADD153 by 10.8% at 48 h, and p-PKC1α by 5.8% at 24 h. However, the expression of pAKT1/2/3 and p-PKC1α by 300 µg/mL PTX were increased to 102% at 48h and 106.9% at 12 h, respectively, compared to those by 10 µg/mL PTX. 10 µg/mL PTX enhanced RAS/NFkB signaling by upregulating KRAS, pAKT1/2/3, p-ERK1, NFkB, p-p38, GADD153, and p-PKC1α compared to the untreated controls, while 300 µg/mL PTX attenuated RAS/NFkB signaling by downregulating pAKT1/2/3, p-ERK1, NFkB, p-p38, and GADD153 (Figs. 17 C and D).

Inflammatory protein expression by 10 µg/mL and 300 µg/mL PTX

300 µg/mL PTX markedly decreased the expression of inflammation-associated proteins in RAW 264.7 cells compared to 10 µg/mL PTX, that is, TNFα by 11% at 12 h, CD4 by 21.8% at 24 h, CD80 by 6.9% at 24 h, M-CSF by 15% at 48 h, CXCR4 by 7.1% at 24 h, MMP1 by 19.3% at 48 h, and lactoferrin by 15.7% at 24 h, but increased the expression of an inflammation suppressor TGF-β1 by 23.5% at 48 h. It was evident 10 µg/mL PTX stimulated the inflammatory reaction of RAW 264.7 cells by upregulating TNFα, IL-6, CD4, CD80, M-CSF, CXCR4,MMP1, lactoferrin, and downregulating TGF-β1 compared to the untreated controls,

bioRxiv preprint doi: https://doi.org/10.1101/2021.12.13.472401; this version posted December 13, 2021. The copyright holder for this preprint (which was not certified by peer review) is the author/funder, who has granted bioRxiv a license to display the preprint in perpetuity. It is made available under aCC-BY 4.0 International license.

while 300 μg/mL PTX showed anti-inflammatory effect on cells by downregulating TNFα, IL-6, CD4, M-CSF, MMP1, lactoferrin, and upregulating TGF-β1 (Figs. 17 E and F).

Apoptosis protein expression by 10 μg/mL and 300 μg/mL PTX

300 μg/mL PTX was found to have different effect on the expression of oncogenesis proteins in RAW 264.7 cells from 10 μg/mL PTX. The expressions of tumor suppressor protein p53, anti-apoptotic protein BCL2, apoptosis trigger FASL, and TGF-β1 by 300 μg/mL PTX were higher by 7.9% at 24 h, 13.3% at 48 h, 5.5% at 24 h, and 23.5% at 48 h, respectively, than those by 10 μg/mL PTX, while the expressions of FAS-associated protein with death domain (FADD), apoptosis executors c-caspase 8 and c-caspase 3 by 300 μg/mL PTX were lower by 7.3% at 12 h, 9.9% at 24 h, and 13.3% at 48 h, respectively, than those by 10 μg/mL PTX. 10 μg/mL PTX induced significant apoptosis effect on RAW 264.7 cells through FAS-mediated apoptosis by upregulating FAS, FADD, c-caspase 8, and c-caspase 3 compared to the untreated controls, while 300 μg/mL PTX slightly reduced the apoptosis effect by downregulating FADD, c-caspase 8, and c-caspase 3 compared to PTX (Figs. 17 G and H).

Figure 17. IP-HPLC comparison between the protein expression of 10 μg/mL and 300 μg/mL PTX-treated RAW 264.7 cells. Expression of proliferation-related proteins (A and B), RAS/NFkB signaling proteins (C and D), inflammatory proteins (E and F), and apoptosis proteins (G and H) as determined by IP-HPLC. Line graphs, A, C, E, and G show 10 μg/mL PTX-induced protein expressions, whereas B, D, F, H show 300 μg/mL PTX-induced protein expressions on the same scale (%) versus culture time (12, 24, or 48 h).

ER stress protein expression by 10 μg/mL and 300 μg/mL PTX

bioRxiv preprint doi: https://doi.org/10.1101/2021.12.13.472401; this version posted December 13, 2021. The copyright holder for this preprint (which was not certified by peer review) is the author/funder, who has granted bioRxiv a license to display the preprint in perpetuity. It is made available under aCC-BY 4.0 International license.

300 μg/mL PTX increased the expression of ER stress proteins in RAW 264.7 cells compared to 10 μg/mL PTX, that is, eIF2AK3 (PERK) by 14.9% at 12 h, p-eIF2α by 12.8% at 48 h, ATF6α by 13.7% at 48 h, BIP by 10.3% at 12 h. and IRE1α by 3.3% at 24 h. And 300 μg/mL PTX minimally affected the expression of GADD153 (CHOP) compared to 10 μg/mL PTX. It was found that 10 μg/mL PTX reduced ER stress by downregulating eIF2AK3, p-eIF2α, ATF6α, BIP, and IRE1α, while 100 μg/mL PTX alleviated the reduction of ER stress by upregulating eIF2AK3, p-eIF2α, ATF6α, and BIP compared to 10 μg/mL PTX, particularly, the expression of eIF2AK3, p-eIF2α, ATF6α, and BIP were increased by 300 μg/mL PTX to 106% at 48 h, 106.4% at 48 h, 105.8% at 48 h, an 104.4% at 24 h, respectively, versus the untreated controls (Figs. 18 A and B).

Fibrosis protein expression by 10 μg/mL and 300 μg/mL PTX

300 μg/mL PTX increased the expression of fibrosis proteins in RAW 264.7 cells compared to 10 μg/mL PTX, that is, FGF1 by 7.1% at 24 h, FGF2 by 8.3% at 12 h, CTGF by 15.6% at 12 h, collagen 3A1 by 29.1% at 24 h, laminin α5 by 28% at 48 h, and α1-antitrypsin by 21.6% at 24 h. 10 μg/mL PTX showed potent anti-fibrosis effect on RAW 264.7 cells by downregulating FGF1, FGF2, CTGF, collagen 3A1 and 5A, laminin α5, and α1-antitrypsin, while 300 μg/mL PTX showed no anti-fibrosis effect rather increased the expression of FGF1 (by 6.4% at 48 h), collagen 3A1 (14% at 24 h), collage 5A (4.6% at 24 h), and laminin α5 (9.8% at 48 h) compared to the untreated controls (Figs. 18 C and D).

Neuromuscular differentiation protein expression by 10 μg/mL and 300 μg/mL PTX

300 μg/mL PTX decreased the expression of neuromuscular differentiation proteins in RAW 264.7 cells compared to 10 μg/mL PTX, that is, NSEγ by 7.6% at 48 h, GFAP by 5.2% at 12 h, MYH2 by 18.1% at 24 h,

bioRxiv preprint doi: https://doi.org/10.1101/2021.12.13.472401; this version posted December 13, 2021. The copyright holder for this preprint (which was not certified by peer review) is the author/funder, who has granted bioRxiv a license to display the preprint in perpetuity. It is made available under aCC-BY 4.0 International license.

desmin by 8.5% at 24 h, and α-SMA by 21.5% at 12 h, but the expression of myosin 1a (membrane binding class I myosin) was increased by 11.3% at 12 h. 10 μg/mL PTX induced nerve differentiation by upregulating NSEγ and GFAP, and muscle differentiation by upregulating MYH2 (skeletal muscle heavy chain 2), desmin, and α-SMA, while 300 μg/mL PTX only slightly increased the expression of NSEγ, GFAP, MYH2, desmin and α-SMA compared to the untreated controls (Figs. 18 E and F).

Osteogenesis protein expression by 10 μg/mL and 300 μg/mL PTX

300 μg/mL PTX decreased the expression of osteogenesis proteins in RAW 264.7 cells compared to 10 μg/mL PTX, that is, BMP2 by 25.8% at 48 h, RUNX2 by 27.7% at 12 h, osterix by 8.7% at 24 h, osteocalcin by 5.2% at 24 h, osteopontin by 11.3% at 48 h, and osteonectin by 9.4% at 24 h. However, the expression ratios of OPG and RANKL, which are essential signaling molecules of RANKL/RANK/OPG system regulating osteoclast differentiation/activation and calcium release from the skeleton, were increased by 6.6% and 9.6% at 12 h, respectively. It was found 10 μg/mL PTX showed strong osteogenic effect on RAW 264.7 cells by upregulating BMP2, RUNX2, osterix, osteocalcin, osteopontin, osteonectin, and OPG, while 300 μg/mL PTX alleviated the osteogenic effect by downregulating RUNX2, BMP2, and osteocalcin compared to the untreated controls (Figs. 18 G and H).

Figure 18. IP-HPLC comparison between the protein expression of 10 μg/mL and 300 μg/mL PTX-treated RAW 264.7 cells. Expression of ER stress proteins (A and B) fibrosis proteins (C and D), neuromuscular differentiation proteins (E and F) and osteogenesis proteins (G and H) as determined by IP-HPLC. Line graphs, A, C, E, and G show 10 μg/mL PTX-induced protein expressions, whereas B, D, F, H show 300 μg/mL PTX-induced protein expressions on the same scale (%) versus culture time (12, 24, or 48 h).

bioRxiv preprint doi: https://doi.org/10.1101/2021.12.13.472401; this version posted December 13, 2021. The copyright holder for this preprint (which was not certified by peer review) is the author/funder, who has granted bioRxiv a license to display the preprint in perpetuity. It is made available under aCC-BY 4.0 International license.

Discussion

The pharmacological effect of PTX was frequently investigated in different cell types including RAW 264.7 cells [19-22] and animals [50-53] by using higher dose PTX, 100 – 500 μg/mL, rather than the therapeutic dose in human (about 10 μg/mL). It was also reported that the low dose PTX, 10, 25, 50 mg/kg, led to an increase in the expression of caspase 3 and TNFα in the rat hippocampus following lipopolysaccharide (LPS)-induced inflammation [54]. And the TNFα production by lipopolysaccharide (LPS)-stimulated human alveolar macrophages was significantly suppressed in the presence of PTX at concentration of 2 mM and 1 mM (278.3 μg/mL), but not at 0.5 mM, 0.1mM (27.8 μg/mL), and 0.01 mM, while production of IL-1β, IL-6, and GM-CSF remained unaffected. These data indicate PTX showed anti-inflammatory effect selectively depending on its concentration [55].

In the present study, RAW 264.7 cells, which are originally murine monocytes, were explored for PTX-induced protein expression changes by administrating with two different doses, 10 μg/mL PTX similar to the therapeutic dose in human, and 300 μg/mL PTX which was frequently used in cell and animal experiments. First of all, the 10 μg/mL PTX-induced effect was compared with the 300 μg/mL PTX-induced effect. However, in clinical application, even the therapeutic dose PTX, about 10 μg/mL, produces diverse side effects including belching, bloating, stomach discomfort or upset, nausea, vomiting, indigestion, dizziness, flushing, angina, palpitations, hypersensitivity, itchiness, rash, hives, bleeding, hallucinations, arrhythmias, and aseptic meningitis [56, 57]. Therefore, it is thought that the low dose 10 μg/mL PTX-induced protein expression may be more informative to know the real pharmacological effect of PTX in human than the high dose 300 μg/mL PTX-induced protein expression in cell culture. Therefore, in the present study, 10 μg/mL PTX-induced effect on cells was more extensively investigated than 300 μg/mL PTX-induced effect.

bioRxiv preprint doi: https://doi.org/10.1101/2021.12.13.472401; this version posted December 13, 2021. The copyright holder for this preprint (which was not certified by peer review) is the author/funder, who has granted bioRxiv a license to display the preprint in perpetuity. It is made available under aCC-BY 4.0 International license.

In the global protein expression of RAW 264.7 cells by 10 μg/mL PTX, a competitive non-selective phosphodiesterase inhibitor which is known to raise intracellular cAMP and activate PKA, actually enhanced RAS signaling by upregulating AKAP13, pAKT1/2/3, PKC, p-PKC1α, KRAS, and HRAS, and subsequently activated histone/DNA demethylation and acetylation by upregulating KDMD4 and PCAF, and downregulating HDAC10, MBD4, DMAP1, DNMT1 and EZH2, and subsequently induced cellular proliferation by upregulating cMyc/MAX/MAD network proteins, Wnt/β-catenin signaling objective protein TCF1, proliferation activating proteins Ki-67, PCNA, PLK4, cyclin D2, and cdc25A in this study. On the other hand, the expression of CDK inhibitors, p14, p15/16, and p21 were compensatory upregulated. The double IP-HPLC to assess the amount of protein complex containing two different target proteins showed the increase of cMyc-MAX heterodimer and β-catenin-TCF1 complex which led to cell cycle progression [58], and the decrease of cMyc-MAD1 heterodimer and CDK4-p27 complex concomitantly. On the other hand, the double IP-HPLC also revealed the increase of E2F1-Rb1 and CDK4-p21 complexes, which mitigated cell cycle progression [59].

Although the expression of cMyc and MAX were decreased by 10 μg/mL PTX at 12, 24, and 48 h, the expression of MAD1 was increased in western blot and IP-HPLC, and the double IP-HPLC showed dominant increase of cMyc-MAX heterodimer and decrease of cMyc-MAD heterodimer versus the untreated controls. Therefore, it is suggested that cMyc and MAX are competitively utilized to form cMyc-MAX heterodimer against cMyc-MAD heterodimer at 12, 24, and 48 h after 10 μg/mL PTX treatment, and then the unbound cMyc and MAX are gradually reduced in amount as detected in western blot (Fig. 5) and IP-HPLC. And more, although the expression of E2F1 was increased by 10 μg/mL PTX at 12, 24, and 48 h, the phosphorylated Rb1 (p-Rb1) was decreased, and both E2F1-Rb1 and CDK4-p21 complexes were increased in double IP-HPLC.

bioRxiv preprint doi: https://doi.org/10.1101/2021.12.13.472401; this version posted December 13, 2021. The copyright holder for this preprint (which was not certified by peer review) is the author/funder, who has granted bioRxiv a license to display the preprint in perpetuity. It is made available under aCC-BY 4.0 International license.

993 Therefore, it is suggested p53/Rb/E2F signaling rarely exerts to enhance cell proliferation in 10 μg/mL
994 PTX-treated RAW 264.7 cells.

995 Cell counting assay of 10 μg/mL PTX-treated cells showed the increase of cell number at 12, 24, and 48
996 h. And regarding some proliferation-related proteins, ICC revealed strong positive reaction of Ki-67 at 12, 24,
997 and 48 h compared to the untreated controls, and western blot showed strong bands of Ki-67, E2F1, Wnt1,
998 and TCF1 at 12, 24, and 48 h. Taken together, it is evident that 10 μg/mL PTX enhances RAS signaling, and
999 subsequently activates histone/DNA demethylation and acetylation, cMyc/MAX/MAD network, and
1000 Wnt/β-catenin signaling, and resulted in the proliferation of RAW 264.7 cells. Whereas 300 μg/mL PTX
1001 showed a trend to decrease the expression of proliferation-related proteins, Ki-67, cMyx, MAX, p-Rb1, E2F1,
1002 and cyclin D2 compared to 10 μg/mL PTX.

1003 The non-selective phosphodiesterase inhibitor, PTX specifically induced RAS signaling, and
1004 subsequently stimulated NFkB signal by upregulating PKC, p-PKC-1α, AKAP13, MDR, GADD45, p38, and
1005 p-p38, and eventually influenced on the expression of protection-, ER stress-, apoptosis-, and inflammatory
1006 proteins in RAW 264.7 cells. Regarding cellular protection, 10 μg/mL PTX upregulated antioxidant proteins,
1007 SOD1, GSTO1/2, and SVCT2, but downregulated NRF2 regulating antioxidant expression, PGC-1α
1008 regulating mitochondrial biogenesis, and AMPK1α that plays a role in cellular energy homeostasis. And 10
1009 μg/mL PTX mitigated ER stress by downregulating eIF2AK3, p-eIF2AK3, eIF2α, p-eIF2α, GADD153,
1010 p-GADD153, BIP, IRE1α, and ATF6α. Therefore, it is suggested that 10 μg/mL PTX-treated in RAW 264.7
1011 cells are relatively safe under control of cellular protection and homeostasis. And more, the 10 μg/mL
1012 PTX-induced RAS signal by cAMP accumulation activated epigenetic modification through histone/DNA
1013 demethylation or acetylation, and subsequently elevated protein translation, which eventually positively
1014 influenced on cell proliferation, differentiation, protection and survival of RAW 264.7 cells.

bioRxiv preprint doi: https://doi.org/10.1101/2021.12.13.472401; this version posted December 13, 2021. The copyright holder for this preprint (which was not certified by peer review) is the author/funder, who has granted bioRxiv a license to display the preprint in perpetuity. It is made available under aCC-BY 4.0 International license.

10 μg/mL PTX-induced NFkB signal also influenced on the expression of inflammatory protein positively or negatively in RAW 264.7 cells. It was found some acute inflammatory proteins (TNFα, IL-1, IL-6, MCP1, CXCR4, granzyme B, and MMP1), innate immunity proteins (β-defensin 1, lactoferrin, versican, TLR 3 and 4), and cell-mediated immunity proteins (CD4, CD8, CD80, HLA-DR, perforin, and CTLA4) were upregulated, while some chronic inflammatory proteins including IL-12, CD68, CD106, lysozyme, cathepsin C and G, COX2, and α1-antitrypsin were downregulated. Therefore, it is suggested 10 μg/mL PTX-treated cells are tend to differentiate into M1 type macrophages, which are pro-inflammatory type and important for phagocytosis and secretion of pro-inflammatory cytokines and microbicidal molecules to defend against pathogens, such as bacteria, virus [60-62], etc. This activation of M1 type macrophage polarization after 10 μg/mL PTX treatment was correlated with the increase of FAS-mediated apoptosis contrary to p53-mediated apoptosis in RAW 264.7 cells.

On the other hand, 300 μg/mL PTX consistently decreased the expression of inflammatory proteins, TNFα, IL-6, CD4, CD80, M-CSF, CXCR4, MMP1, and lactoferrin but compensatory increased the expression of anti-inflammatory protein TGF-β1 compared to 10 μg/mL PTX. And 300 μg/mL PTX increased the expression of anti-apoptosis protein, BCL2, but minimally affected the expression of tumor suppressor protein, p53, compared to 10 μg/mL PTX, whereas the apoptosis triggering TNF family protein, FASL, and the initiator caspase, c-caspase 8 were more upregulated by 300 μg/mL PTX than 10 μg/mL PTX. Therefore, it is suggested 300 μg/mL PTX-treated cells showed anti-inflammatory effect and FAS-mediated apoptosis.

The 10 μg/mL PTX-treated RAW 264.7 cells showed crosstalk between activated RAS and NFkB signalings, and were progressed into cytodifferentiation by upregulating some growth factors and SHH/PTCH signaling. Particularly, it is evident that the 10 μg/mL PTX-treated RAW 264.7 cells have potentials of neuromuscular and osteoblastic differentiation, which are able to influence on objective adjacent cells [63-65].

bioRxiv preprint doi: https://doi.org/10.1101/2021.12.13.472401; this version posted December 13, 2021. The copyright holder for this preprint (which was not certified by peer review) is the author/funder, who has granted bioRxiv a license to display the preprint in perpetuity. It is made available under aCC-BY 4.0 International license.

1037 The active neuromuscular and osteoblastic differentiations were also observed in ICC and western blot in this
1038 study. On the other hand, regarding the expression of osteogenesis proteins, 300 μg/mL PTX downregulated
1039 the osteoblastic differentiation proteins, BMP2, RUNX2, osterix, osteocalcin, osteopontin, and osteonectin,
1040 but upregulated the osteoclastic differentiation protein, RANKL, and compensatory increased the expression
1041 of OPG compared to 10 μg/mL PTX.

1042 In the present study, 300 μg/mL PTX consistently decreased the expression of proliferation-, RAS/NFkB
1043 signaling-, inflammation-, and osteogenesis proteins but apoptosis proteins compared to 10 μg/mL PTX,
1044 therefore, it is thought that the high dose 300 μg/mL PTX may somehow disturb the protein expressions and
1045 give a harmful effect on RAW 264.7 cells, and resulted in the increase of FAS-mediated apoptosis, whereas
1046 the low dose 10 μg/mL PTX showed characteristic protein expression of competitive
1047 non-selective phosphodiesterase inhibitor, which may be helpful for the investigation of PTX pharmacological
1048 effect in human.

1049 Contrary to the neuromuscular and osteoblastic differentiation in PTX-treated RAW 264.7 cells, 10
1050 μg/mL PTX suppressed fibroblastic differentiation and attenuated collagen production by downregulating the
1051 fibrosis-inducing proteins, FGF1, FGF2, TGF-β1, CTGF, collagen 3A1, 4, and 5, laminin α5, integrin β1,
1052 α1-antitrypsin, and upregulating the fibrosis-inhibiting proteins, plasminogen, CMG2, integrin α2 and α5. On
1053 the other hand, 10 μg/mL PTX increased the expression of endothelin-1 having a key role of vascular
1054 homeostasis. In the global expression of 10 μg/mL PTX-treated RAW 264.7 cells, the anti-fibrotic protein
1055 expression is closely relevant to the reduction of chronic inflammation-associated M2 macrophage
1056 polarization by downregulating CD68, CD106, lysozyme, MMP9, and α1-antitrypsin, and the low level of
1057 ROS damage and ER stress after 10 μg/mL PTX treatment. Therefore, it is suggested that 10 μg/mL PTX
1058 inhibits M2 type macrophage polarization through RAS/NFkB/TNFα signaling [66], and reduces ER stress

bioRxiv preprint doi: https://doi.org/10.1101/2021.12.13.472401; this version posted December 13, 2021. The copyright holder for this preprint (which was not certified by peer review) is the author/funder, who has granted bioRxiv a license to display the preprint in perpetuity. It is made available under aCC-BY 4.0 International license.

1059 through eIF2α/eIF2AK3/GADD153/ATF6 signaling, which negatively regulates the growth factors, TGF-β1,
1060 β2, β3, FGF1, FGF2, and CTGF, and extracellular matrix-associated proteins, collagen-3A1, -4, -5A, laminin
1061 α5, integrin β1, plasminogen, PAI-1, α1-antitrypsin, and elafin, and eventually resulted in anti-fibrotic effect
1062 on RAW 264.7 cells.

1063 10 μg/mL PTX reduced the expression of many angiogenic proteins, angiogenin, VEGF-A, VEGF-D,
1064 vWF, FLT-4, LYVE-1, FGF-2, CD1056 (VCAM-1), MMP-2, MMP-10, PAI-1, CD54, and CD56, but
1065 upregulated some angiogenic proteins responsible for wound and damage, that is, HIF-1α, VEGF-C, VEGFR2,
1066 CMG2, plasminogen, endothelin-1, and CD44. These results indicate 10 μg/mL PTX primarily inhibited
1067 angiogenesis but secondarily maintained *de novo* angiogenesis for wound healing [67].

1068 In addition, 10 μg/mL PTX was found to increase the potential of oncogenesis by upregulating the
1069 oncogenic proteins, CEA, 14-3-3θ, survivin, mucin 4, and YAP1, and downregulating the tumor suppressor
1070 proteins, P53, Rb1, BRCA1, BRCA2, NF1, ATM, maspin, and DMBT1. Nevertheless, 10 μg/mL PTX did not
1071 increase the expression of DNA repair enzymes, MBD4 and PARP-1, and exogenous stress responsible
1072 proteins, JNK1 and JAK2, but showed the overexpression of antioxidant proteins, SOD1 and GSTO1/2, and
1073 cell protection proteins, HSP70, sirtuin 6, and leptin, and resulted in the attenuation of ER stress. Therefore, it
1074 is suggested that 10 μg/mL PTX does not exert oncogenesis in RAW 264.7 cells, but maintains the cellular
1075 homeostasis, even though there appears slight elevation of oncogenic protein expression.

1076 The 10 μg/mL PTX-induced protein expression changes of different signaling pathways were
1077 summarized in a diagram of Fig. 19. The protein signaling diagram illustrated main axes of protein signaling
1078 pathways in cells based on IP-HPLC data obtained in this study, therefore, it may indicate the real status of
1079 phamarcological effect of PTX in RAW 264.7 cells. We thought this PTX-induced protein expression changes

bioRxiv preprint doi: https://doi.org/10.1101/2021.12.13.472401; this version posted December 13, 2021. The copyright holder for this preprint (which was not certified by peer review) is the author/funder, who has granted bioRxiv a license to display the preprint in perpetuity. It is made available under aCC-BY 4.0 International license.

of different signaling pathways should be corrected or added by further precise protein expression investigation using different cells and animals.

Figure 16. A diagram of 10 μg/mL PTX-induced protein expression change in global protein signaling pathways of RAW 264.7 cells. The main axis of cellular signaling, that is, proliferation, RAS signaling, NFkB signaling, and inflammation were consistently activated by 10 μg/mL PTX, followed by activation of epigenetic modification, protein translation, Wnt/β-catenin, cMyc/MAX/MAD network, neuromuscular and osteoblastic differentiation, acute inflammation, innate immunity, cell-mediated immunity, and FAS-mediated apoptosis, while inactivation of p53/Rb/E2F signaling, ER stress, angiogenesis, fibrosis, and chronic inflammation. Red letter: upregulated signaling and proteins. Blue letter: downregulated signaling and proteins.

Conclusions

PTX as a non-selective phosphodiesterase inhibitor showed different biological effect on RWA 264.7 cells depending on the concentration of low dose 10 μg/mL or high dose 300 μg/mL PTX. 10 μg/mL PTX enhanced a central protein expression pathways, RAS signaling, and subsequently induced proliferation, epigenetic activation, neuromuscular and osteoblastic differentiation, and stimulated acute inflammation, innate immunity, and cell mediated immunity, while reduced chronic inflammation, ER stress, and fibrosis but reactively increased FAS-mediated apoptosis and oncogenic potential in RAW 264.7 cells. On the other hand, 300 μg/mL PTX was found to decrease RAS/NFkB signaling compared to 10 μg/mL PTX, and subsequently attenuated proliferation, epigenetic activation, inflammation, neuromuscular and osteoblastic differentiation but increased apoptosis and fibrosis.

bioRxiv preprint doi: https://doi.org/10.1101/2021.12.13.472401; this version posted December 13, 2021. The copyright holder for this preprint (which was not certified by peer review) is the author/funder, who has granted bioRxiv a license to display the preprint in perpetuity. It is made available under aCC-BY 4.0 International license.

Acknowledgments

We express our gratitude to the late Professor Je Geun Chi who encouraged us to perform IP-HPLC, and to the late Dr. Soo Il Chung who taught us the biological usefulness of IP-HPLC.

Conflicts of Interest

The authors declare no conflict of interest.

Author Contributions

M.H. Seo contributed to the conception and design of the study, data acquisition, analysis and interpretation and drafted and critically revised the manuscript: D.W. Kim and Y.S. Kim contributed to the data acquisition, analysis and interpretation: S.K. Lee contributed to the study design and interpretation and critically reviewed the manuscript. All authors approved the manuscript and agreed to be accountable for all aspects of the work.

References

1. Angelides NS. Continuous infusion treatment with pentoxifylline in patients with severe peripheral vascular occlusive disease. Angiology. 1986;37(8):555-64. http://www.ncbi.nlm.nih.gov/pubmed/3740545 Epub 1986/08/01.
2. Roekaerts F, Deleers L. Trental 400 in the treatment of intermittent claudication: results of long-term, placebo-controlled administration. Angiology. 1984;35(7):396-406. http://www.ncbi.nlm.nih.gov/pubmed/6380348 Epub 1984/07/01.
3. Arcaro CA, Assis RP, Zanon NM, Paula-Gomes S, Navegantes LCC, Kettelhut IC, et al. Involvement of cAMP/EPAC/Akt signaling in the antiproteolytic effects of pentoxifylline on skeletal muscles of diabetic rats. J Appl Physiol (1985). 2018;124(3):704-16. http://www.ncbi.nlm.nih.gov/pubmed/29357512 Epub 2018/01/24.
4. Lin SL, Chen RH, Chen YM, Chiang WC, Tsai TJ, Hsieh BS. Pentoxifylline inhibits platelet-derived growth factor-stimulated cyclin D1 expression in mesangial cells by blocking Akt membrane translocation. Molecular pharmacology. 2003;64(4):811-22. http://www.ncbi.nlm.nih.gov/pubmed/14500737 Epub 2003/09/23.

bioRxiv preprint doi: https://doi.org/10.1101/2021.12.13.472401; this version posted December 13, 2021. The copyright holder for this preprint (which was not certified by peer review) is the author/funder, who has granted bioRxiv a license to display the preprint in perpetuity. It is made available under aCC-BY 4.0 International license.

5. Luo M, Dong L, Li J, Wang Y, Shang B. Protective effects of pentoxifylline on acute liver injury induced by thioacetamide in rats. International journal of clinical and experimental pathology. 2015;8(8):8990-6. http://www.ncbi.nlm.nih.gov/pubmed/26464641 Epub 2015/10/16.

6. Speer EM, Dowling DJ, Ozog LS, Xu J, Yang J, Kennady G, et al. Pentoxifylline inhibits TLR- and inflammasome-mediated in vitro inflammatory cytokine production in human blood with greater efficacy and potency in newborns. Pediatric research. 2017;81(5):806-16. http://www.ncbi.nlm.nih.gov/pubmed/28072760 Epub 2017/01/11.

7. Speer EM, Dowling DJ, Xu J, Ozog LS, Mathew JA, Chander A, et al. Pentoxifylline, dexamethasone and azithromycin demonstrate distinct age-dependent and synergistic inhibition of TLR- and inflammasome-mediated cytokine production in human newborn and adult blood in vitro. PloS one. 2018;13(5):e0196352. http://www.ncbi.nlm.nih.gov/pubmed/29715306 Epub 2018/05/02.

8. Zhang J, Tao X, Xie J, Xiang M, Fu W. Prophylactic anti-inflammation inhibits cigarette smoke-induced emphysema in guinea pigs. Journal of Huazhong University of Science and Technology Medical sciences = Hua zhong ke ji da xue xue bao Yi xue Ying De wen ban = Huazhong keji daxue xuebao Yixue Yingdewen ban. 2003;23(4):365-8. http://www.ncbi.nlm.nih.gov/pubmed/15015637 Epub 2004/03/16.

9. Lee JG, Shim S, Kim MJ, Myung JK, Jang WS, Bae CH, et al. Pentoxifylline Regulates Plasminogen Activator Inhibitor-1 Expression and Protein Kinase A Phosphorylation in Radiation-Induced Lung Fibrosis. BioMed research international. 2017;2017:1279280. http://www.ncbi.nlm.nih.gov/pubmed/28337441 Epub 2017/03/25.

10. Kaidar-Person O, Marks LB, Jones EL. Pentoxifylline and vitamin E for treatment or prevention of radiation-induced fibrosis in patients with breast cancer. The breast journal. 2018;24(5):816-9. http://www.ncbi.nlm.nih.gov/pubmed/29687536 Epub 2018/04/25.

11. Chiao TB, Lee AJ. Role of pentoxifylline and vitamin E in attenuation of radiation-induced fibrosis. The Annals of pharmacotherapy. 2005;39(3):516-22. http://www.ncbi.nlm.nih.gov/pubmed/15701781 Epub 2005/02/11.

12. Yalcin-Ulker GM, Cumbul A, Duygu-Capar G, Uslu U, Sencift K. Preventive Effect of Phosphodiesterase Inhibitor Pentoxifylline Against Medication-Related Osteonecrosis of the Jaw: An Animal Study. Journal of oral and maxillofacial surgery : official journal of the American Association of Oral and Maxillofacial Surgeons. 2017;75(11):2354-68. http://www.ncbi.nlm.nih.gov/pubmed/28529150 Epub 2017/05/23.

13. Kim JH, Shin BC, Park WS, Lee J, Kuh HJ. Antifibrotic effects of pentoxifylline improve the efficacy of gemcitabine in human pancreatic tumor xenografts. Cancer science. 2017;108(12):2470-7. http://www.ncbi.nlm.nih.gov/pubmed/28940685 Epub 2017/09/25.

14. Nidhyanandan S, Thippeswamy BS, Chandrasekhar KB, Reddy ND, Kulkarni NM, Karthikeyan K, et al. Enhanced anticancer efficacy of histone deacetyl inhibitor, suberoylanilide hydroxamic acid, in combination with a phosphodiesterase inhibitor, pentoxifylline, in human cancer cell lines and in-vivo tumor xenografts. Anti-cancer drugs. 2017;28(9):1002-17. http://www.ncbi.nlm.nih.gov/pubmed/28727579 Epub 2017/07/21.

15. Golunski G, Woziwodzka A, Piosik J. Potential Use of Pentoxifylline in Cancer Therapy. Current pharmaceutical biotechnology. 2018;19(3):206-16. http://www.ncbi.nlm.nih.gov/pubmed/29804530 Epub 2018/05/29.

16. Napolitano R, De Matteis S, Lucchesi A, Carloni S, Cangini D, Musuraca G, et al. Pentoxifylline-Induced Apoptosis in Chronic Lymphocytic Leukemia: New Insights into Molecular Mechanism. Mini reviews in medicinal chemistry. 2018;18(3):287-94. http://www.ncbi.nlm.nih.gov/pubmed/28969553 Epub 2017/10/04.

17. Smith RV, Waller ES, Doluisio JT, Bauza MT, Puri SK, Ho I, et al. Pharmacokinetics of orally administered pentoxifylline in humans. Journal of pharmaceutical sciences. 1986;75(1):47-52.

bioRxiv preprint doi: https://doi.org/10.1101/2021.12.13.472401; this version posted December 13, 2021. The copyright holder for this preprint (which was not certified by peer review) is the author/funder, who has granted bioRxiv a license to display the preprint in perpetuity. It is made available under aCC-BY 4.0 International license.

1176 http://www.ncbi.nlm.nih.gov/pubmed/3958905 Epub 1986/01/01.
1177 18. V. SR, S. WE, Doluisio JT, Bauza MT, Puri SK, Ho I, et al. Pharmacokinetics of orally administered
1178 pentoxifylline in humans. Journal of pharmaceutical sciences. 1986;75(1):47-52.
1179 19. Strutz F, Heeg M, Kochsiek T, Siemers G, Zeisberg M, Muller GA. Effects of pentoxifylline, pentifylline
1180 and gamma-interferon on proliferation, differentiation, and matrix synthesis of human renal fibroblasts.
1181 Nephrology, dialysis, transplantation : official publication of the European Dialysis and Transplant
1182 Association - European Renal Association. 2000;15(10):1535-46.
1183 http://www.ncbi.nlm.nih.gov/pubmed/11007820 Epub 2000/09/29.
1184 20. Chao CC, Hu S, Close K, Choi CS, Molitor TW, Novick WJ, et al. Cytokine release from microglia:
1185 differential inhibition by pentoxifylline and dexamethasone. The Journal of infectious diseases.
1186 1992;166(4):847-53. http://www.ncbi.nlm.nih.gov/pubmed/1527422 Epub 1992/10/01.
1187 21. Ruan D, Deng S, Liu Z, He J. Pentoxifylline Can Reduce the Inflammation Caused by LPS after Inhibiting
1188 Autophagy in RAW264.7 Macrophage Cells. BioMed research international. 2021;2021:6698366.
1189 http://www.ncbi.nlm.nih.gov/pubmed/33816630.
1190 22. Endres S, Fulle HJ, Sinha B, Stoll D, Dinarello CA, Gerzer R, et al. Cyclic nucleotides differentially
1191 regulate the synthesis of tumour necrosis factor-alpha and interleukin-1 beta by human mononuclear cells.
1192 Immunology. 1991;72(1):56-60. http://www.ncbi.nlm.nih.gov/pubmed/1847694 Epub 1991/01/01.
1193 23. Kim YS, Lee SK. High Performance Liquid Chromatography Analysis of Human Salivary Protein
1194 Complexes. Kor J Oral Maxillofac Pathol. 2014;36(381-388).
1195 24. Kim YS, Lee SK. IP-HPLC Analysis of Human Salivary Protein Complexes. Korean Journal of Oral and
1196 Maxillofacial Pathology. 2015;39(2):615-22.
1197 25. Kim SM, Eo MY, Cho YJ, Kim YS, Lee SK. Immunoprecipitation high performance liquid
1198 chromatographic analysis of healing process in chronic suppurative osteomyelitis of the jaw. Journal of
1199 cranio-maxillo-facial surgery : official publication of the European Association for Cranio-Maxillo-Facial
1200 Surgery. 2018;46(1):119-27. http://www.ncbi.nlm.nih.gov/pubmed/29191501 Epub 2017/12/02.
1201 26. Kim SM, Eo MY, Cho YJ, Kim YS, Lee SK. Wound healing protein profiles in the postoperative exudate of
1202 bisphosphonate-related osteonecrosis of mandible. Eur Arch Otorhinolaryngol. 2017.
1203 http://www.ncbi.nlm.nih.gov/pubmed/28647850 Epub 2017/06/26.
1204 27. Kim SM, Eo MY, Cho YJ, Kim YS, Lee SK. Differential protein expression in the secretory fluids of
1205 maxillary sinusitis and maxillary retention cyst. Eur Arch Otorhinolaryngol. 2017;274(1):215-22.
1206 http://www.ncbi.nlm.nih.gov/pubmed/27422628 Epub 2016/07/17.
1207 28. Seo MH, Myoung H, Lee JH, Kim SM, Lee SK. Changes in oncogenic protein levels in peri-implant oral
1208 malignancy: a case report. Maxillofacial plastic and reconstructive surgery. 2019;41(1):46.
1209 http://www.ncbi.nlm.nih.gov/pubmed/31763327.
1210 29. Kim SM, Jeong D, Kim MK, Lee SS, Lee SK. Two different protein expression profiles of oral squamous
1211 cell carcinoma analyzed by immunoprecipitation high-performance liquid chromatography. World journal of
1212 surgical oncology. 2017;15(1):151. http://www.ncbi.nlm.nih.gov/pubmed/28789700 Epub 2017/08/10.
1213 30. Yoon CS, Kim MK, Kim YS, Lee SK. In vivo protein expression changes in mouse livers treated with
1214 dialyzed coffee extract as determined by IP-HPLC. Maxillofacial plastic and reconstructive surgery.
1215 2018;40(1):44. http://www.ncbi.nlm.nih.gov/pubmed/30613574.
1216 31. Yoon CS, Kim MK, Kim YS, Lee SK. In vitro protein expression changes in RAW 264.7 cells and HUVECs
1217 treated with dialyzed coffee extract by immunoprecipitation high performance liquid chromatography.
1218 Scientific reports. 2018;8(1):13841. http://www.ncbi.nlm.nih.gov/pubmed/30218035.
1219 32. Kim MK, Kim SG, Lee SK. 4-Hexylresorcinol-in duced angiogenesis potential in human endothelial cells.

bioRxiv preprint doi: https://doi.org/10.1101/2021.12.13.472401; this version posted December 13, 2021. The copyright holder for this preprint (which was not certified by peer review) is the author/funder, who has granted bioRxiv a license to display the preprint in perpetuity. It is made available under aCC-BY 4.0 International license.

Maxillofacial plastic and reconstructive surgery. 2020;42(1):23. http://www.ncbi.nlm.nih.gov/pubmed/32642459.

33. Kim MK, Yoon CS, Kim SG, Park YW, Lee SS, Lee SK. Effects of 4-Hexylresorcinol on Protein Expressions in RAW 264.7 Cells as Determined by Immunoprecipitation High Performance Liquid Chromatography. Scientific reports. 2019;9(1):3379. http://www.ncbi.nlm.nih.gov/pubmed/30833641.

34. Kim YS. Preliminary study on hydrogen peroxide-induced cellular responses in RAW 264.7 cells as determined by IP-HPLC. Korean Journal of Maxillofacial Pathology. 2019;43(6):255-67.

35. Lee IS, Kim DW, Oh JH, Lee SK, Choi JY, Kim SG, et al. Effects of 4-Hexylresorcinol on Craniofacial Growth in Rats. International journal of molecular sciences. 2021;22(16). http://www.ncbi.nlm.nih.gov/pubmed/34445640.

36. Taciak B, Bialasek M, Braniewska A, Sas Z, Sawicka P, Kiraga L, et al. Evaluation of phenotypic and functional stability of RAW 264.7 cell line through serial passages. PloS one. 2018;13(6):e0198943. http://www.ncbi.nlm.nih.gov/pubmed/29889899.

37. Park MH, Wolff EC. Hypusine, a polyamine-derived amino acid critical for eukaryotic translation. The Journal of biological chemistry. 2018;293(48):18710-8. http://www.ncbi.nlm.nih.gov/pubmed/30257869.

38. Chung SI. Comparative studies on tissue transglutaminase and factor XIII. Annals of the New York Academy of Sciences. 1972;202:240-55. http://www.ncbi.nlm.nih.gov/pubmed/4629552.

39. Chung SI, Shrager RI, Folk JE. Mechanism of action of guinea pig liver transglutaminase. VII. Chemical and stereochemical aspects of substrate binding and catalysis. The Journal of biological chemistry. 1970;245(23):6424-35. http://www.ncbi.nlm.nih.gov/pubmed/5488783.

40. Lee SS, Kim SM, Kim YS, Lee SK. Extensive protein expression changes induced by pamidronate in RAW 264.7 cells as determined by IP-HPLC. PeerJ. 2020;8:e9202. http://www.ncbi.nlm.nih.gov/pubmed/32509464.

41. Kim YS, Kim DW, Kim SG, Lee SK. 4-hexylresorcinol-induced protein expression changes in human umbilical cord vein endothelial cells as determined by immunoprecipitation high-performance liquid chromatography. PloS one. 2020;15(12):e0243975. http://www.ncbi.nlm.nih.gov/pubmed/33320912.

42. Saaristo A, Tammela T, Farkkila A, Karkkainen M, Suominen E, Yla-Herttuala S, et al. Vascular endothelial growth factor-C accelerates diabetic wound healing. The American journal of pathology. 2006;169(3):1080-7. http://www.ncbi.nlm.nih.gov/pubmed/16936280.

43. Zhang N, Fang Z, Contag PR, Purchio AF, West DB. Tracking angiogenesis induced by skin wounding and contact hypersensitivity using a Vegfr2-luciferase transgenic mouse. Blood. 2004;103(2):617-26. http://www.ncbi.nlm.nih.gov/pubmed/14512298.

44. Sergeeva OA, van der Goot FG. Converging physiological roles of the anthrax toxin receptors. F1000Research. 2019;8. http://www.ncbi.nlm.nih.gov/pubmed/31448094.

45. Shao R, Yan W, Rockey DC. Regulation of endothelin-1 synthesis by endothelin-converting enzyme-1 during wound healing. The Journal of biological chemistry. 1999;274(5):3228-34. http://www.ncbi.nlm.nih.gov/pubmed/9915864.

46. Toriu N, Ueno T, Mizuno H, Sekine A, Hayami N, Hiramatsu R, et al. Brown tumor diagnosed three years after parathyroidectomy in a patient with nail-patella syndrome: A case report. Bone reports. 2019;10:100187. http://www.ncbi.nlm.nih.gov/pubmed/30627596.

47. Price JT, Quinn JM, Sims NA, Vieusseux J, Waldeck K, Docherty SE, et al. The heat shock protein 90 inhibitor, 17-allylamino-17-demethoxygeldanamycin, enhances osteoclast formation and potentiates bone metastasis of a human breast cancer cell line. Cancer research. 2005;65(11):4929-38. http://www.ncbi.nlm.nih.gov/pubmed/15930315.

48. Chang MY, Kang I, Gale M, Jr., Manicone AM, Kinsella MG, Braun KR, et al. Versican is produced by

bioRxiv preprint doi: https://doi.org/10.1101/2021.12.13.472401; this version posted December 13, 2021. The copyright holder for this preprint (which was not certified by peer review) is the author/funder, who has granted bioRxiv a license to display the preprint in perpetuity. It is made available under aCC-BY 4.0 International license.

Trif- and type I interferon-dependent signaling in macrophages and contributes to fine control of innate immunity in lungs. American journal of physiology Lung cellular and molecular physiology. 2017;313(6):L1069-L86. http://www.ncbi.nlm.nih.gov/pubmed/28912382.

49. Zhu L, Li L, Zhang Q, Yang X, Zou Z, Hao B, et al. NOS1 S-nitrosylates PTEN and inhibits autophagy in nasopharyngeal carcinoma cells. Cell death discovery. 2017;3:17011. http://www.ncbi.nlm.nih.gov/pubmed/28243469.

50. Dhulqarnain AO, Takzaree N, Hassanzadeh G, Tooli H, Malekzadeh M, Khanmohammadi N, et al. Pentoxifylline improves the survival of spermatogenic cells via oxidative stress suppression and upregulation of PI3K/AKT pathway in mouse model of testicular torsion-detorsion. Heliyon. 2021;7(4):e06868. http://www.ncbi.nlm.nih.gov/pubmed/33997400.

51. Yang YL, Lee MG, Lee CC, Su PI, Chi CY, Liu CH, et al. Pentoxifylline decreases post-operative intra-abdominal adhesion formation in an animal model. PeerJ. 2018;6:e5434. http://www.ncbi.nlm.nih.gov/pubmed/30155353 Epub 2018/08/30.

52. Dong J, Yuan X, Xie W. Pentoxifylline exerts anti-inflammatory effects on cerebral ischemia reperfusioninduced injury in a rat model via the p38 mitogen-activated protein kinase signaling pathway. Molecular medicine reports. 2018;17(1):1141-7. http://www.ncbi.nlm.nih.gov/pubmed/29115594 Epub 2017/11/09.

53. Kim HK, Hwang SH, Lee SO, Kim SH, Abdi S. Pentoxifylline Ameliorates Mechanical Hyperalgesia in a Rat Model of Chemotherapy-Induced Neuropathic Pain. Pain physician. 2016;19(4):E589-600. http://www.ncbi.nlm.nih.gov/pubmed/27228525 Epub 2016/05/27.

54. Akbari Z, Reisi P, Torkaman-Boutorabi A, Farahmandfar M. The Effect of Pentoxifylline on Passive Avoidance Learning and Expression of Tumor Necrosis Factor-Alpha and Caspase-3 in the Rat Hippocampus Following Lipopolysaccharide-Induced Inflammation. Advanced biomedical research. 2019;8:39. http://www.ncbi.nlm.nih.gov/pubmed/31360680.

55. Poulakis N, Androutsos G, Kazi D, Bastas A, Provata A, Bitsakou C, et al. The differential effect of pentoxifylline on cytokine production by alveolar macrophages and its clinical implications. Respiratory medicine. 1999;93(1):52-7. http://www.ncbi.nlm.nih.gov/pubmed/10464849 Epub 1999/08/28.

56. Annamaraju P, Baradhi KM. Pentoxifylline. StatPearls. Treasure Island (FL)2021.

57. Heifetz-Li JJ, Abdelsamie S, Campbell CB, Roth S, Fielding AF, Mulligan JP. Systematic review of the use of pentoxifylline and tocopherol for the treatment of medication-related osteonecrosis of the jaw. Oral surgery, oral medicine, oral pathology and oral radiology. 2019;128(5):491-7 e2. http://www.ncbi.nlm.nih.gov/pubmed/31488389.

58. Bouchard C, Thieke K, Maier A, Saffrich R, Hanley-Hyde J, Ansorge W, et al. Direct induction of cyclin D2 by Myc contributes to cell cycle progression and sequestration of p27. The EMBO journal. 1999;18(19):5321-33. http://www.ncbi.nlm.nih.gov/pubmed/10508165.

59. Brugarolas J, Bronson RT, Jacks T. p21 is a critical CDK2 regulator essential for proliferation control in Rb-deficient cells. The Journal of cell biology. 1998;141(2):503-14. http://www.ncbi.nlm.nih.gov/pubmed/9548727.

60. Ghasemnejad-Berenji M, Pashapour S, Sadeghpour S. Pentoxifylline: A Drug with Antiviral and Anti-Inflammatory Effects to Be Considered in the Treatment of Coronavirus Disease 2019. Medical principles and practice : international journal of the Kuwait University, Health Science Centre. 2021;30(1):98-100. http://www.ncbi.nlm.nih.gov/pubmed/33049737.

61. Lopez-Iranzo FJ, Lopez-Rodas AM, Franco L, Lopez-Rodas G. Pentoxifylline and Oxypurinol: Potential Drugs to Prevent the "Cytokine Release (Storm) Syndrome" Caused by SARS-CoV-2? Current pharmaceutical

bioRxiv preprint doi: https://doi.org/10.1101/2021.12.13.472401; this version posted December 13, 2021. The copyright holder for this preprint (which was not certified by peer review) is the author/funder, who has granted bioRxiv a license to display the preprint in perpetuity. It is made available under aCC-BY 4.0 International license.

design. 2020;26(35):4515-21. http://www.ncbi.nlm.nih.gov/pubmed/32787748.

62. Assimakopoulos SF, Seintis F, Marangos M. Pentoxifylline and complicated COVID-19: A pathophysiologically based treatment proposal. Medical hypotheses. 2020;143:109926. http://www.ncbi.nlm.nih.gov/pubmed/32485316.

63. Pal S, Porwal K, Singh H, Malik MY, Rashid M, Kulkarni C, et al. Reversal of Osteopenia in Ovariectomized Rats by Pentoxifylline: Evidence of Osteogenic and Osteo-Angiogenic Roles of the Drug. Calcified tissue international. 2019;105(3):294-307. http://www.ncbi.nlm.nih.gov/pubmed/31175387.

64. Tsutsumimoto T, Wakabayashi S, Kinoshita T, Horiuchi H, Takaoka K. A phosphodiesterase inhibitor, pentoxifylline, enhances the bone morphogenetic protein-4 (BMP-4)-dependent differentiation of osteoprogenitor cells. Bone. 2002;31(3):396-401. http://www.ncbi.nlm.nih.gov/pubmed/12231412.

65. Windischhofer W, Zach D, Fauler G, Raspotnig G, Kofeler H, Leis HJ. Involvement of Rho and p38 MAPK in endothelin-1-induced expression of PGHS-2 mRNA in osteoblast-like cells. Journal of bone and mineral research : the official journal of the American Society for Bone and Mineral Research. 2002;17(10):1774-84. http://www.ncbi.nlm.nih.gov/pubmed/12369781.

66. Okunieff P, Augustine E, Hicks JE, Cornelison TL, Altemus RM, Naydich BG, et al. Pentoxifylline in the treatment of radiation-induced fibrosis. Journal of clinical oncology : official journal of the American Society of Clinical Oncology. 2004;22(11):2207-13. http://www.ncbi.nlm.nih.gov/pubmed/15169810 Epub 2004/06/01.

67. Frueh FS, Sanchez-Macedo N, Calcagni M, Giovanoli P, Lindenblatt N. The Crucial Role of Vascularization and Lymphangiogenesis in Skin Reconstruction. European surgical research Europaische chirurgische Forschung Recherches chirurgicales europeennes. 2018;59(3-4):242-54. http://www.ncbi.nlm.nih.gov/pubmed/30244256.

bioRxiv preprint doi: https://doi.org/10.1101/2021.12.13.472401; this version posted December 13, 2021. The copyright holder for this preprint (which was not certified by peer review) is the author/funder, who has granted bioRxiv a license to display the preprint in perpetuity. It is made available under aCC-BY 4.0 International license.

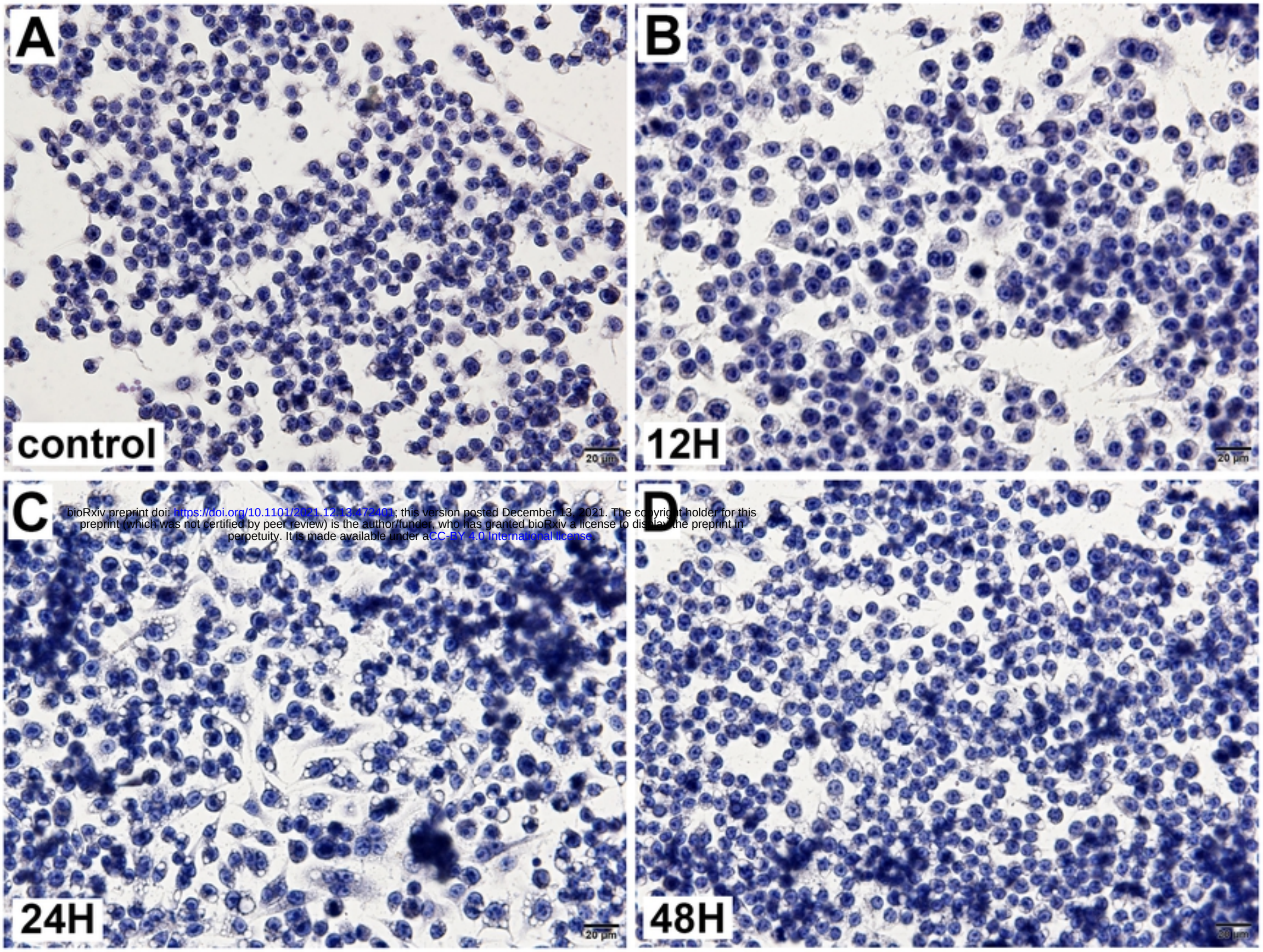

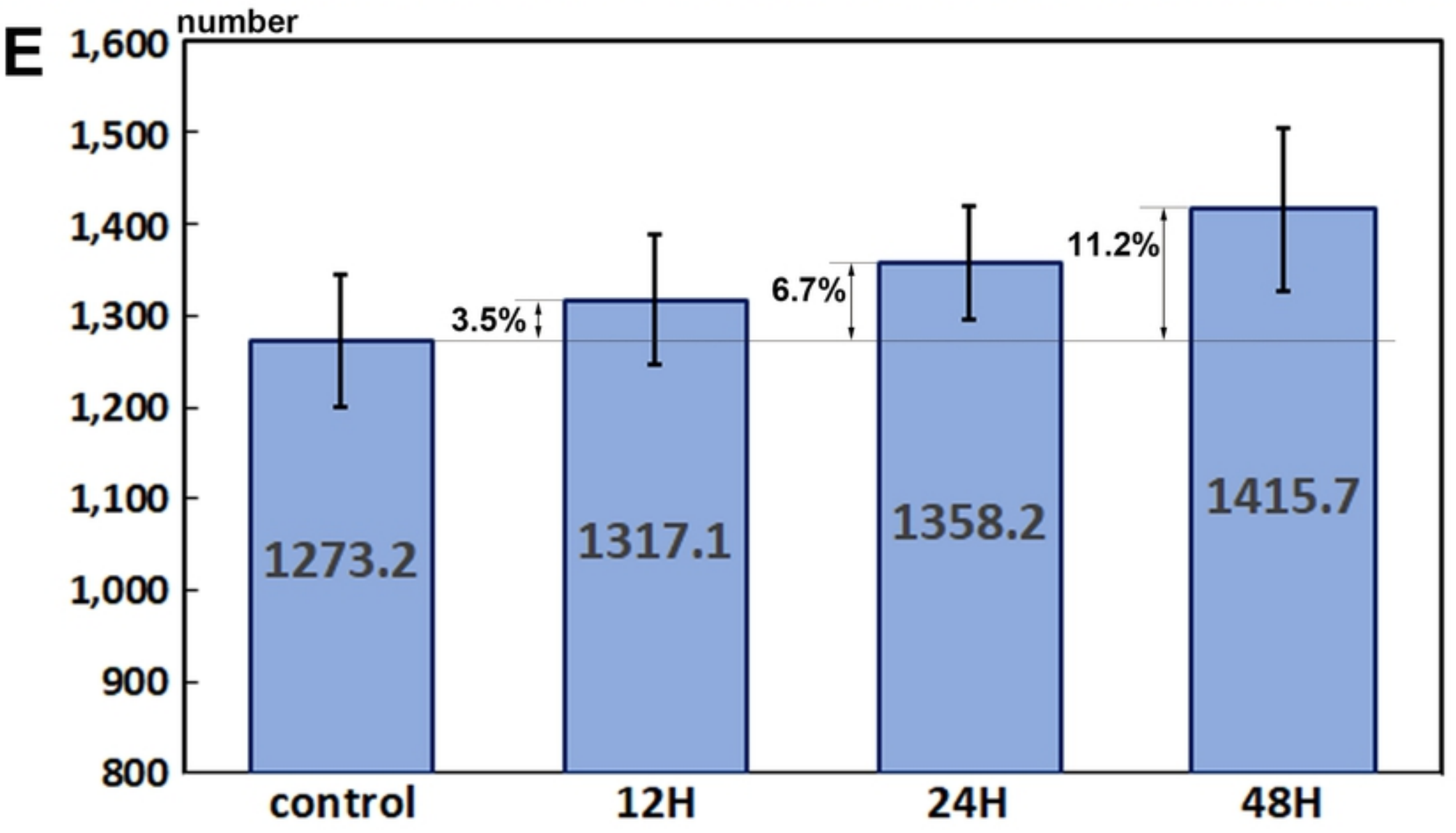

Figure 1

bioRxiv preprint doi: https://doi.org/10.1101/2021.12.13.472401; this version posted December 13, 2021. The copyright holder for this preprint (which was not certified by peer review) is the author/funder, who has granted bioRxiv a license to display the preprint in perpetuity. It is made available under aCC-BY 4.0 International license.

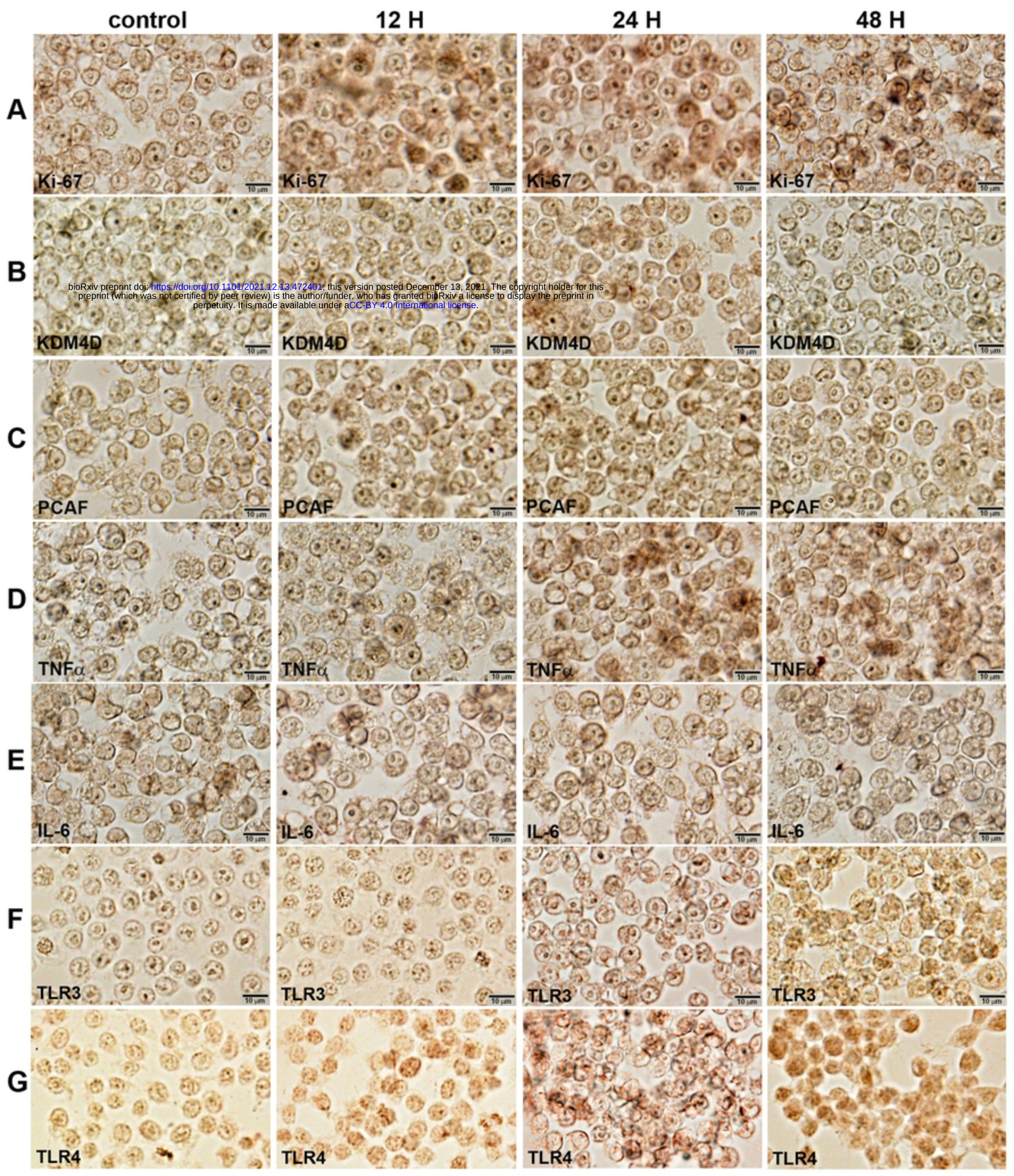

Figure 2

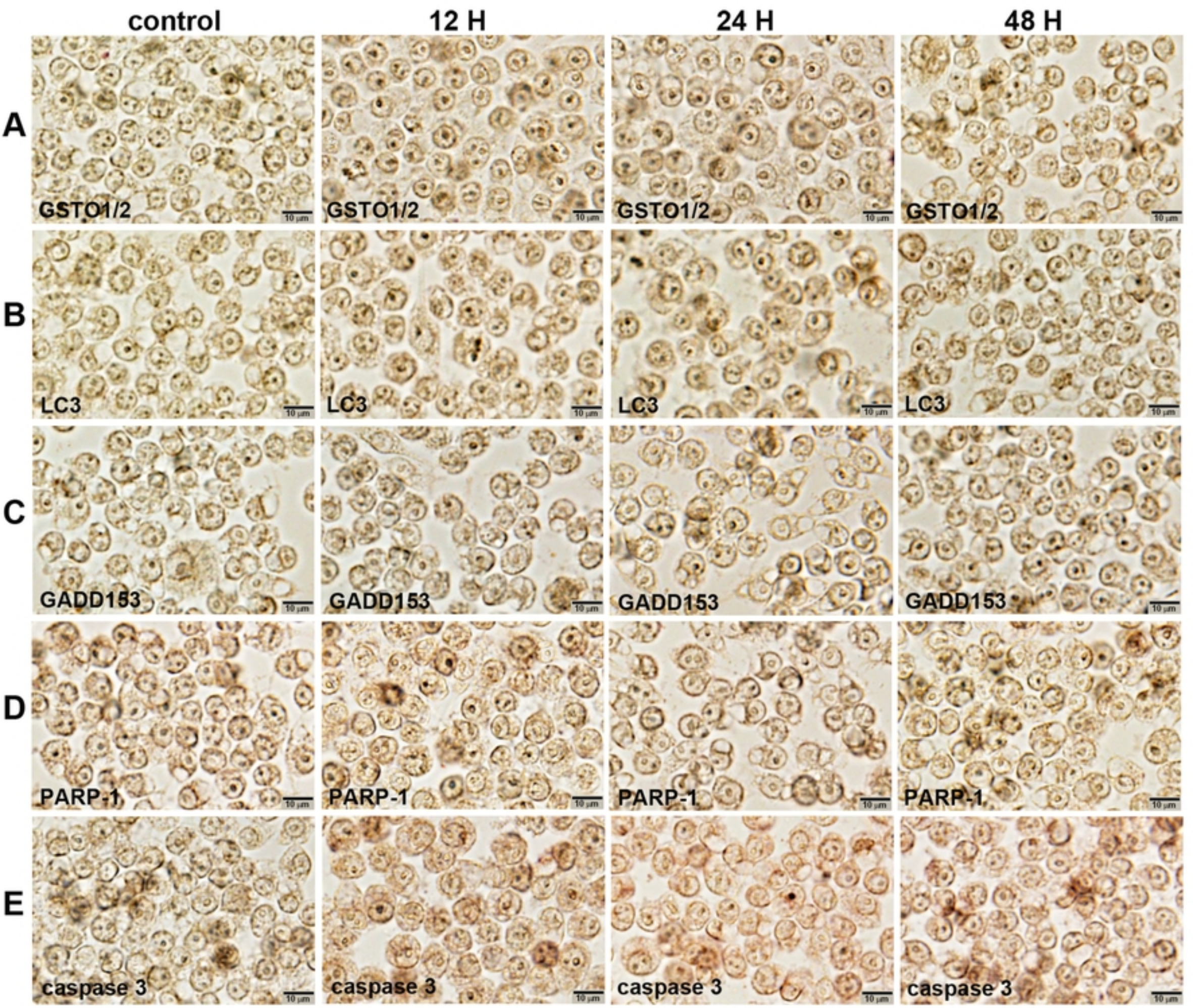
control
12 H
24 H
48 H
A
GSTO1/2
GSTO1/2
GSTO1/2
GSTO1/2
B
LC3
LC3
LC3
LC3
C
GADD153
GADD153
GADD153
GADD153
D
PARP-1
PARP-1
PARP-1
PARP-1
E
caspase 3
caspase 3
caspase 3
caspase 3

Figure 3

bioRxiv preprint doi: https://doi.org/10.1101/2021.12.13.472401; this version posted December 13, 2021. The copyright holder for this preprint (which was not certified by peer review) is the author/funder, who has granted bioRxiv a license to display the preprint in perpetuity. It is made available under aCC-BY 4.0 International license.

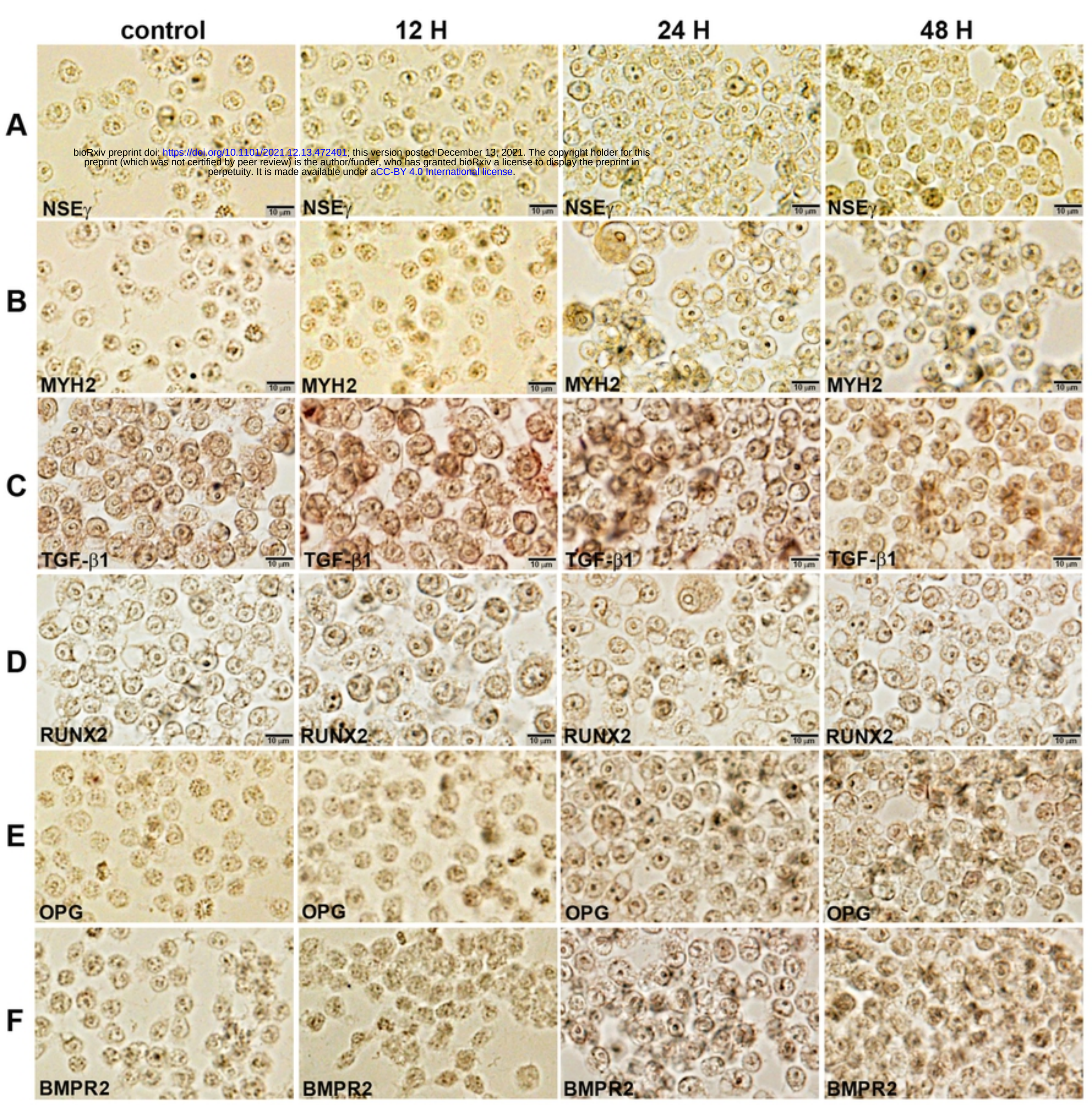

Figure 4

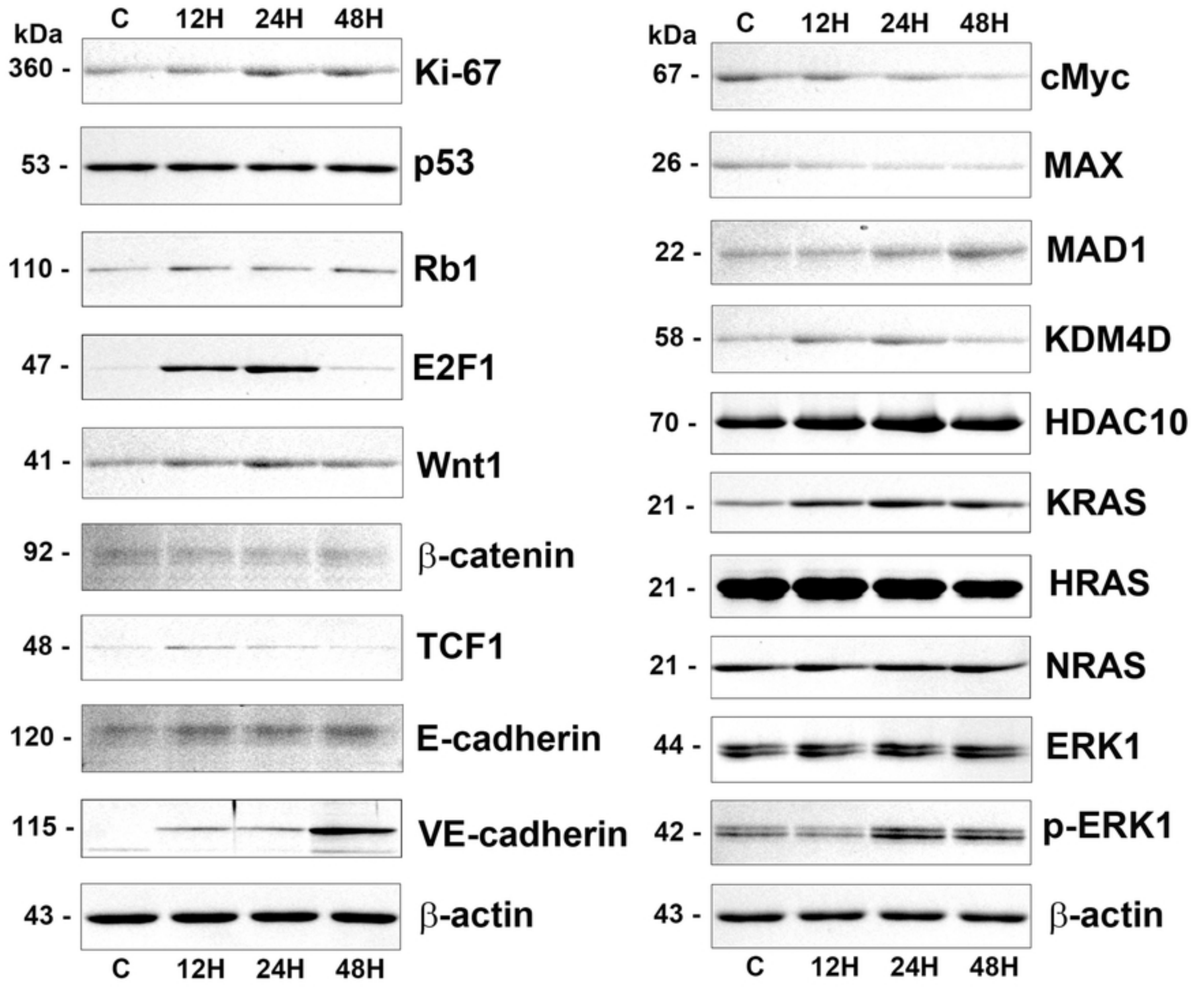
kDa
C
12H
24H
48H
360 -
Ki-67
53 -
p53
110 -
Rb1
47 -
E2F1
41 -
Wnt1
92 -
β-catenin
48 -
TCF1
120 -
E-cadherin
115 -
VE-cadherin
43 -
β-actin
C
12H
24H
48H
kDa
67 -
cMyc
26 -
MAX
22 -
MAD1
58 -
KDM4D
70 -
HDAC10
21 -
KRAS
21 -
HRAS
21 -
NRAS
44 -
ERK1
42 -
p-ERK1
43 -
β-actin
C
12H
24H
48H

Figure 5

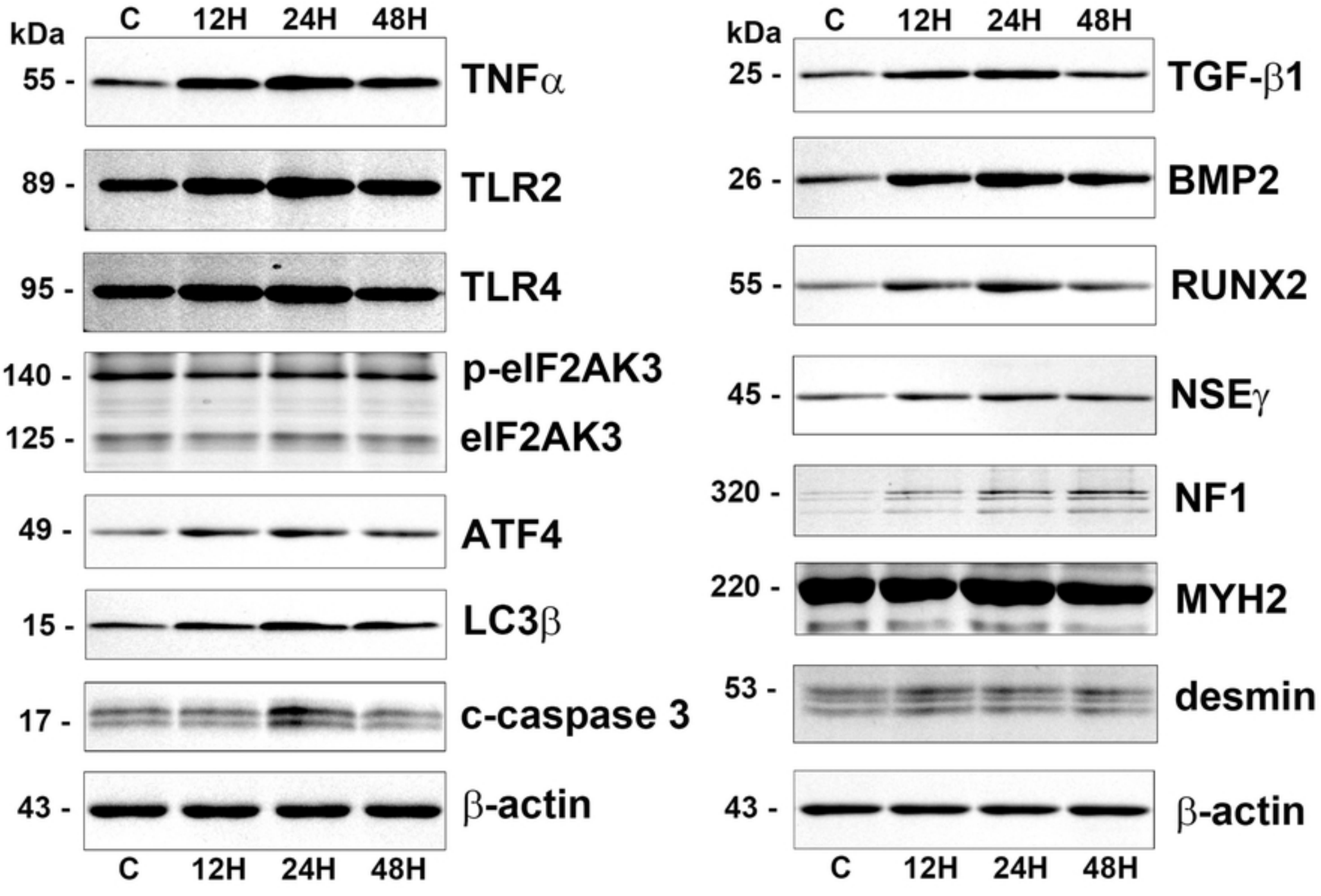
kDa
C
12H
24H
48H
55 -
TNFα
89 -
TLR2
95 -
TLR4
140 -
p-eIF2AK3
125 -
eIF2AK3
49 -
ATF4
15 -
LC3β
17 -
c-caspase 3
43 -
β-actin
C
12H
24H
48H
kDa
25 -
TGF-β1
26 -
BMP2
55 -
RUNX2
45 -
NSEγ
320 -
NF1
220 -
MYH2
53 -
desmin
43 -
β-actin
C
12H
24H
48H

Figure 6

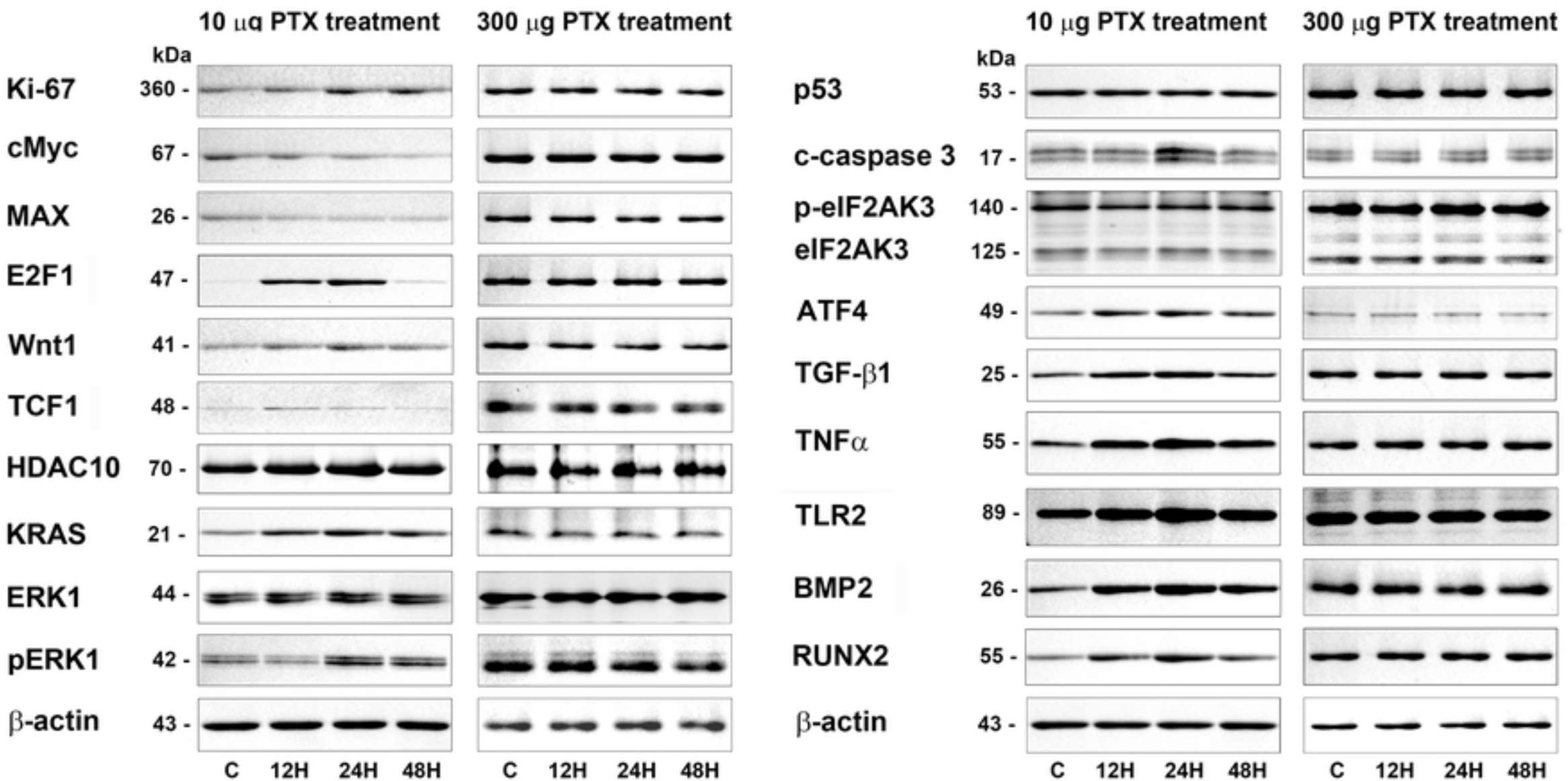
10 μg PTX treatment
300 μg PTX treatment
kDa
Ki-67
360 -
cMyc
67 -
MAX
26 -
E2F1
47 -
Wnt1
41 -
TCF1
48 -
HDAC10
70 -
KRAS
21 -
ERK1
44 -
pERK1
42 -
β-actin
43 -
C
12H
24H
48H
10 μg PTX treatment
300 μg PTX treatment
kDa
p53
53 -
c-caspase 3
17 -
p-eIF2AK3
140 -
eIF2AK3
125 -
ATF4
49 -
TGF-β1
25 -
TNFα
55 -
TLR2
89 -
BMP2
26 -
RUNX2
55 -
β-actin
43 -
C
12H
24H
48H

Figure 7

bioRxiv preprint doi: https://doi.org/10.1101/2021.12.13.472401; this version posted December 13, 2021. The copyright holder for this preprint (which was not certified by peer review) is the author/funder, who has granted bioRxiv a license to display the preprint in perpetuity. It is made available under aCC-BY 4.0 International license.

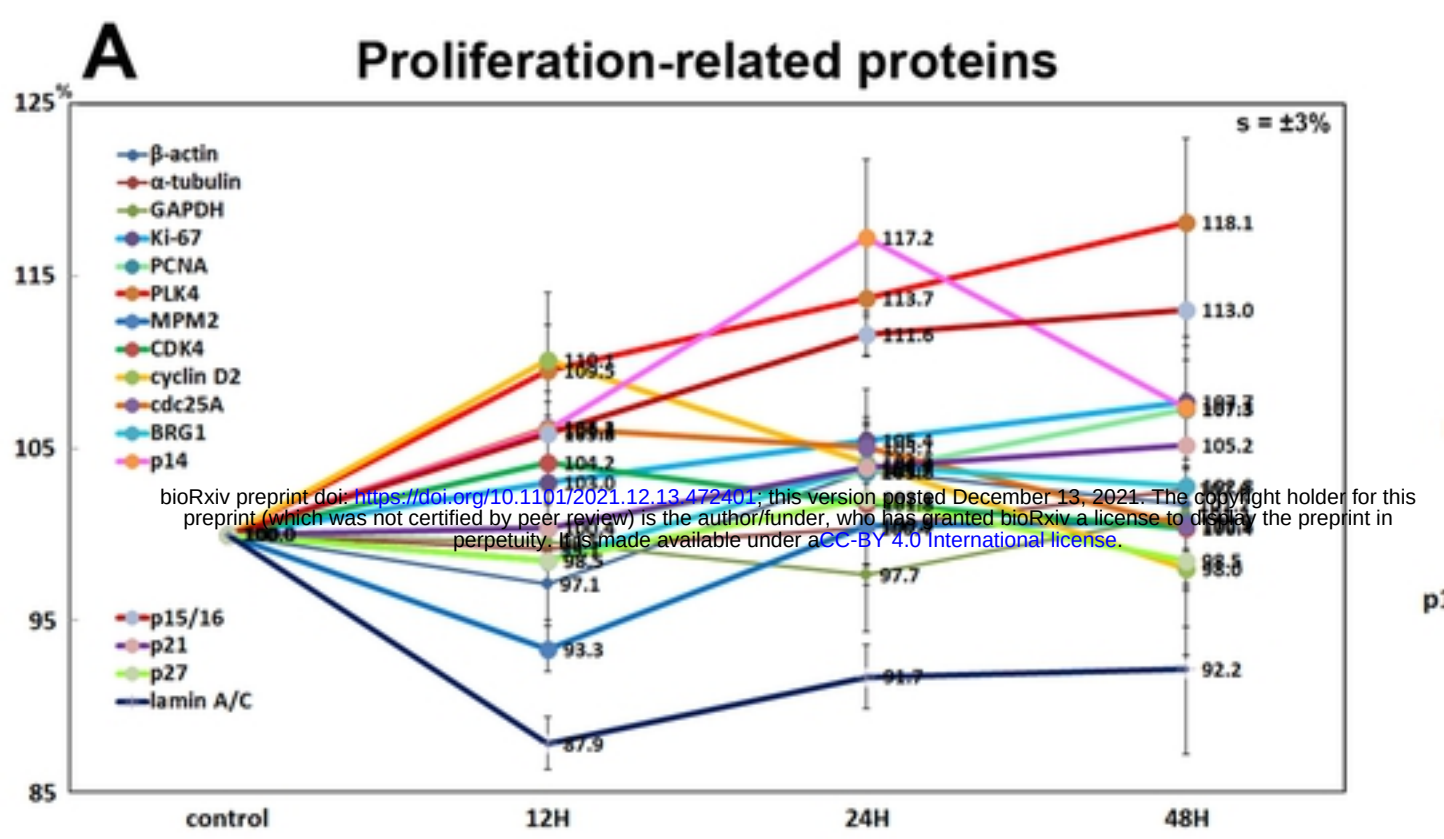

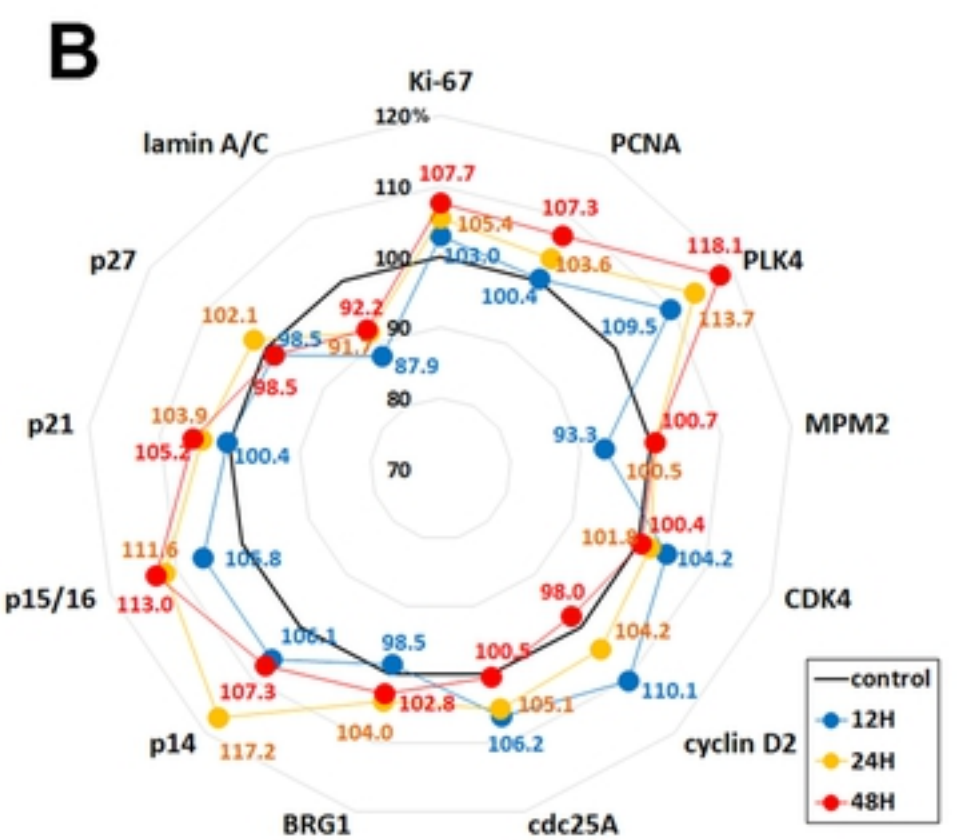

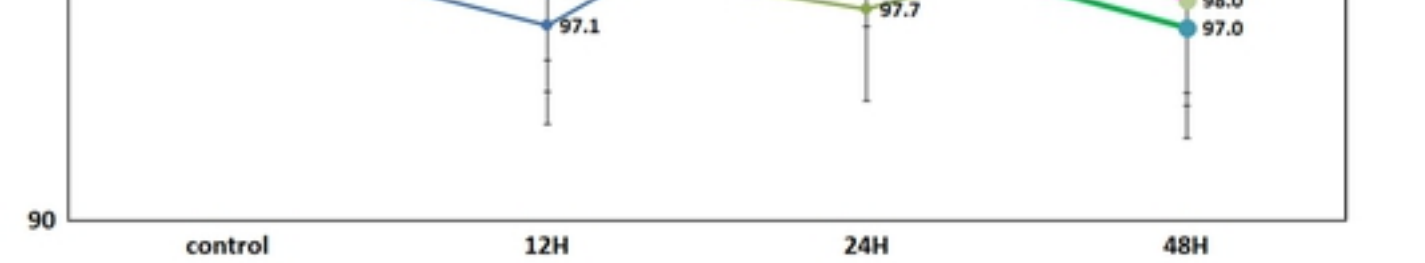

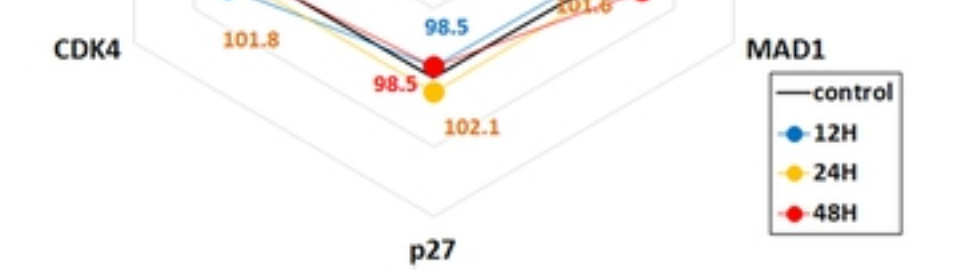

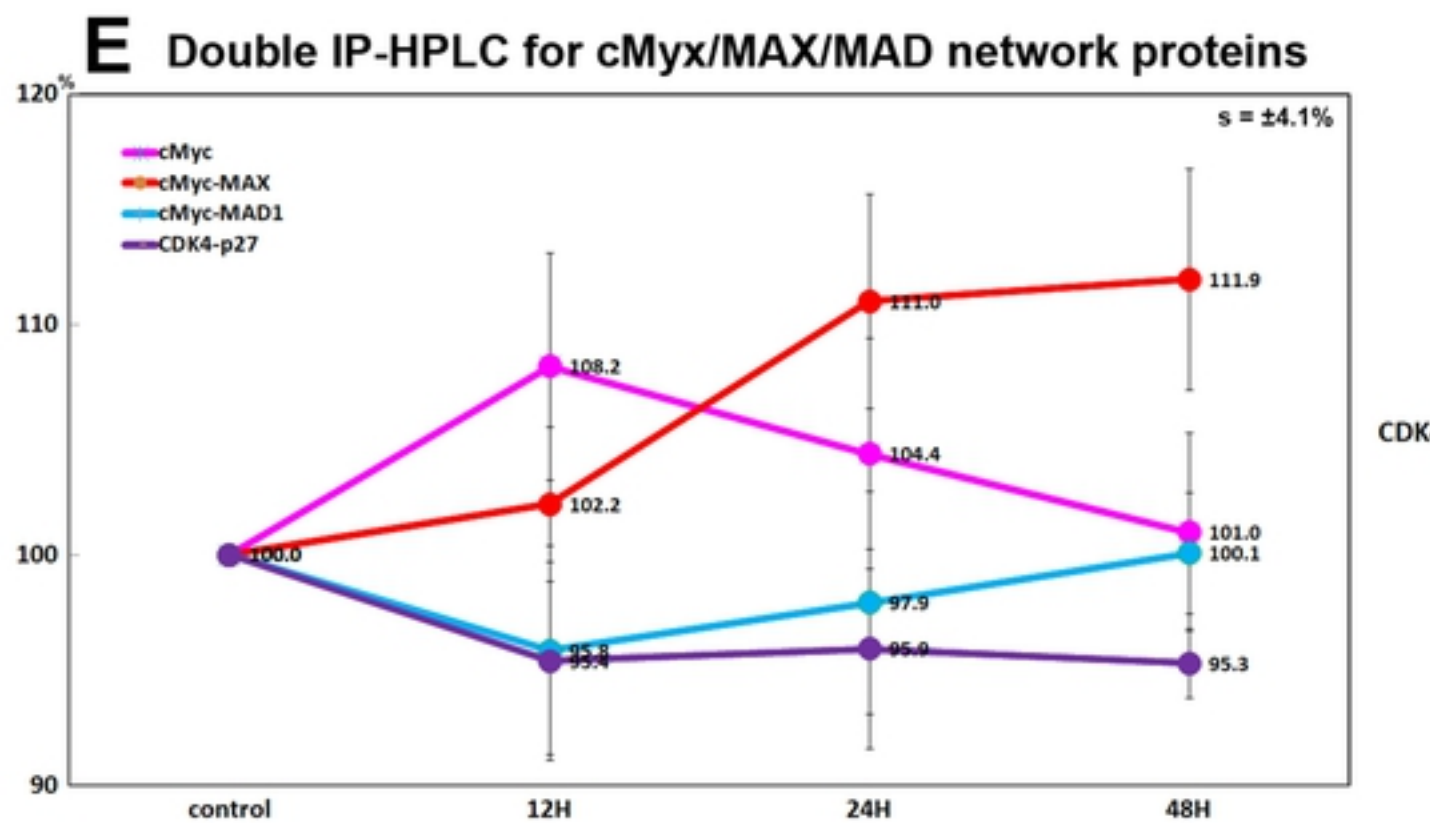

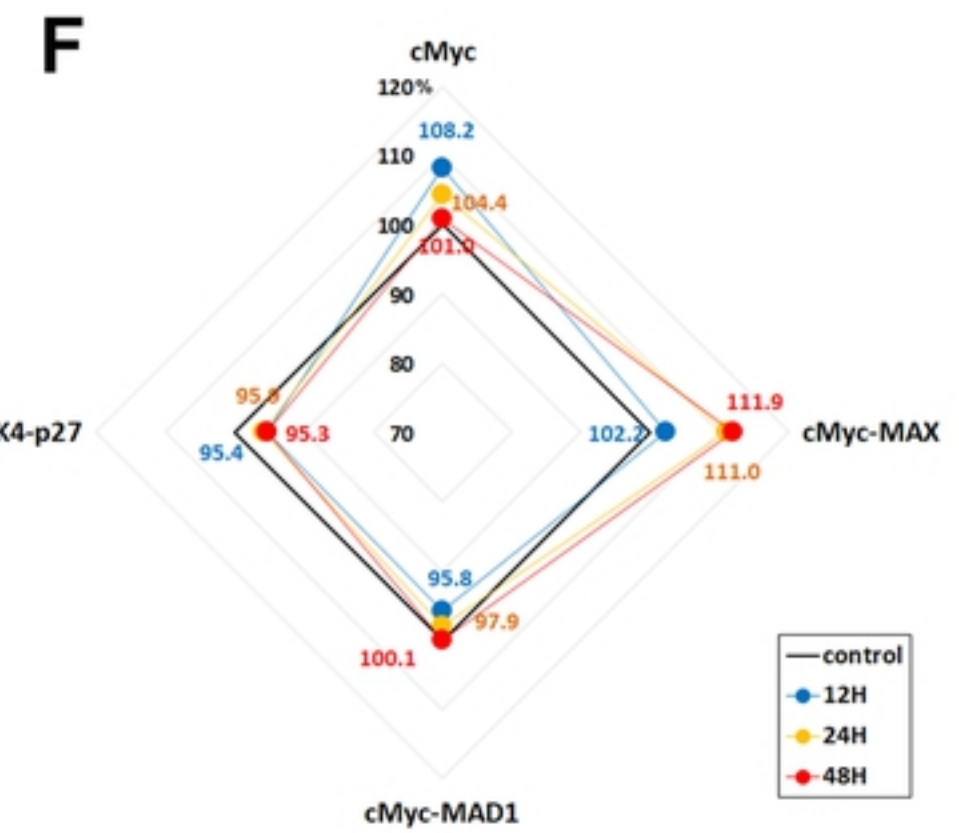

Figure 8

bioRxiv preprint doi: https://doi.org/10.1101/2021.12.13.472401; this version posted December 13, 2021. The copyright holder for this preprint (which was not certified by peer review) is the author/funder, who has granted bioRxiv a license to display the preprint in perpetuity. It is made available under aCC-BY 4.0 International license.

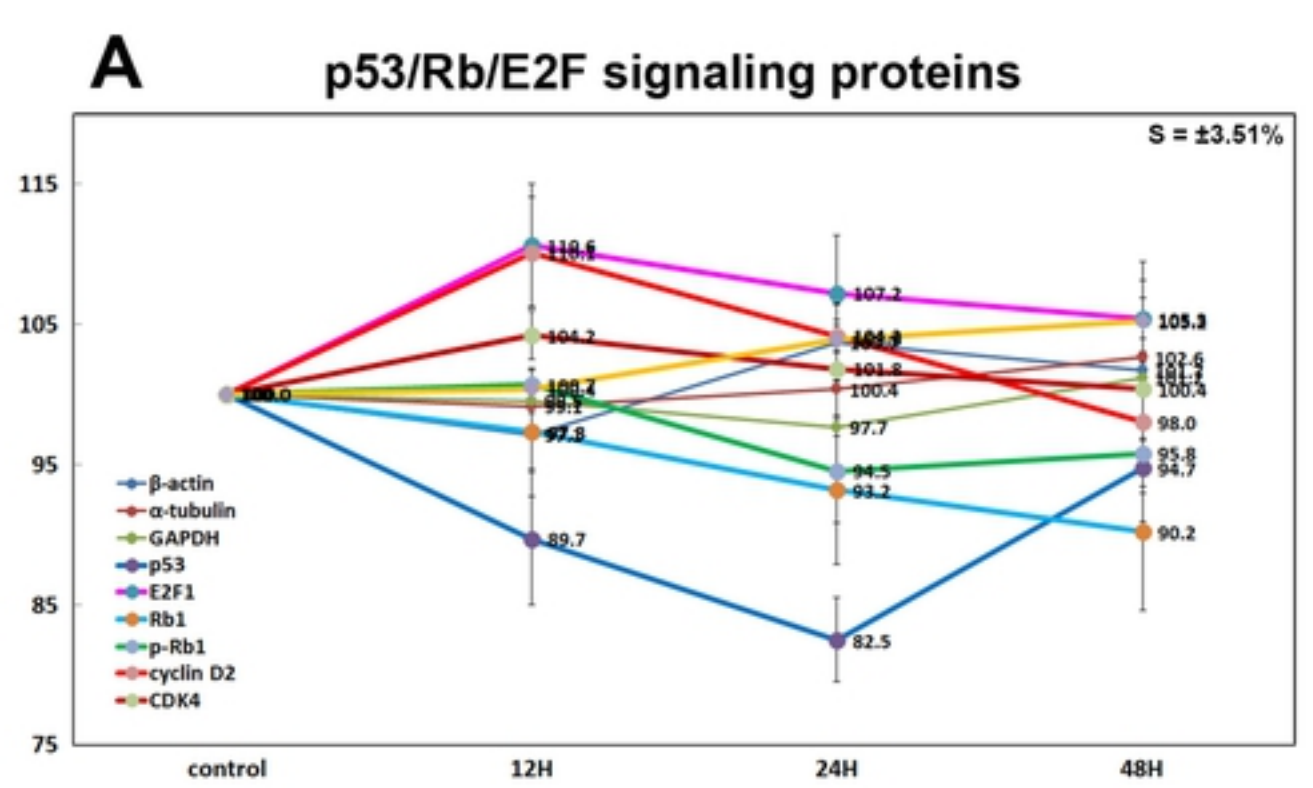

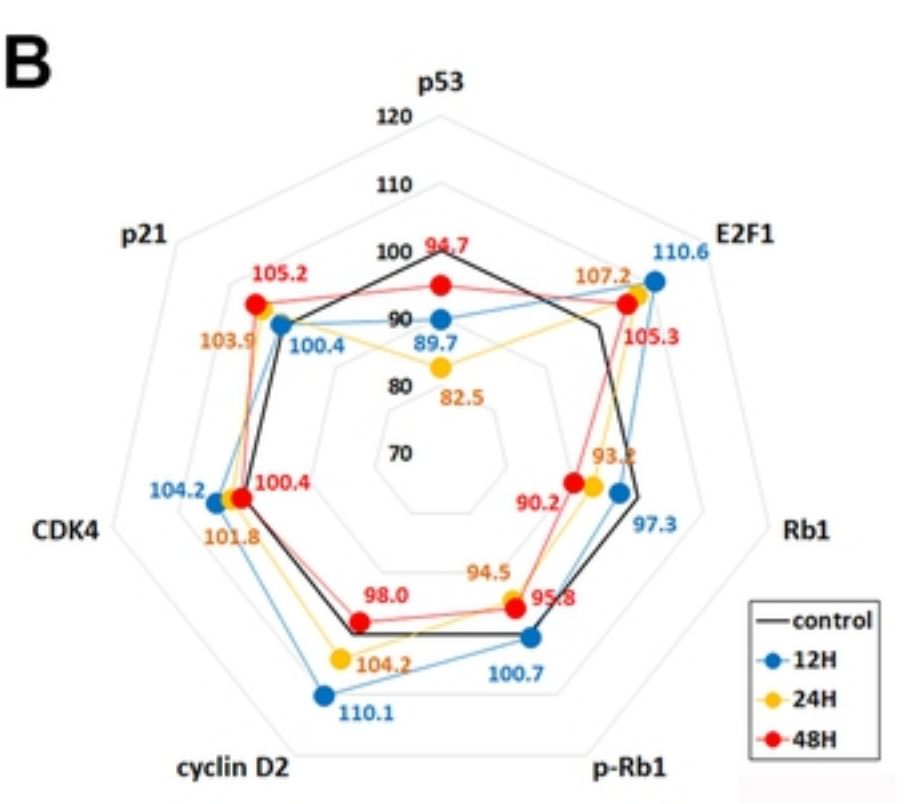

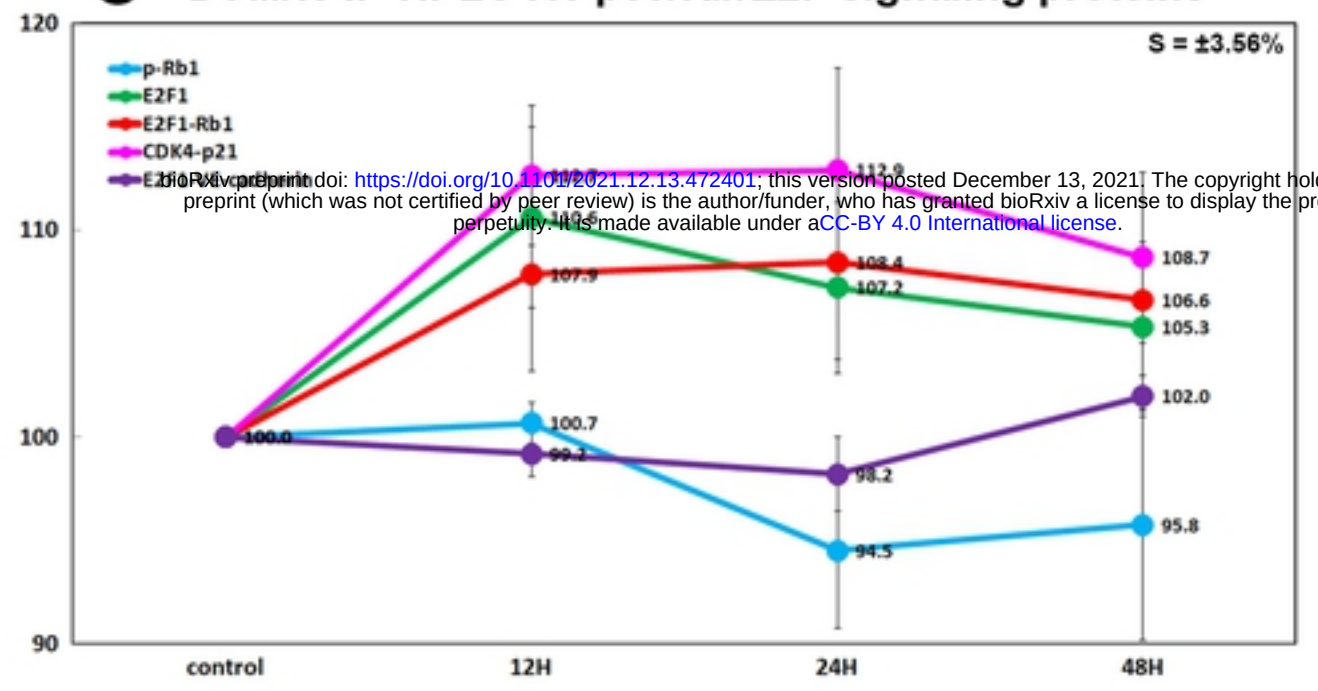

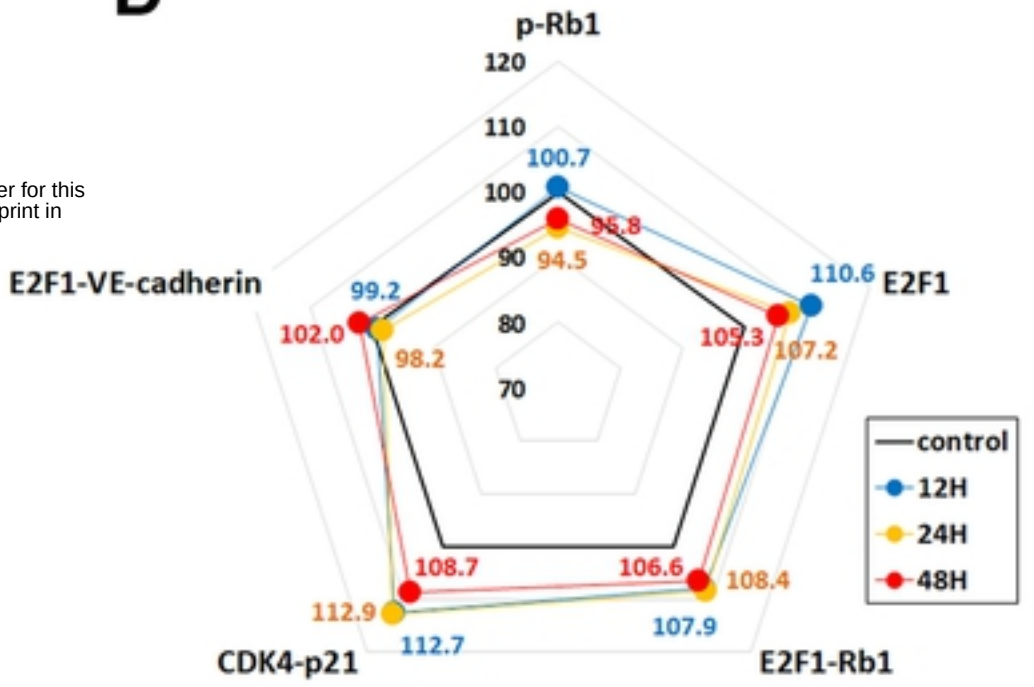

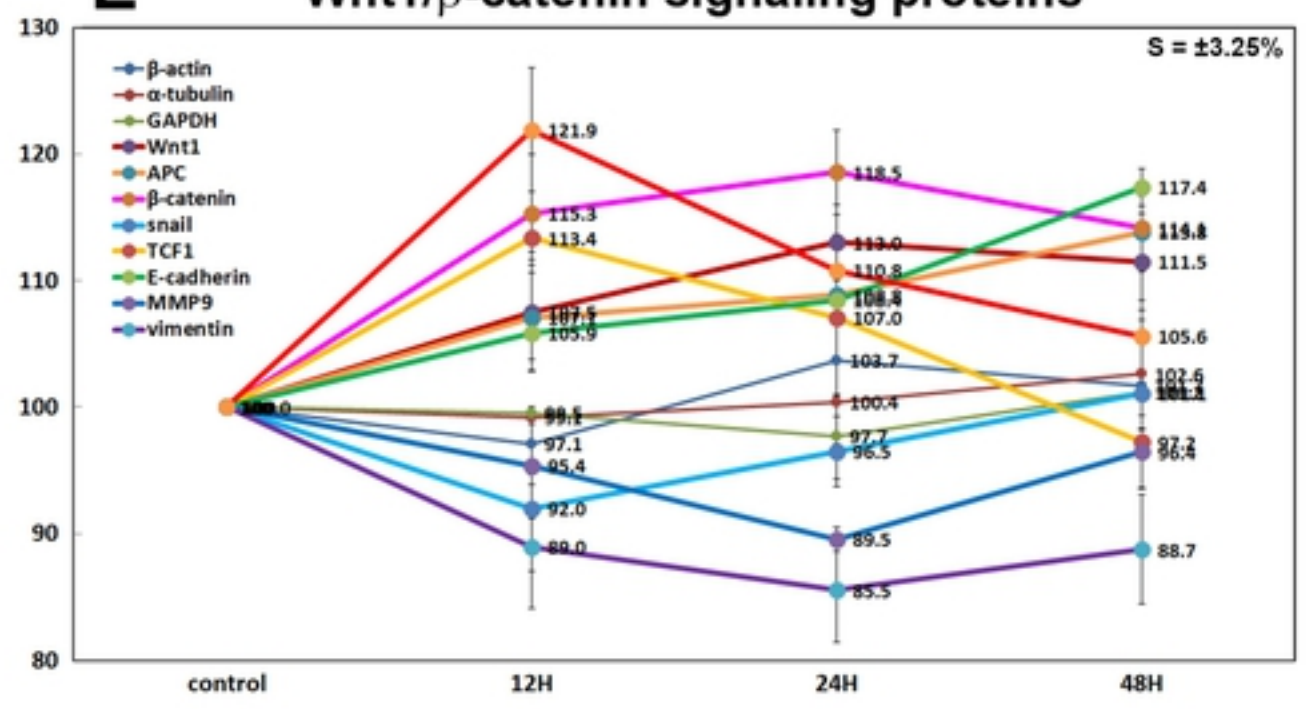

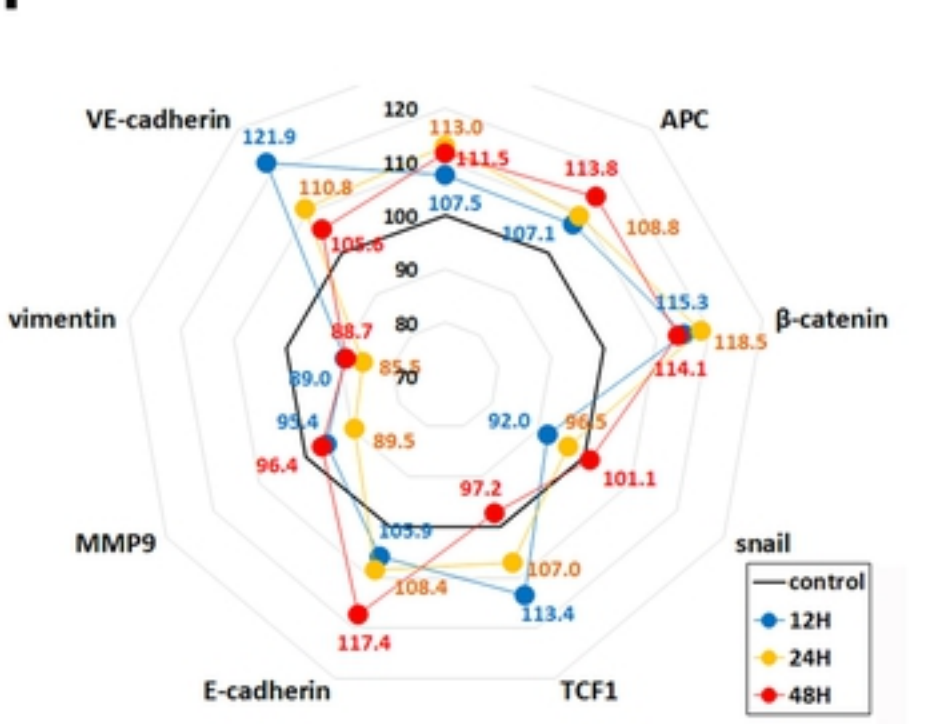

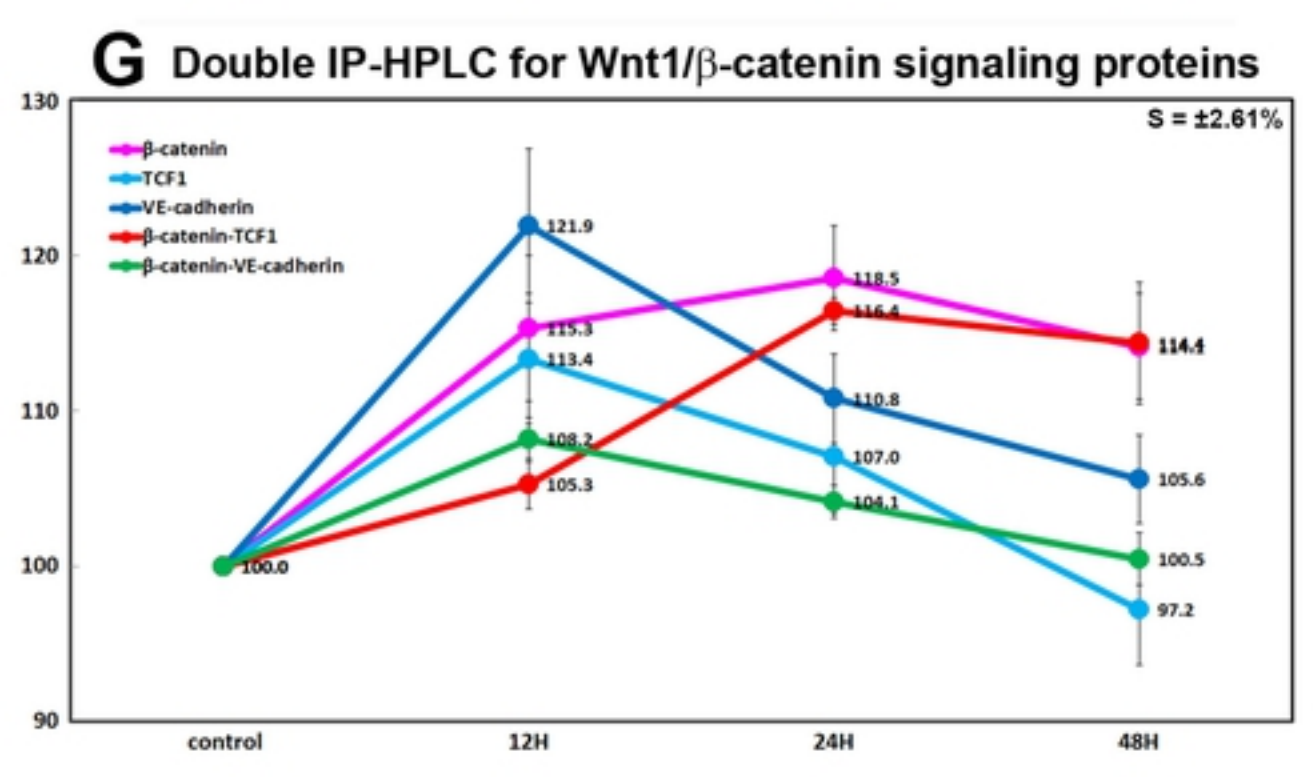

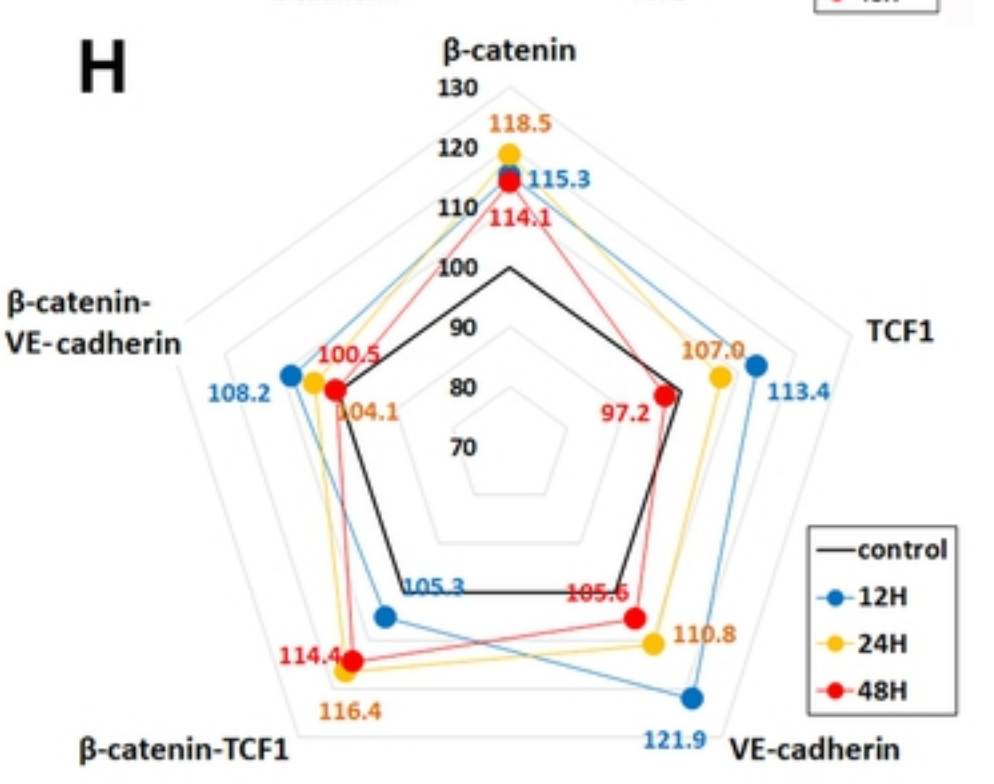

Figure 9

bioRxiv preprint doi: https://doi.org/10.1101/2021.12.13.472401; this version posted December 13, 2021. The copyright holder for this preprint (which was not certified by peer review) is the author/funder, who has granted bioRxiv a license to display the preprint in perpetuity. It is made available under aCC-BY 4.0 International license.

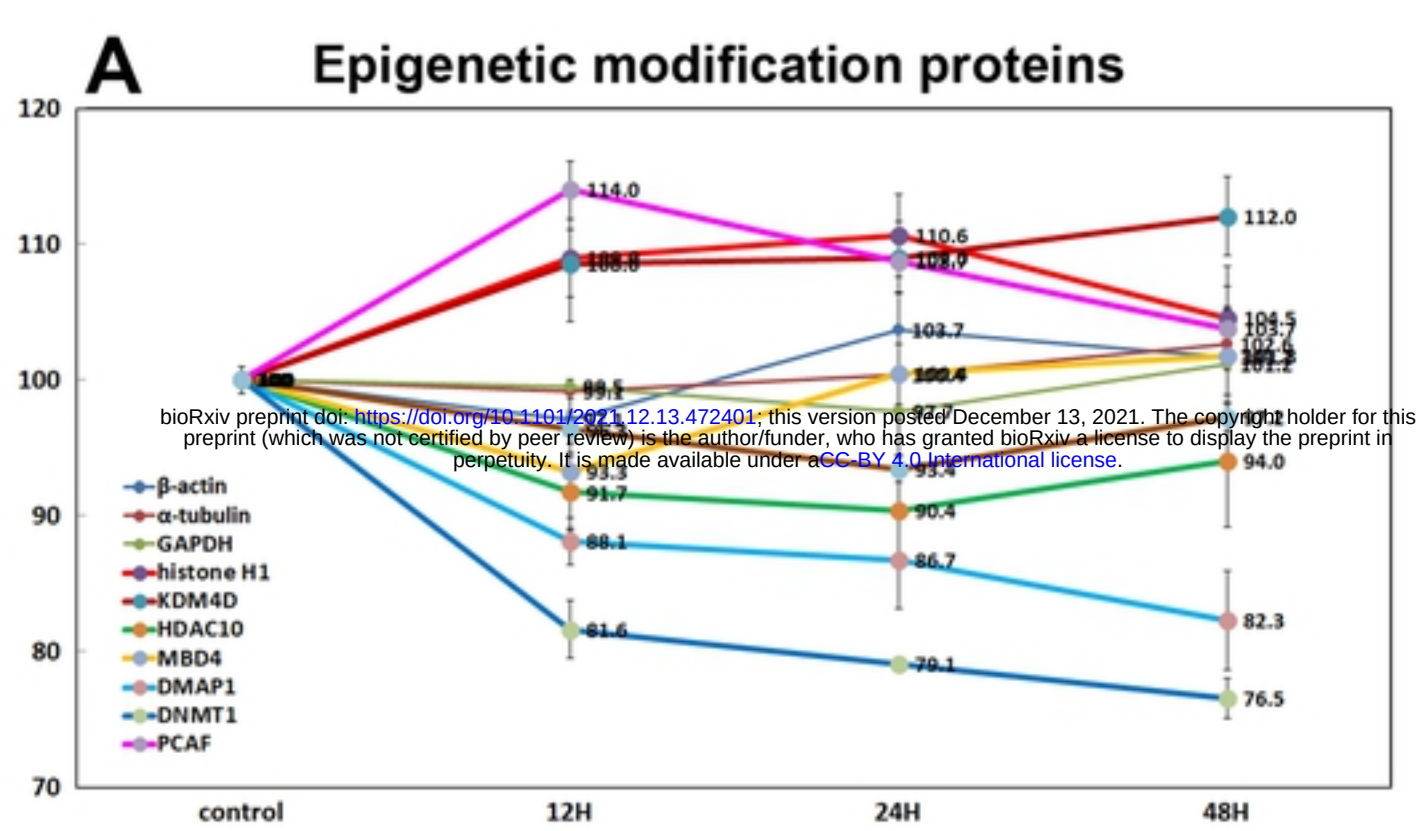

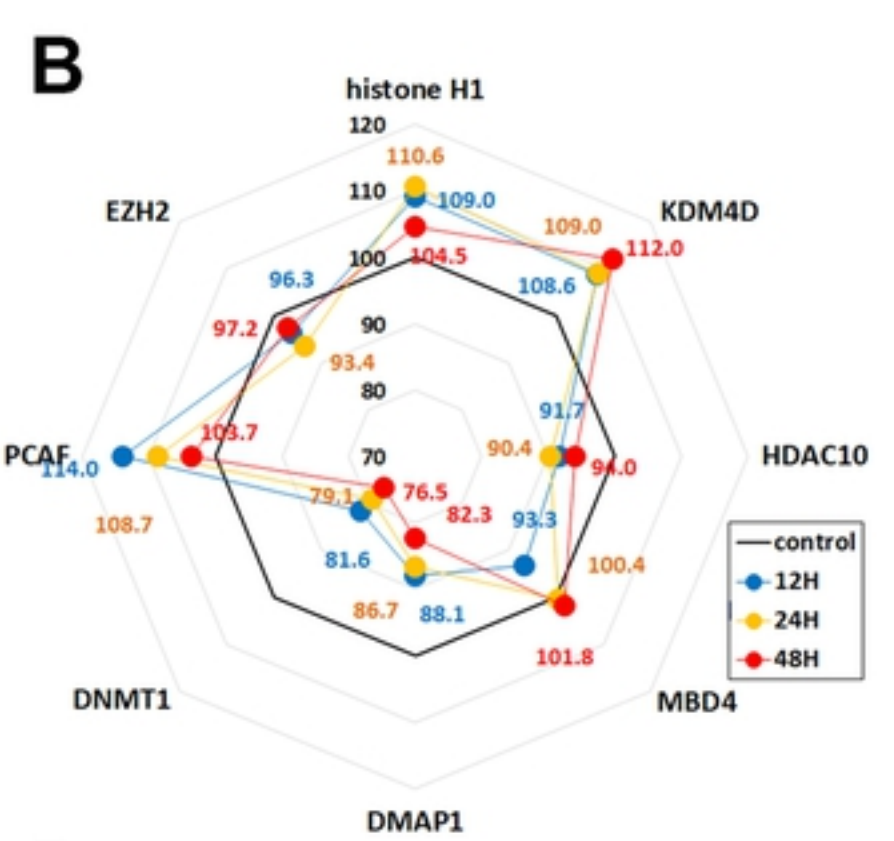

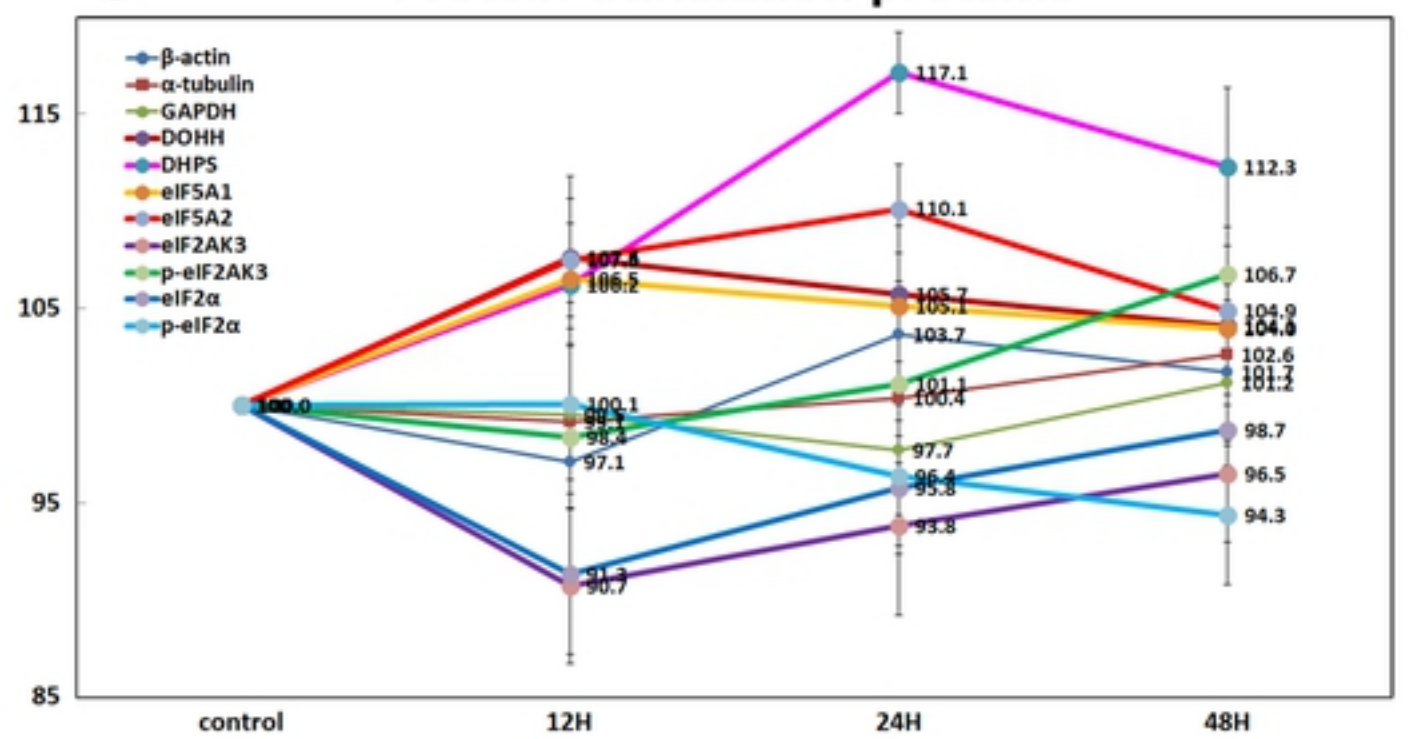

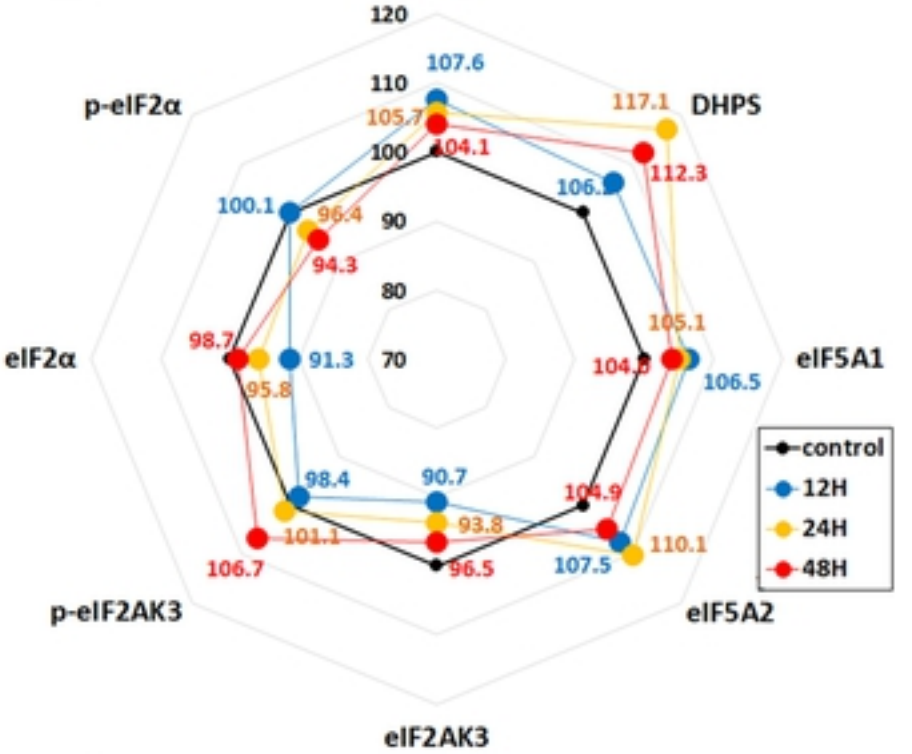

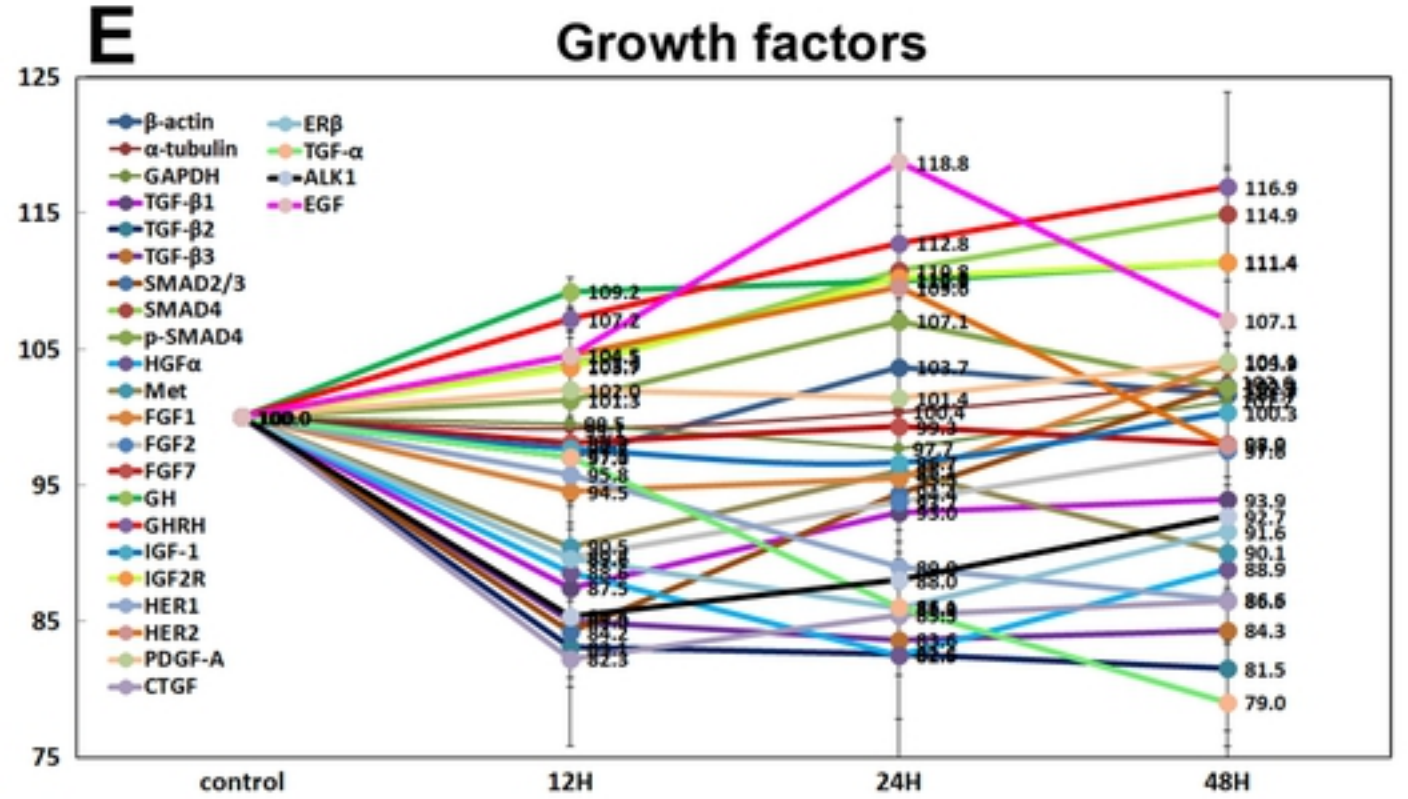

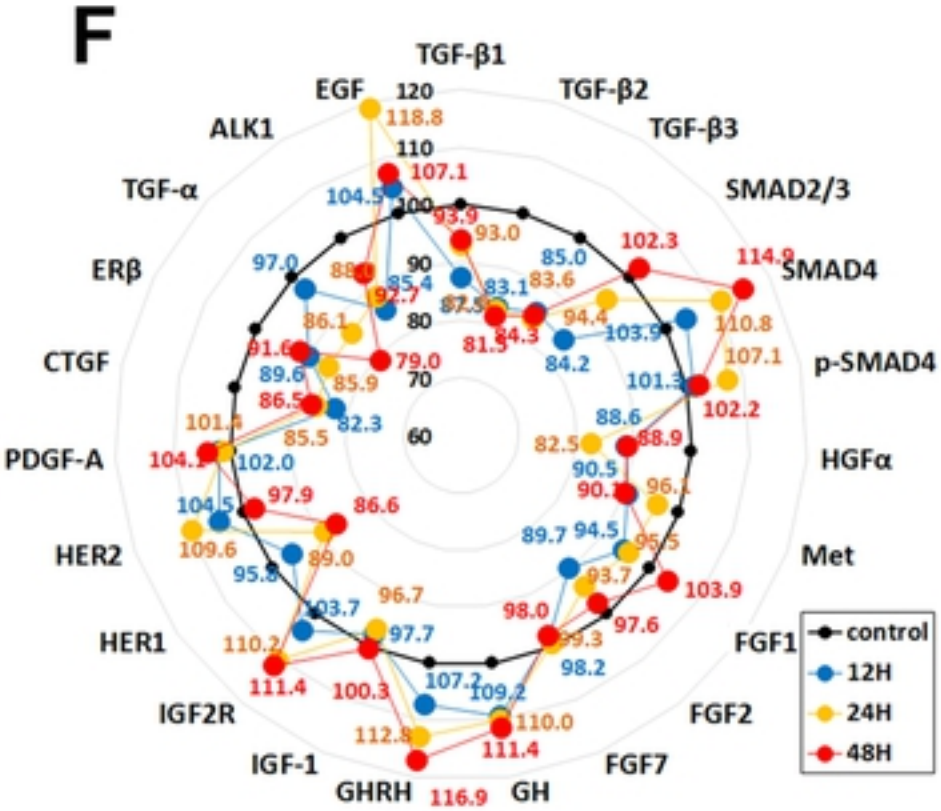

Figure 10

bioRxiv preprint doi: https://doi.org/10.1101/2021.12.13.472401; this version posted December 13, 2021. The copyright holder for this preprint (which was not certified by peer review) is the author/funder, who has granted bioRxiv a license to display the preprint in perpetuity. It is made available under aCC-BY 4.0 International license.

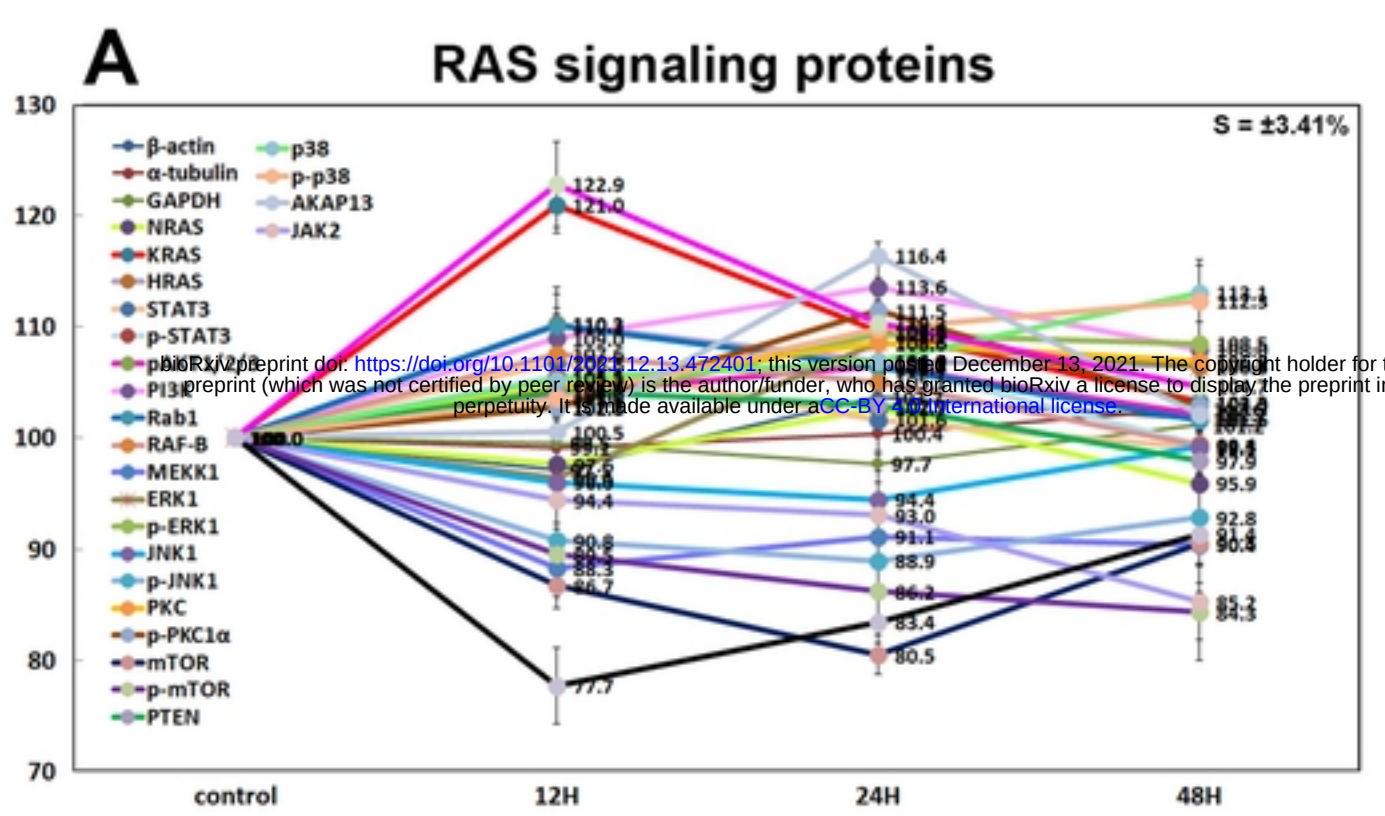

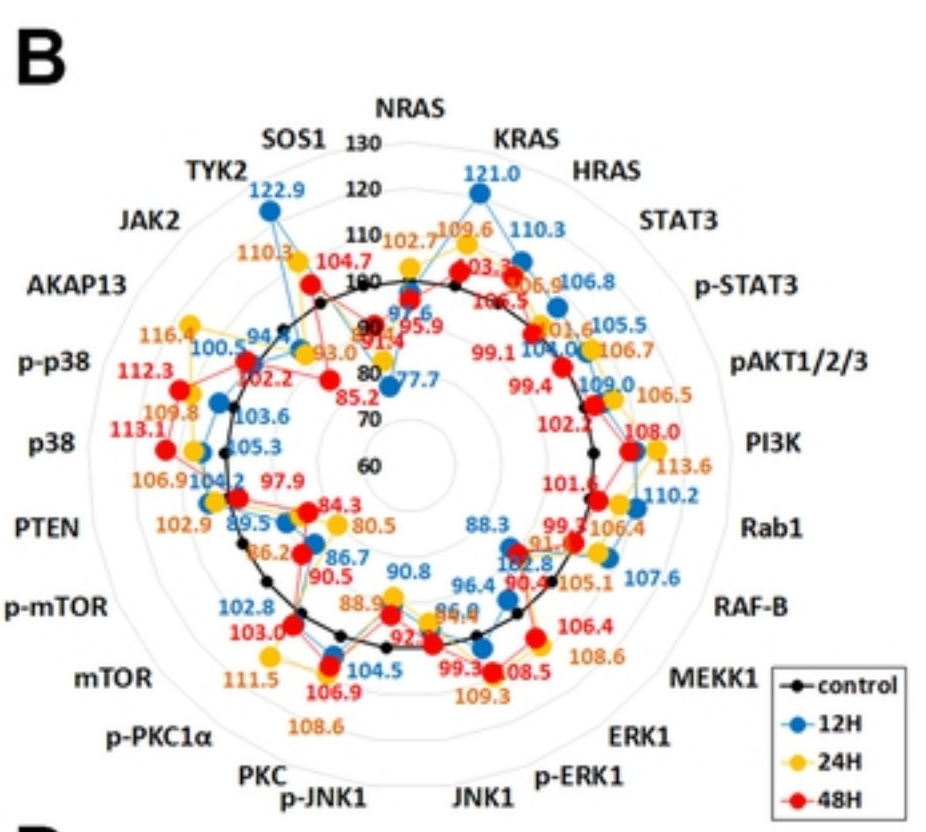

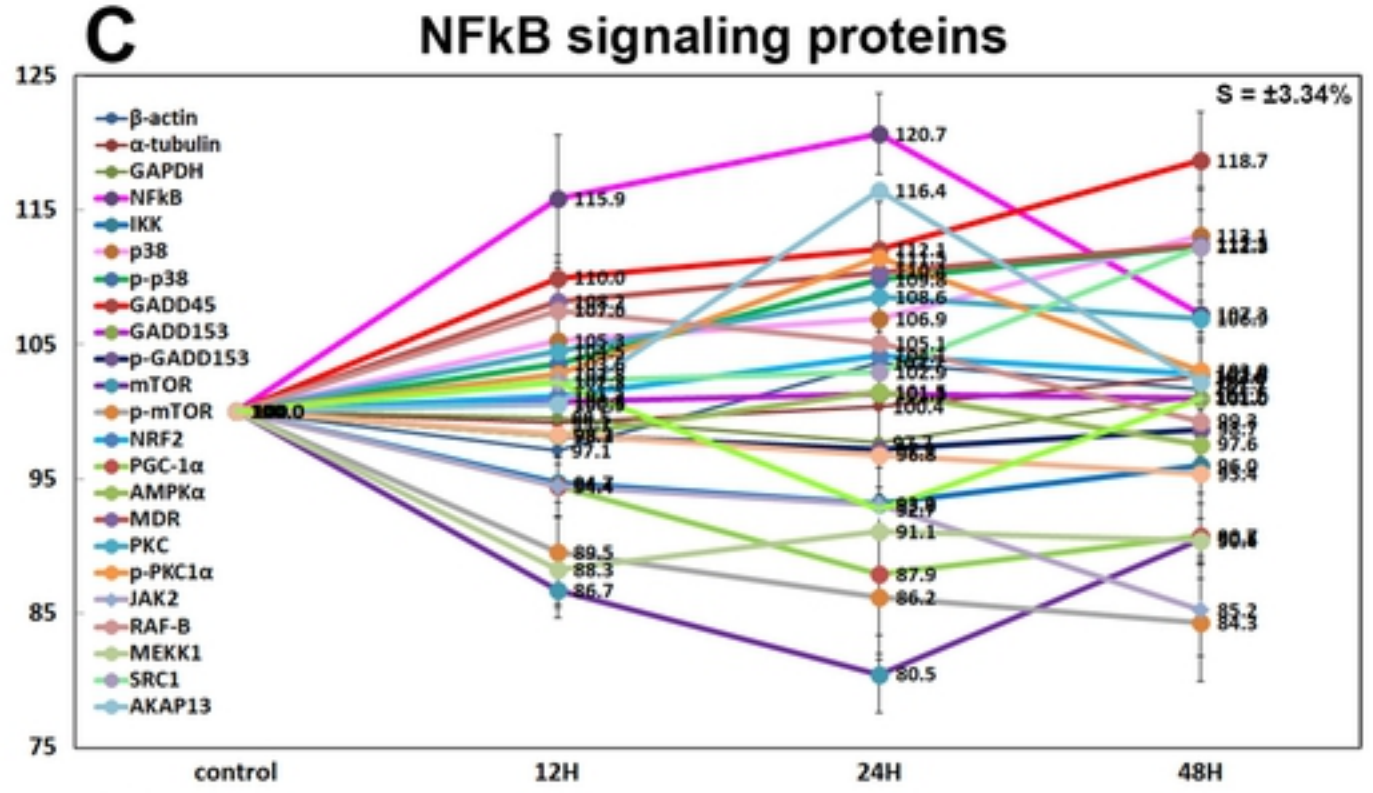

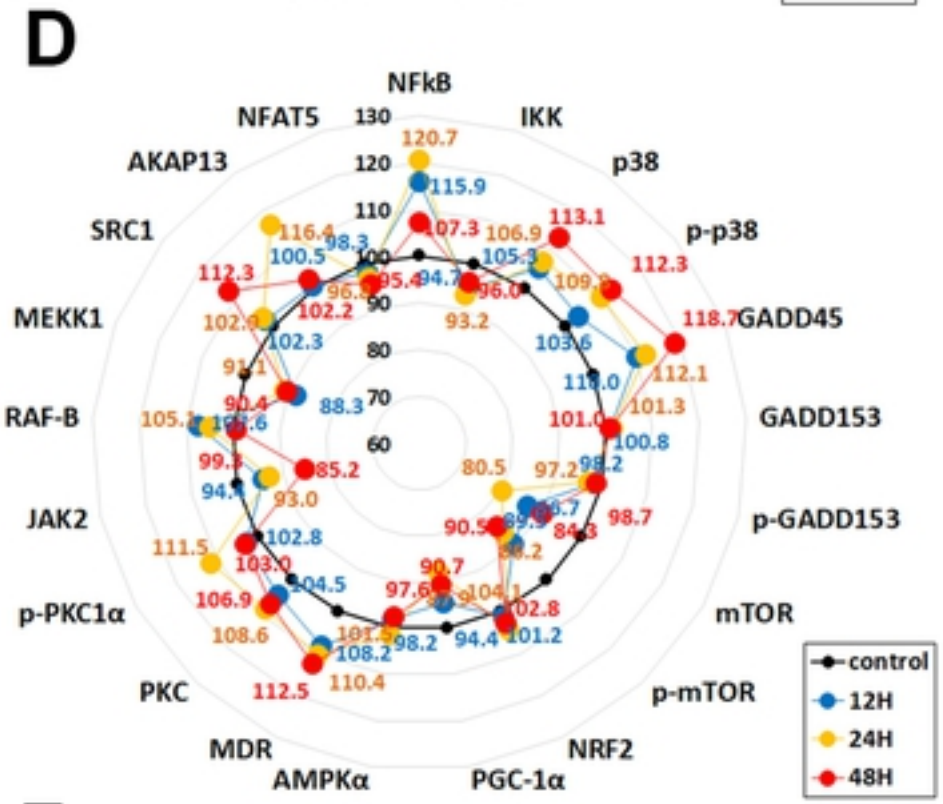

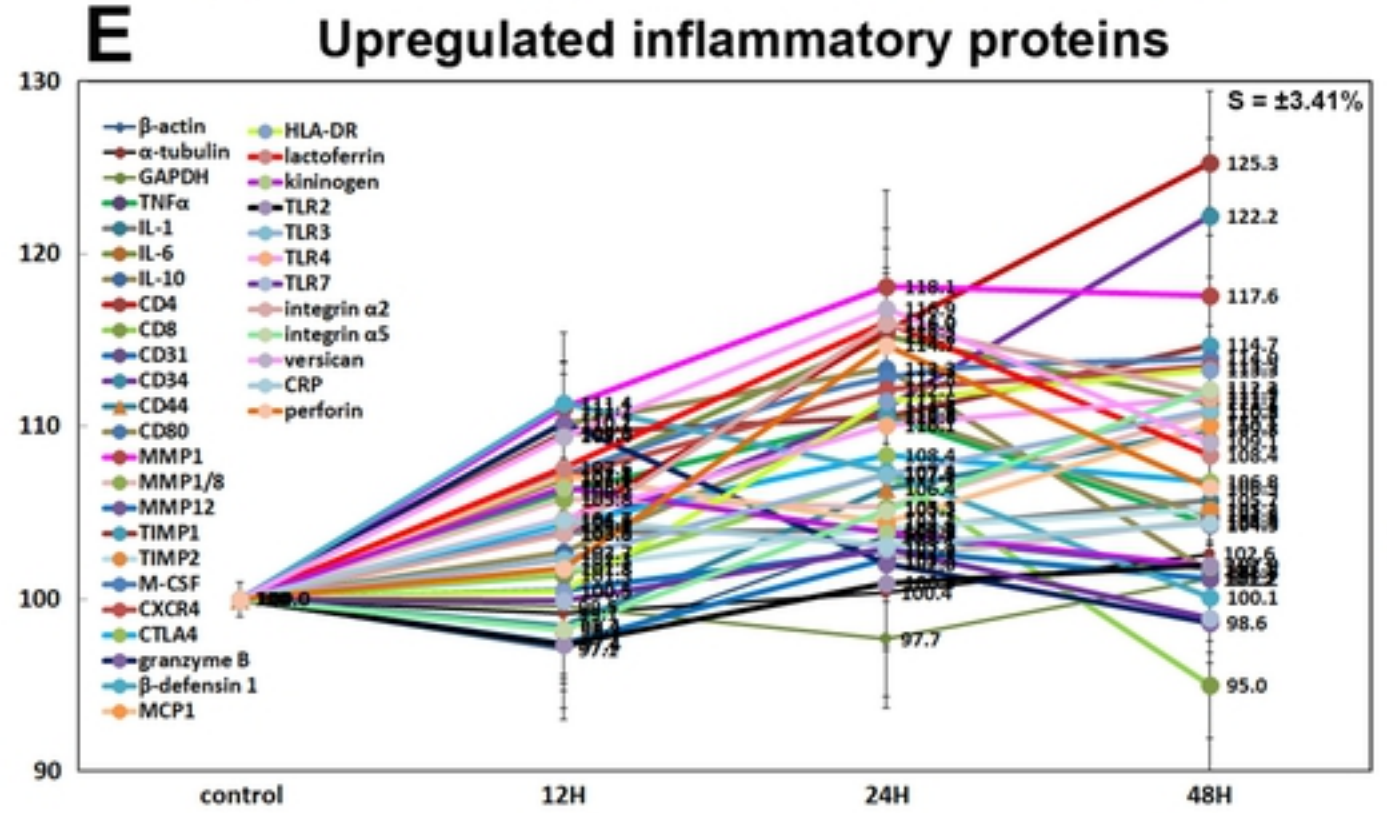

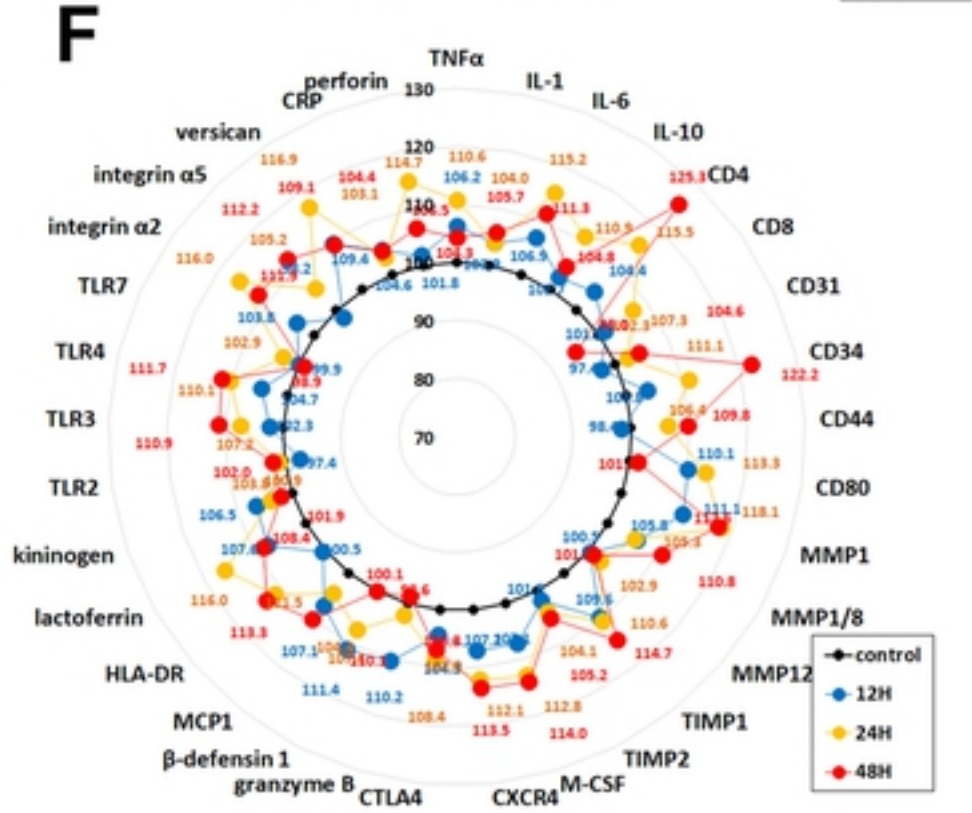

Figure 11

bioRxiv preprint doi: https://doi.org/10.1101/2021.12.13.472401; this version posted December 13, 2021. The copyright holder for this preprint (which was not certified by peer review) is the author/funder, who has granted bioRxiv a license to display the preprint in perpetuity. It is made available under aCC-BY 4.0 International license.

Figure 12

bioRxiv preprint doi: https://doi.org/10.1101/2021.12.13.472401; this version posted December 13, 2021. The copyright holder for this preprint (which was not certified by peer review) is the author/funder, who has granted bioRxiv a license to display the preprint in perpetuity. It is made available under aCC-BY 4.0 International license.

Figure 13

bioRxiv preprint doi: https://doi.org/10.1101/2021.12.13.472401; this version posted December 13, 2021. The copyright holder for this preprint (which was not certified by peer review) is the author/funder, who has granted bioRxiv a license to display the preprint in perpetuity. It is made available under aCC-BY 4.0 International license.

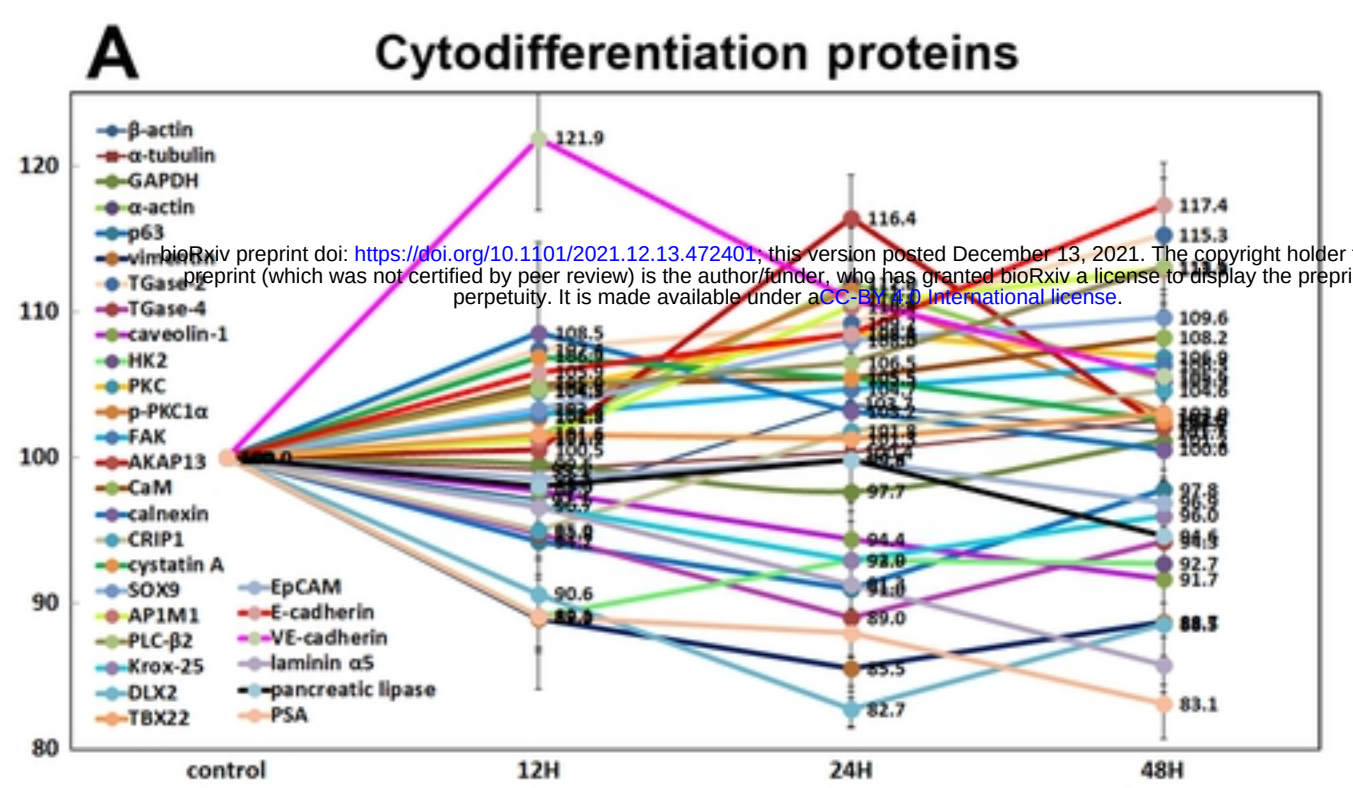

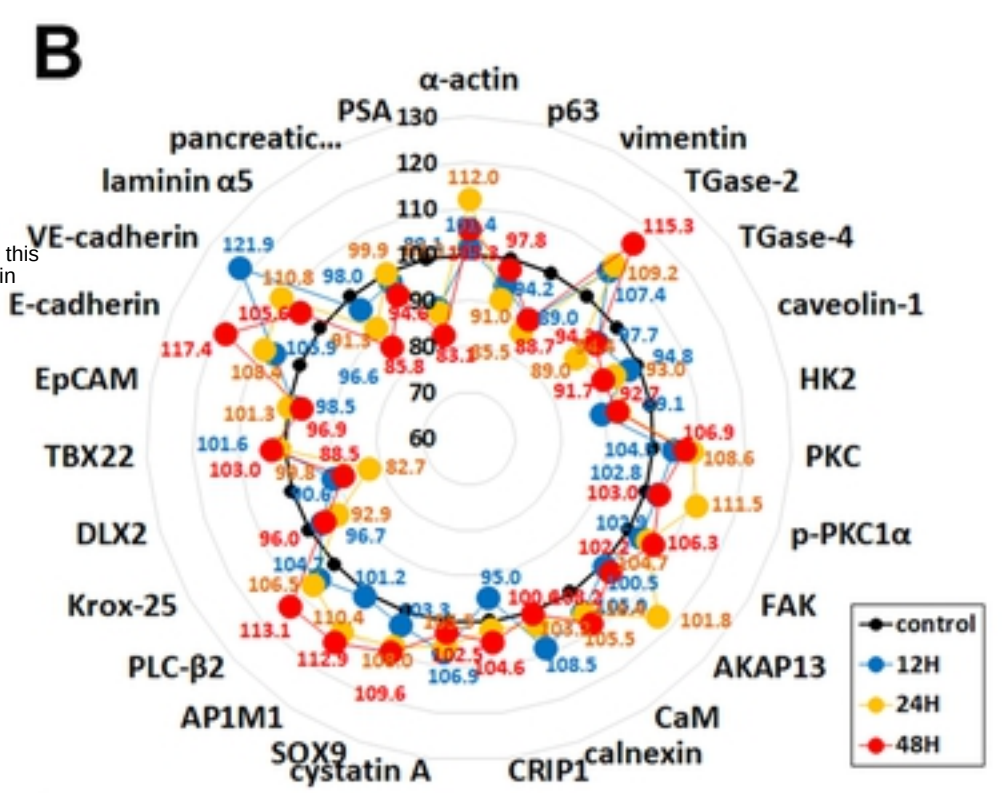

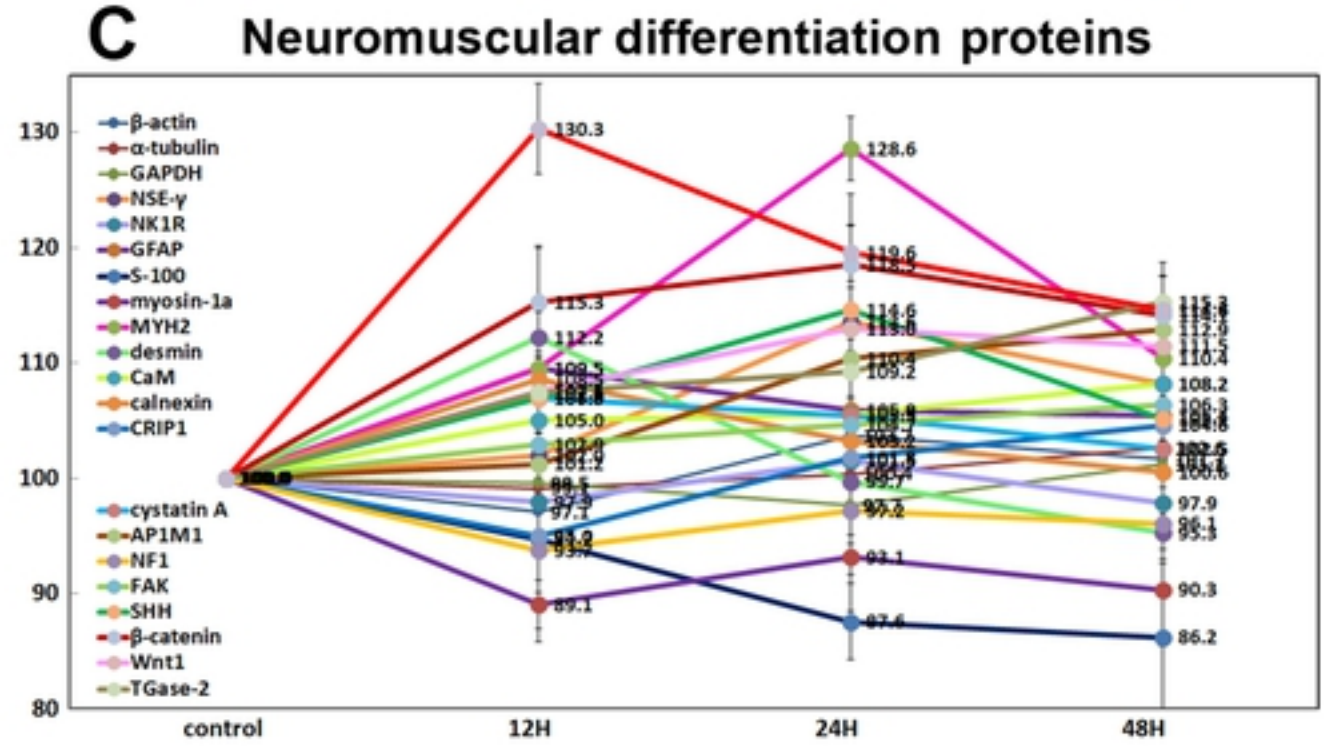

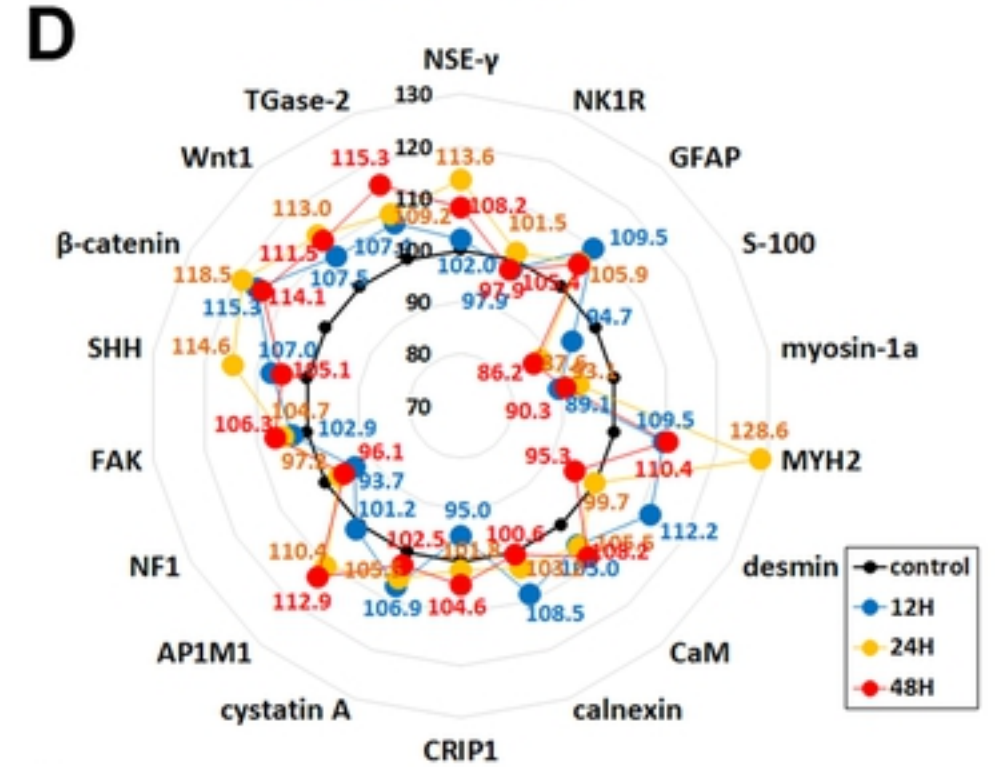

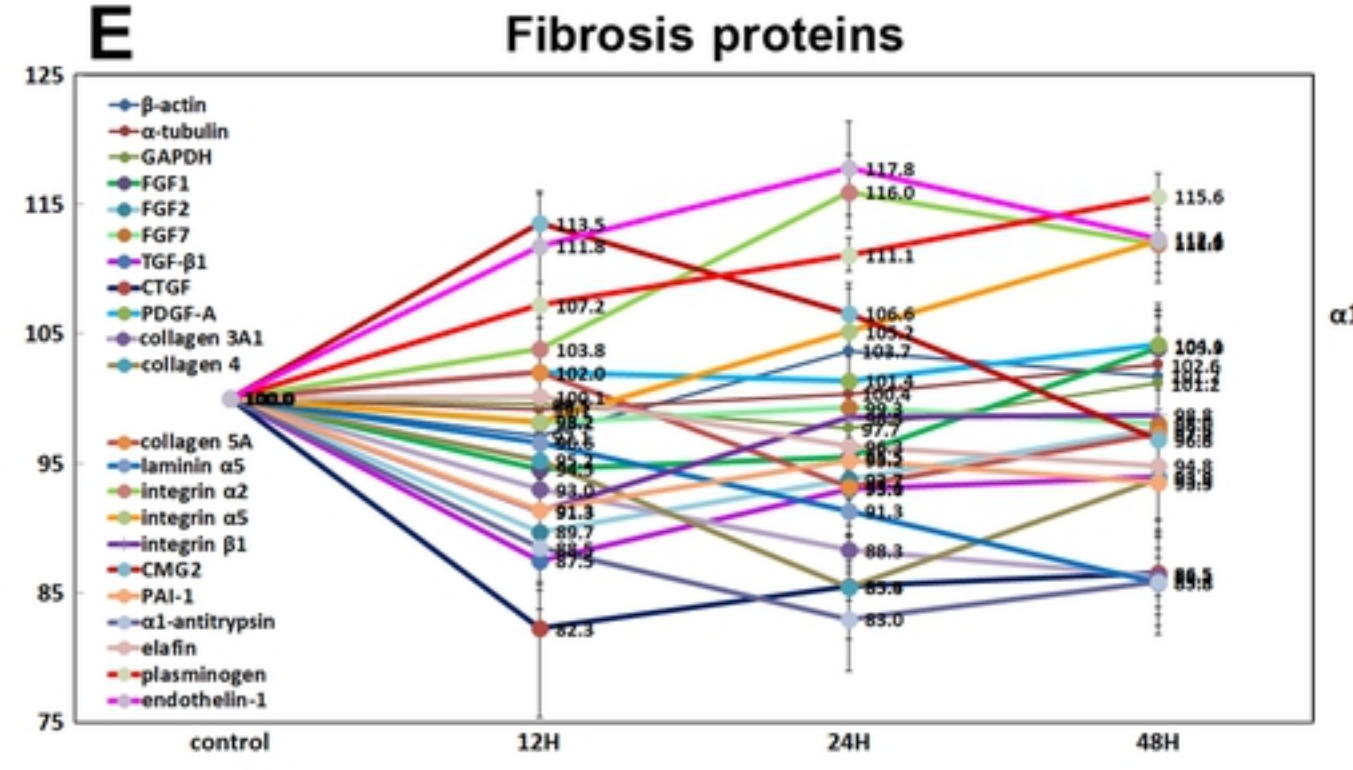

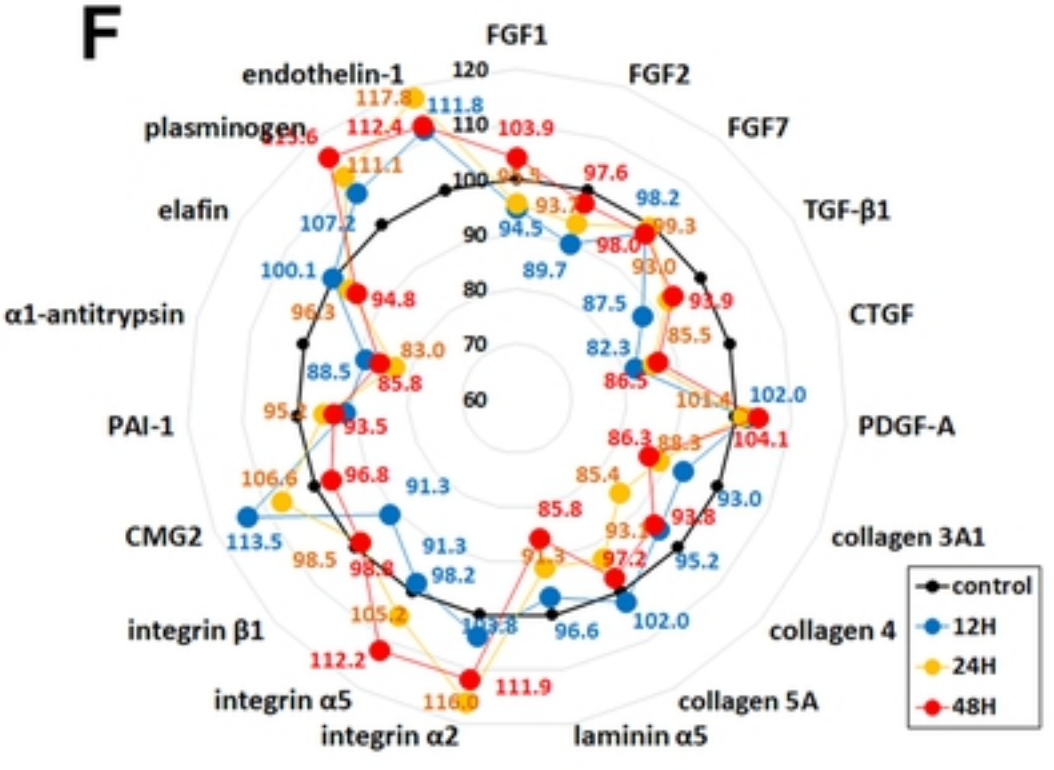

Figure 14

bioRxiv preprint doi: https://doi.org/10.1101/2021.12.13.472401; this version posted December 13, 2021. The copyright holder for this preprint (which was not certified by peer review) is the author/funder, who has granted bioRxiv a license to display the preprint in perpetuity. It is made available under aCC-BY 4.0 International license.

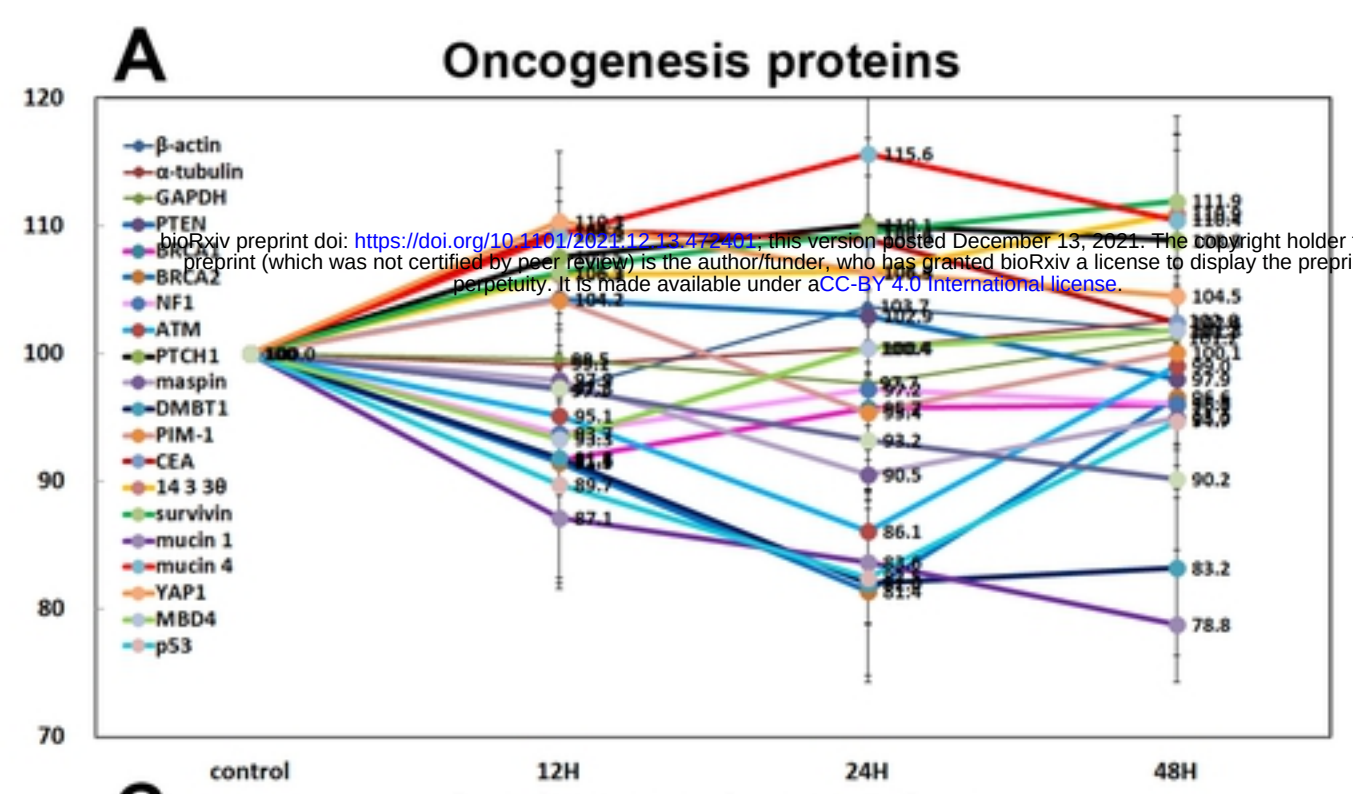

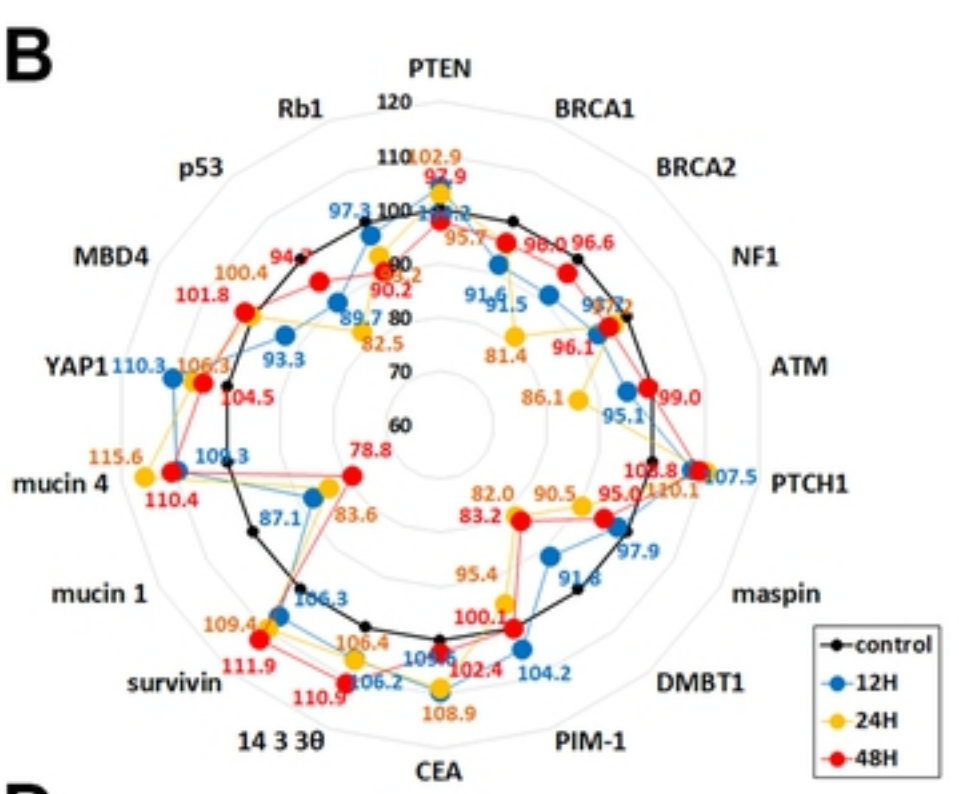

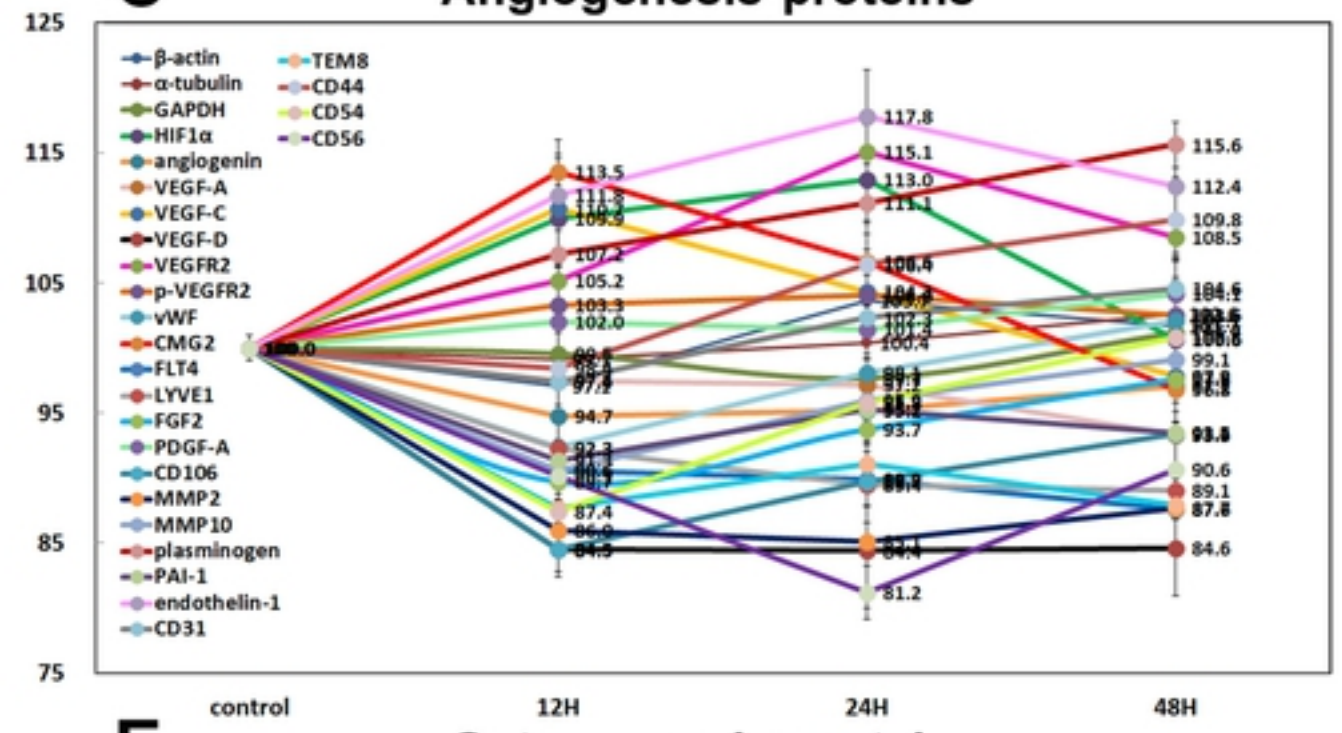

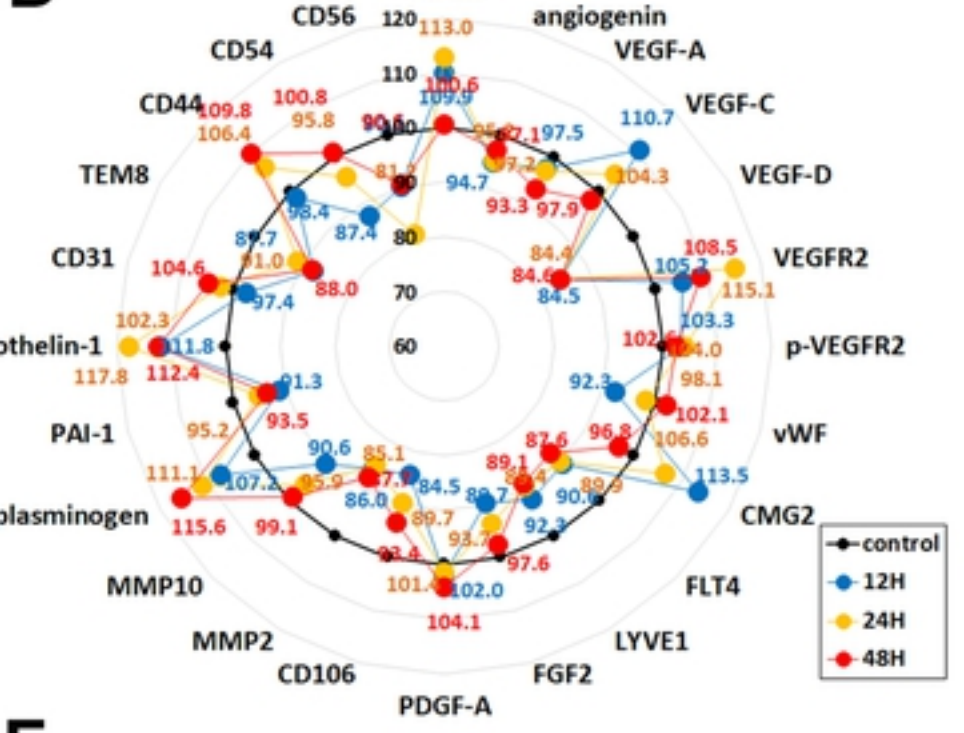

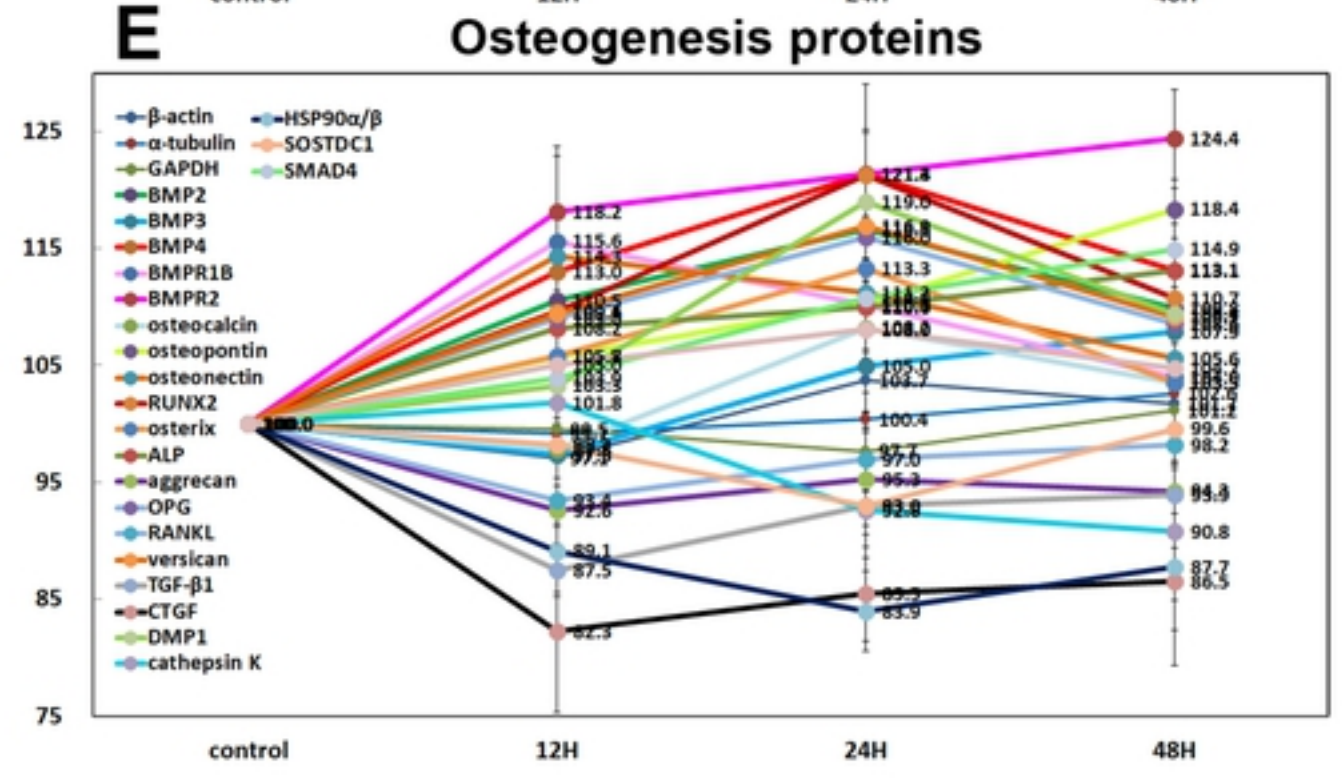

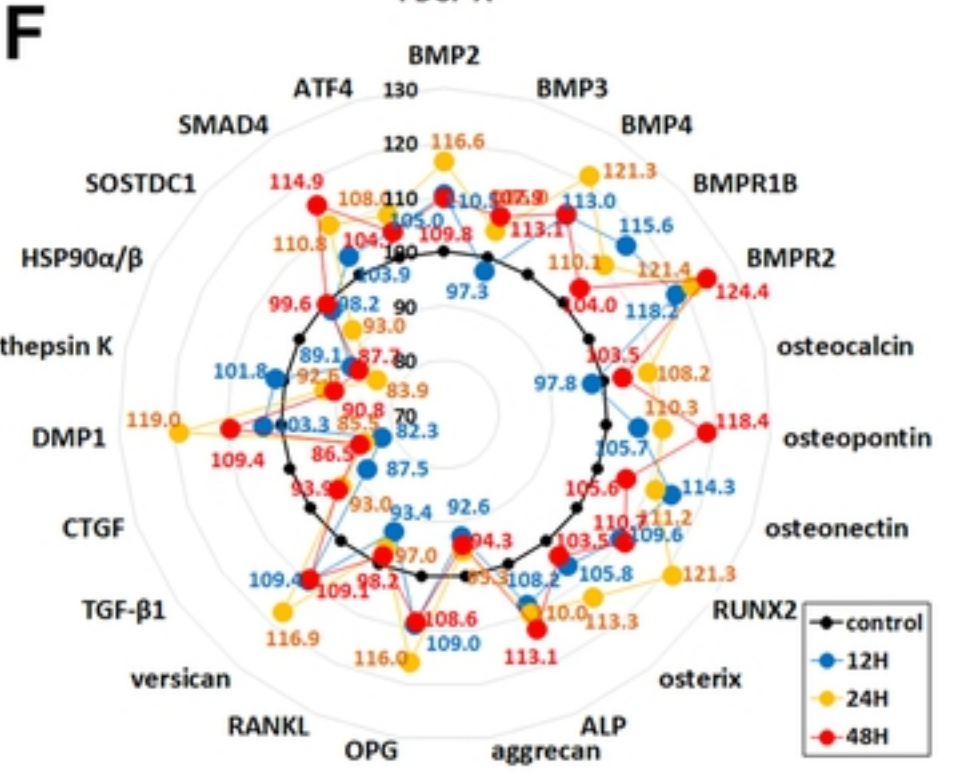

Figure 15

bioRxiv preprint doi: https://doi.org/10.1101/2021.12.13.472401; this version posted December 13, 2021. The copyright holder for this preprint (which was not certified by peer review) is the author/funder, who has granted bioRxiv a license to display the preprint in perpetuity. It is made available under aCC-BY 4.0 International license.

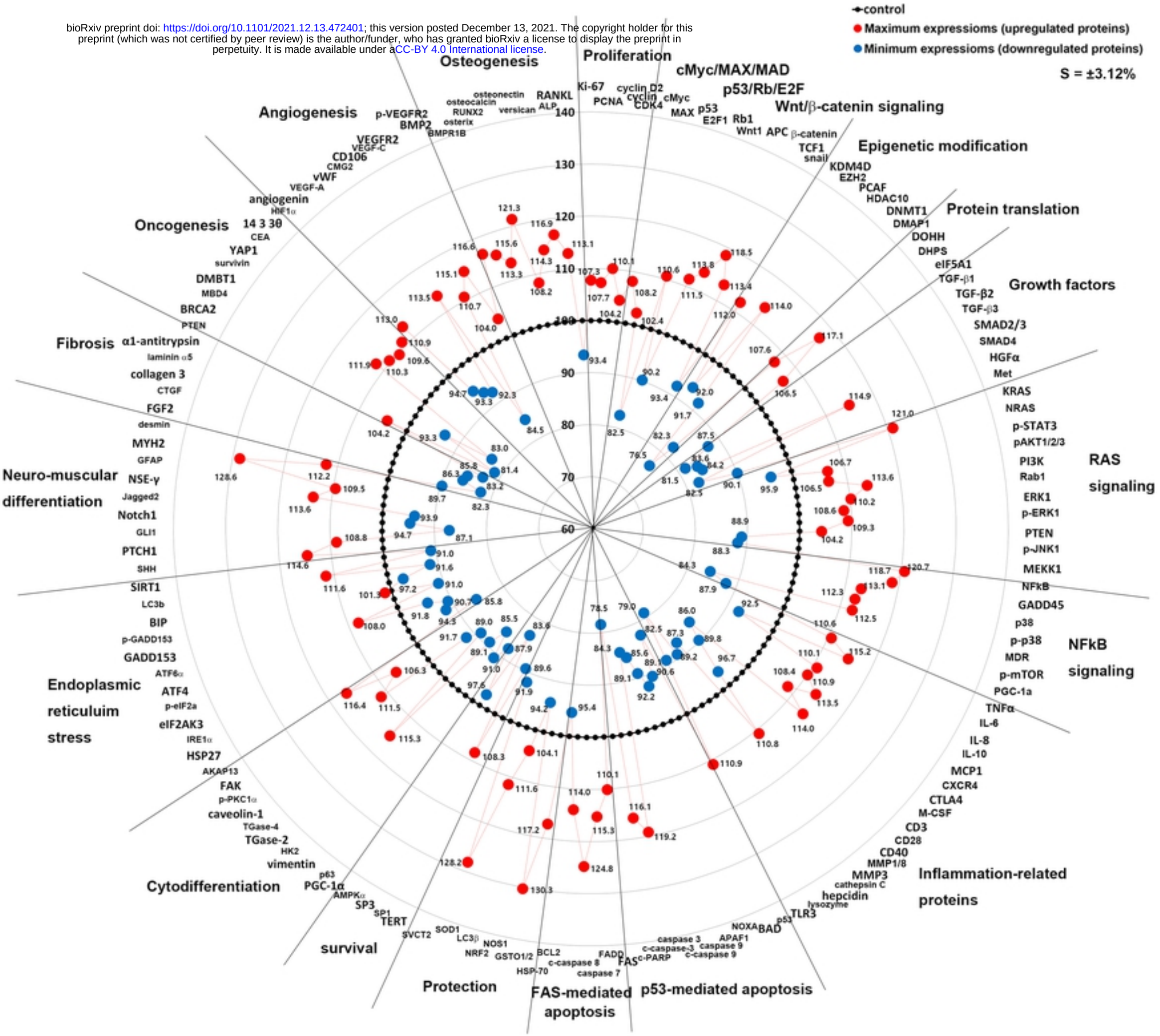

Figure 16

bioRxiv preprint doi: https://doi.org/10.1101/2021.12.13.472401; this version posted December 13, 2021. The copyright holder for this preprint (which was not certified by peer review) is the author/funder, who has granted bioRxiv a license to display the preprint in perpetuity. It is made available under aCC-BY 4.0 International license.

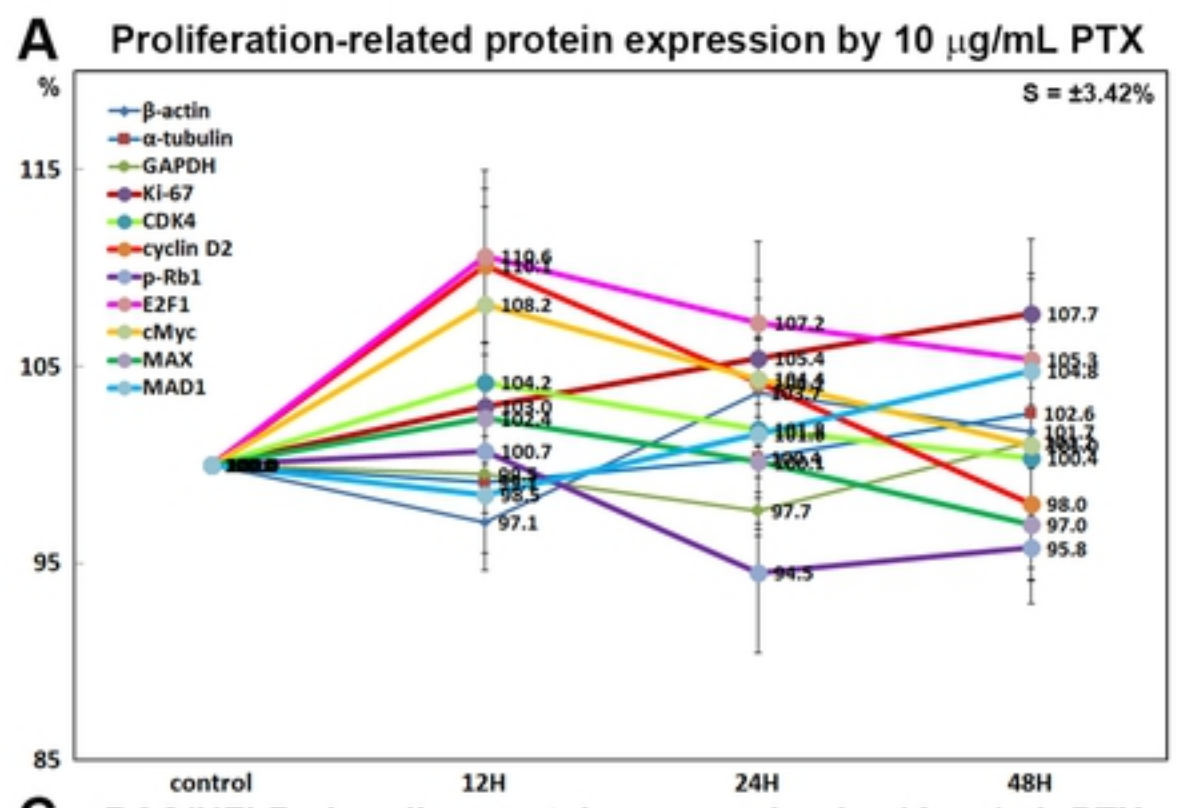

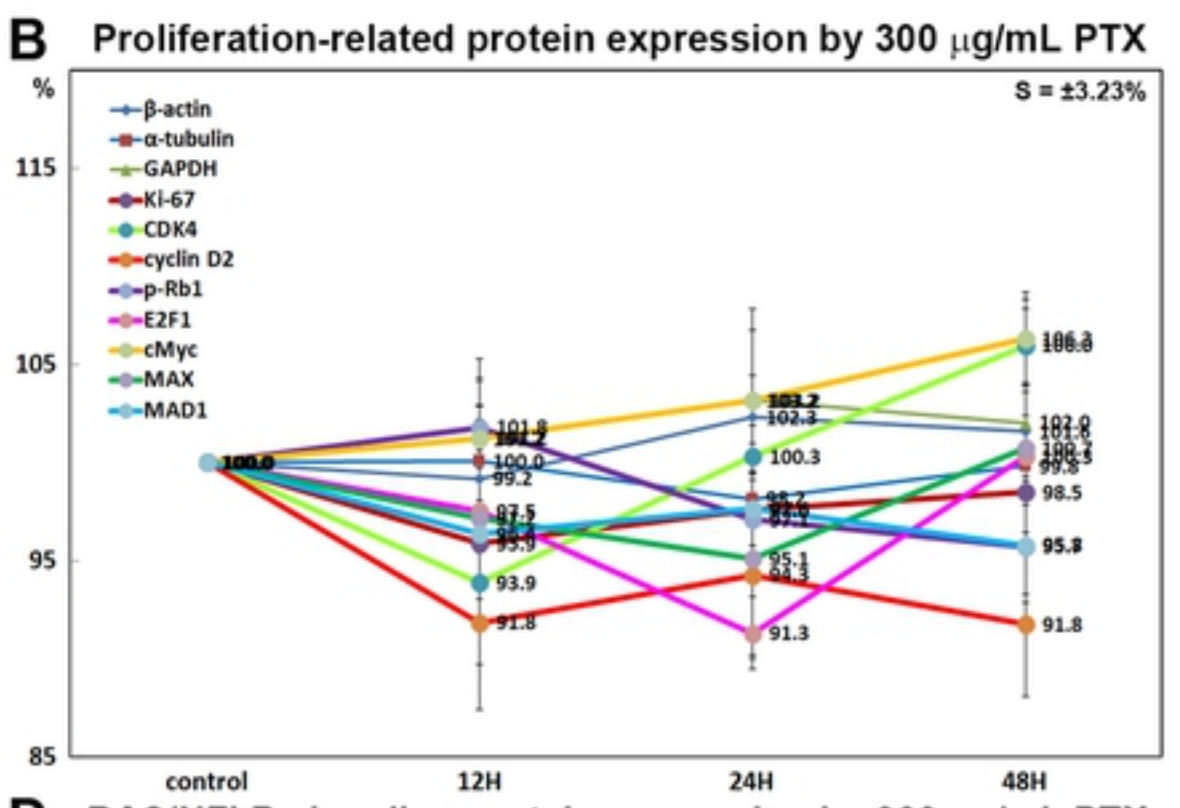

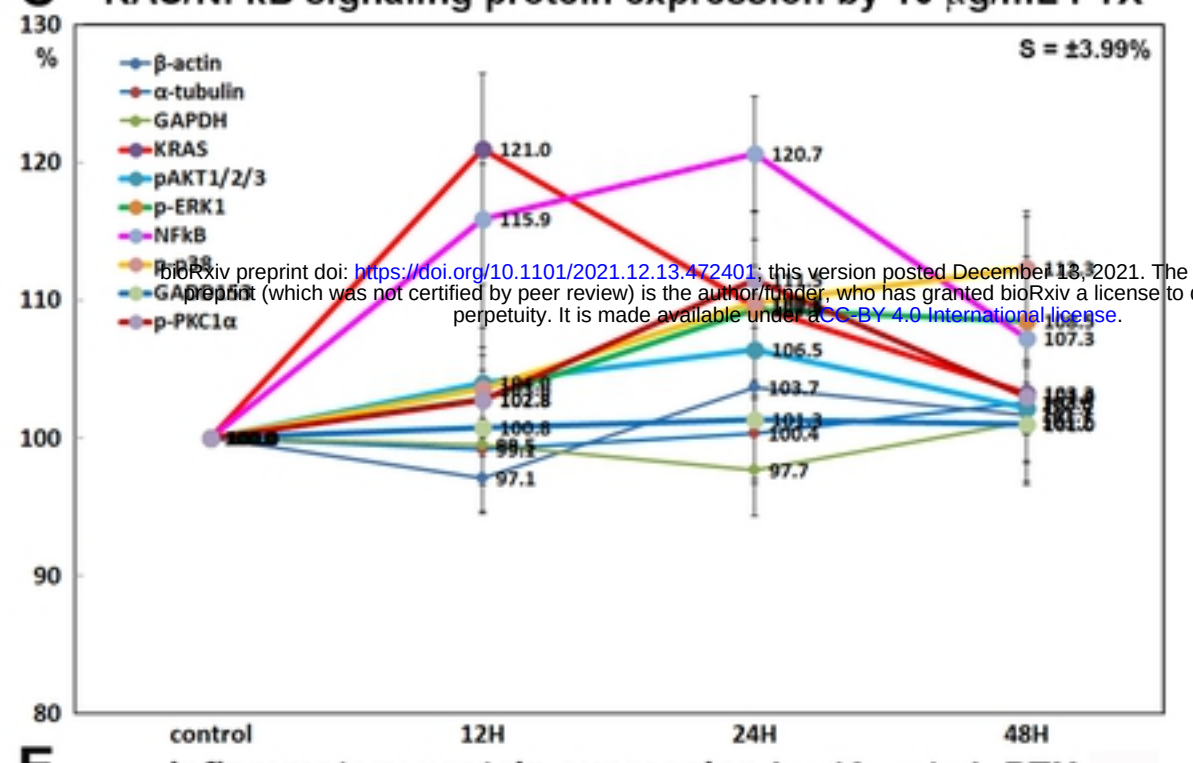

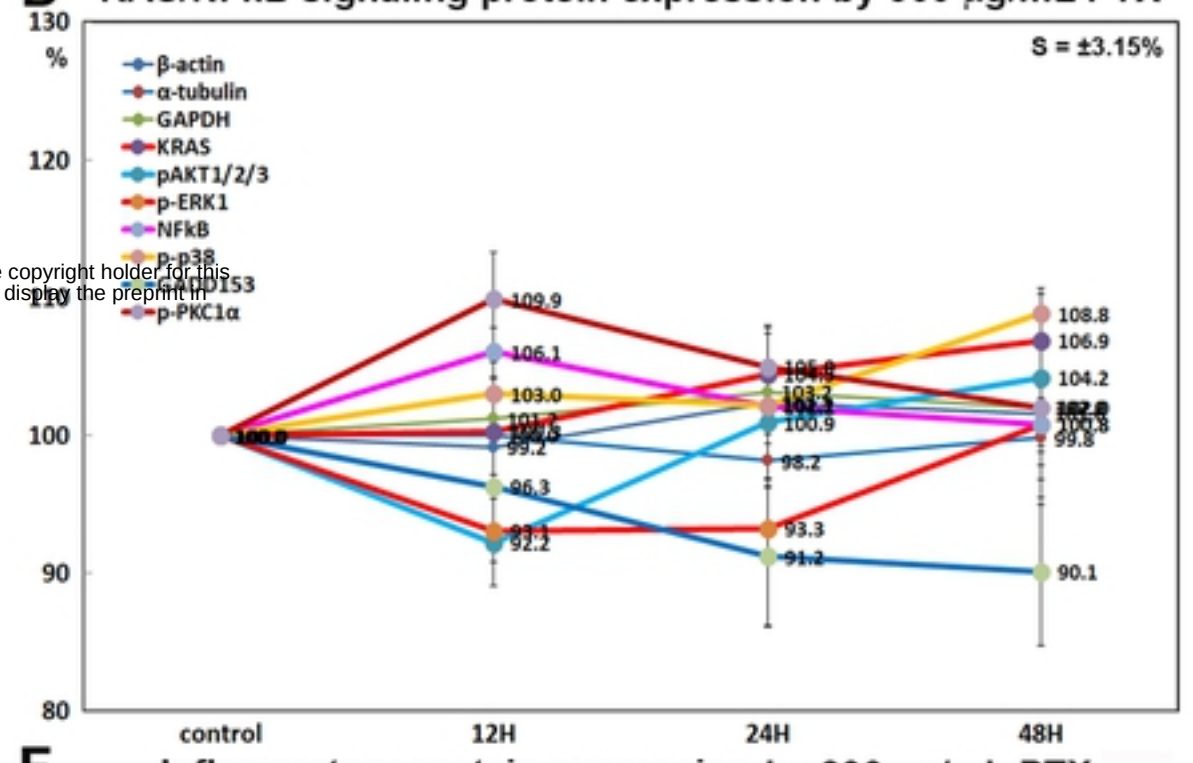

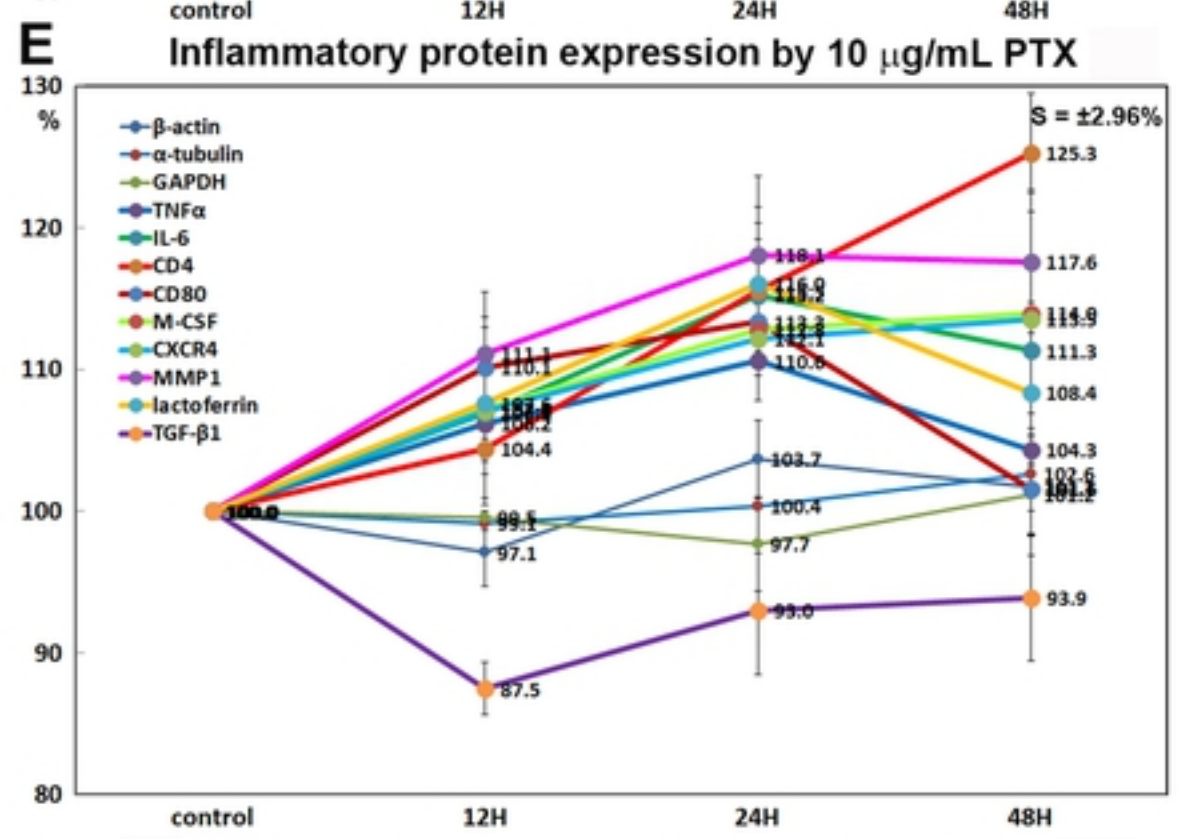

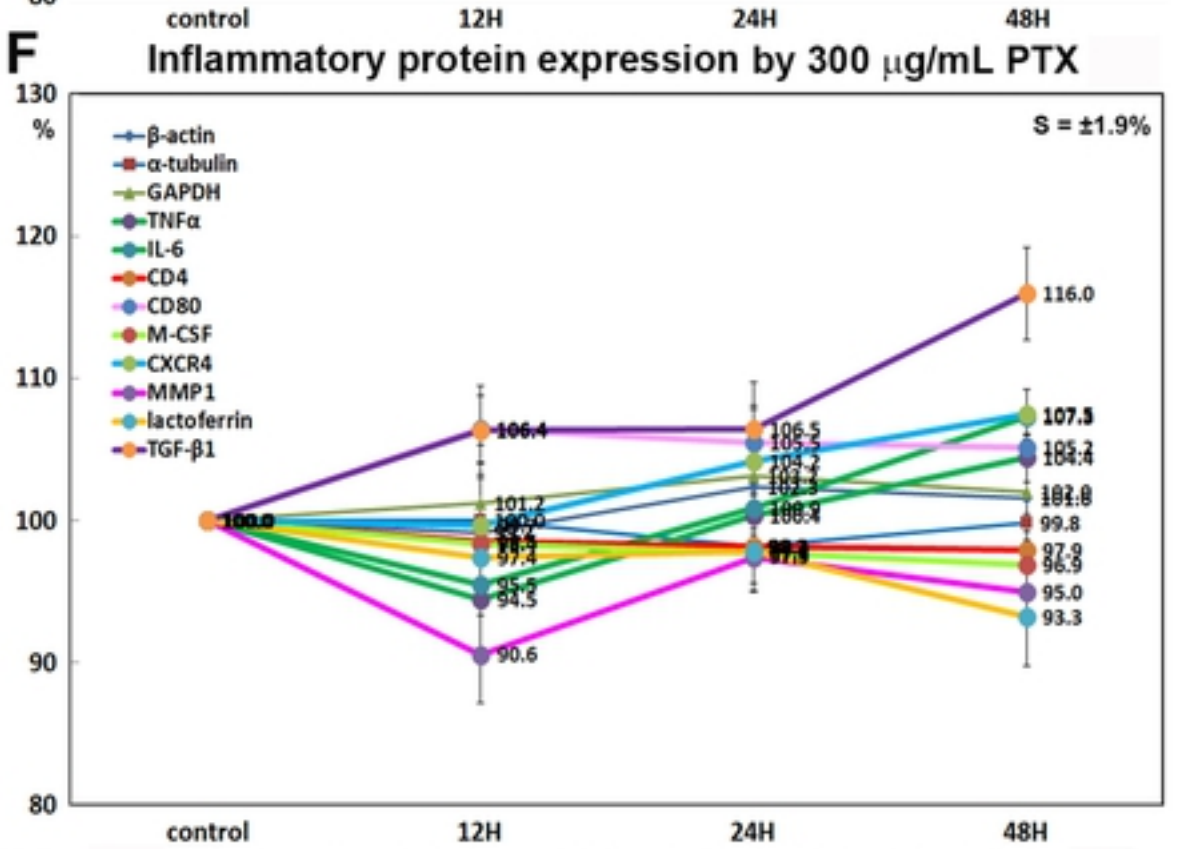

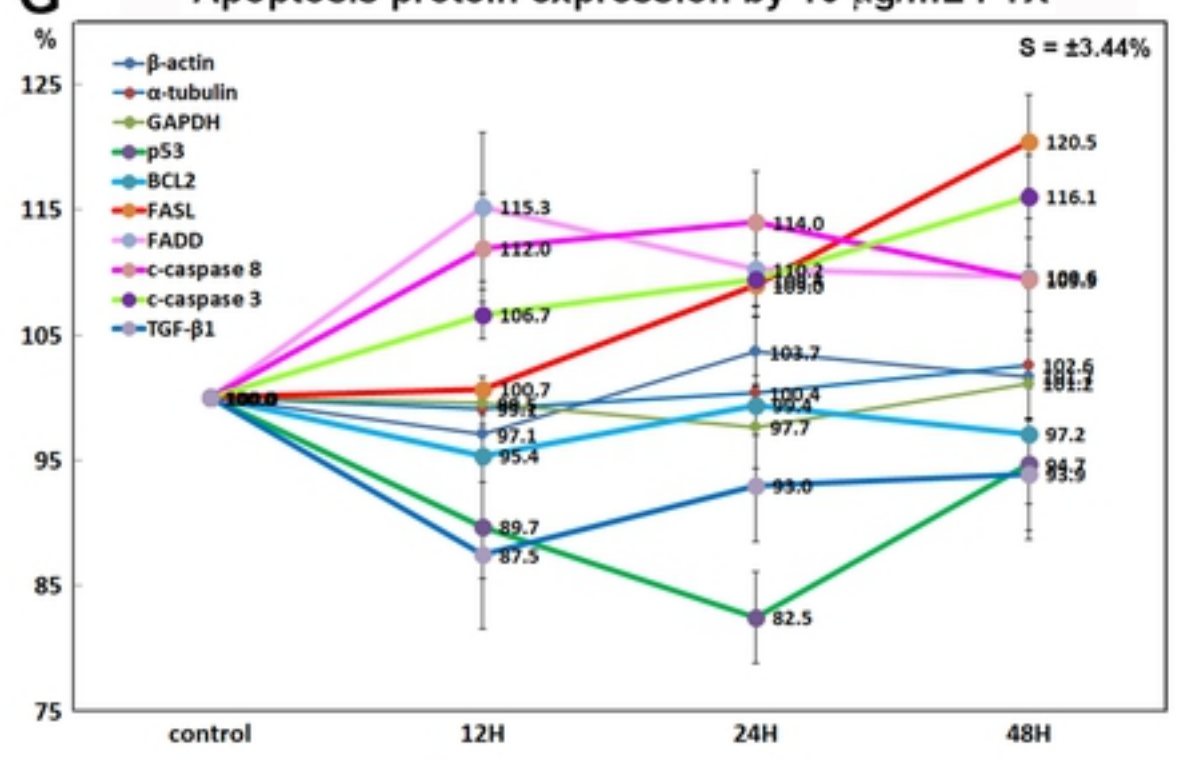

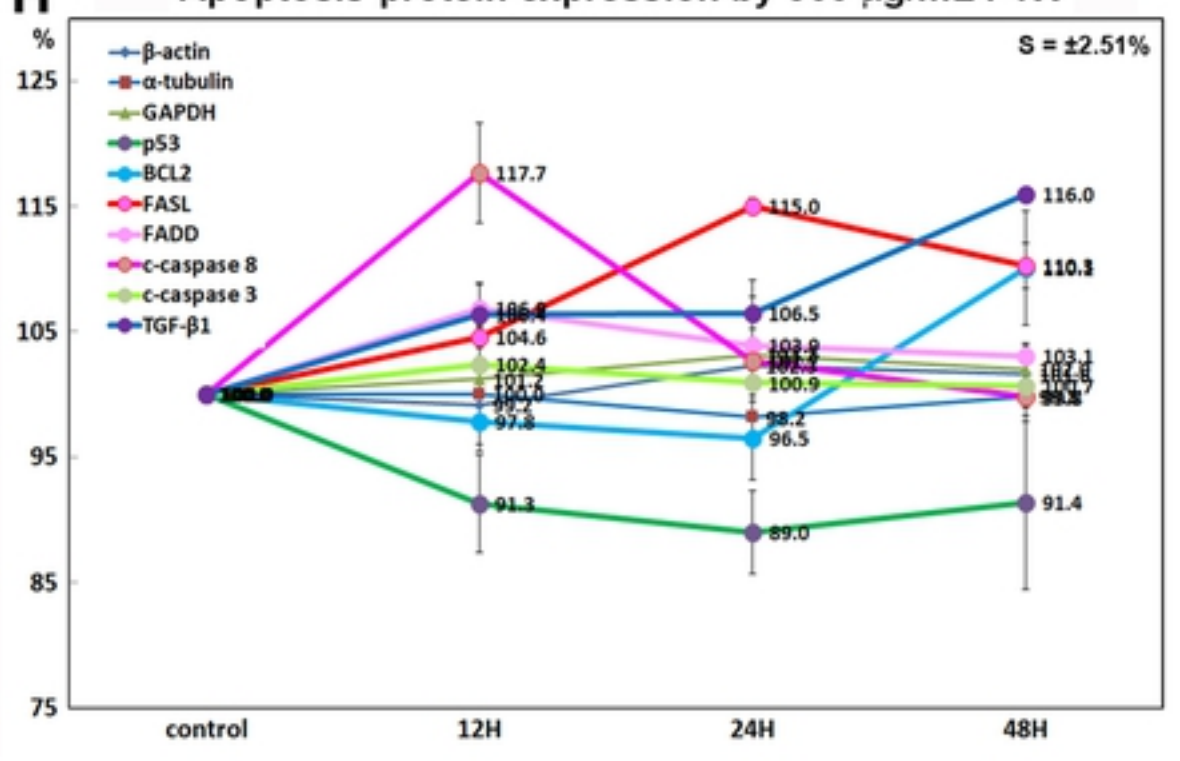

Figure 17

bioRxiv preprint doi: https://doi.org/10.1101/2021.12.13.472401; this version posted December 13, 2021. The copyright holder for this preprint (which was not certified by peer review) is the author/funder, who has granted bioRxiv a license to display the preprint in perpetuity. It is made available under aCC-BY 4.0 International license.

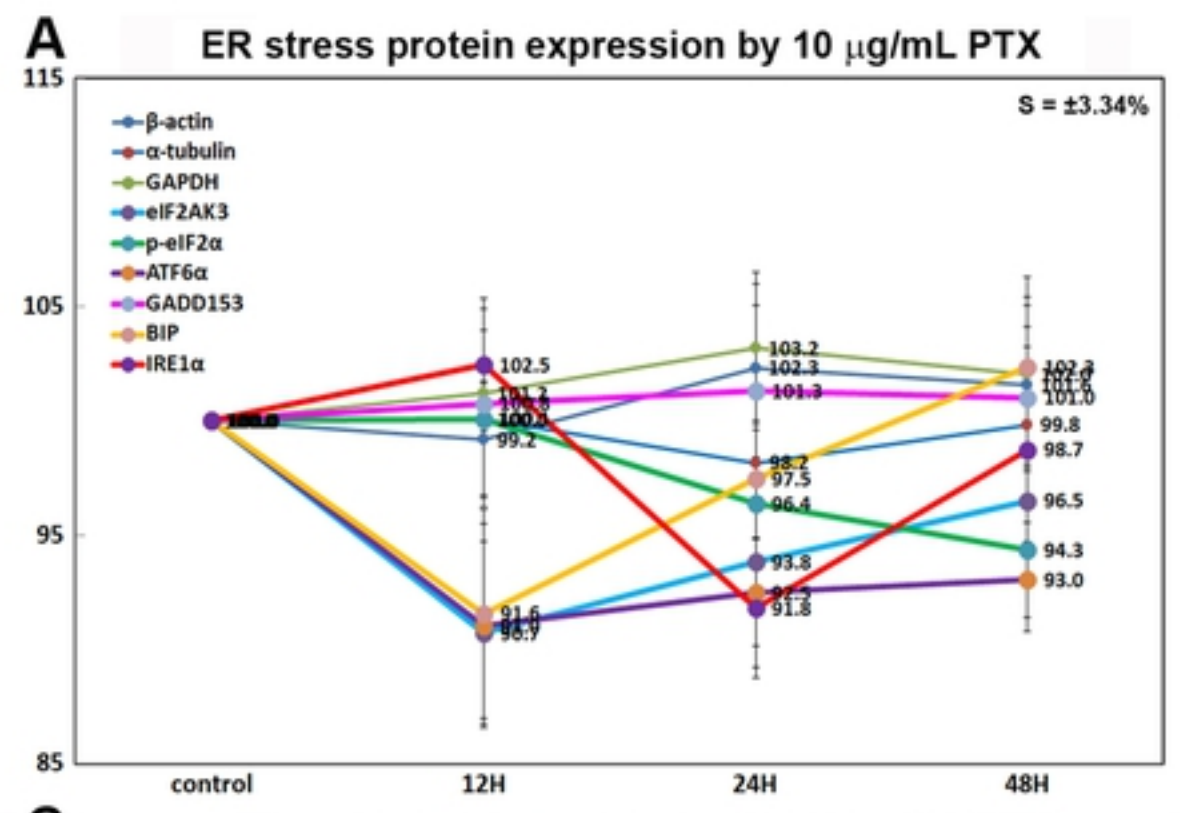

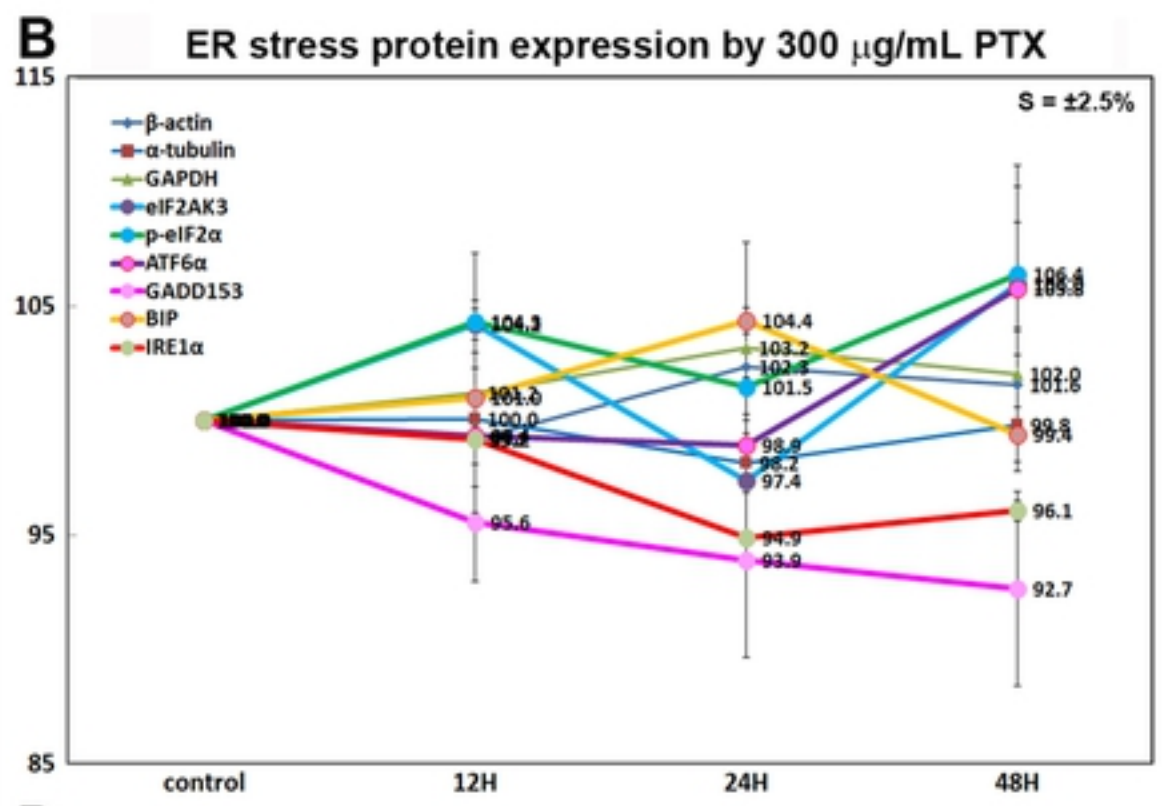

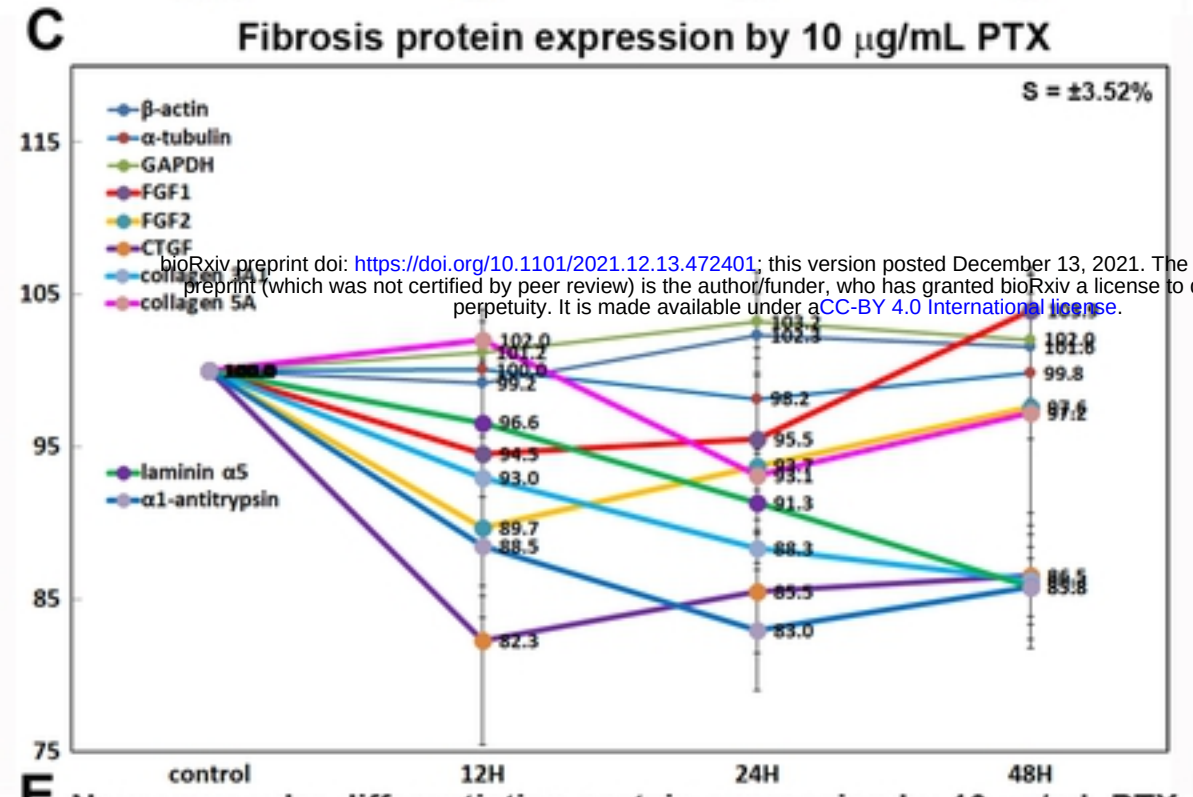

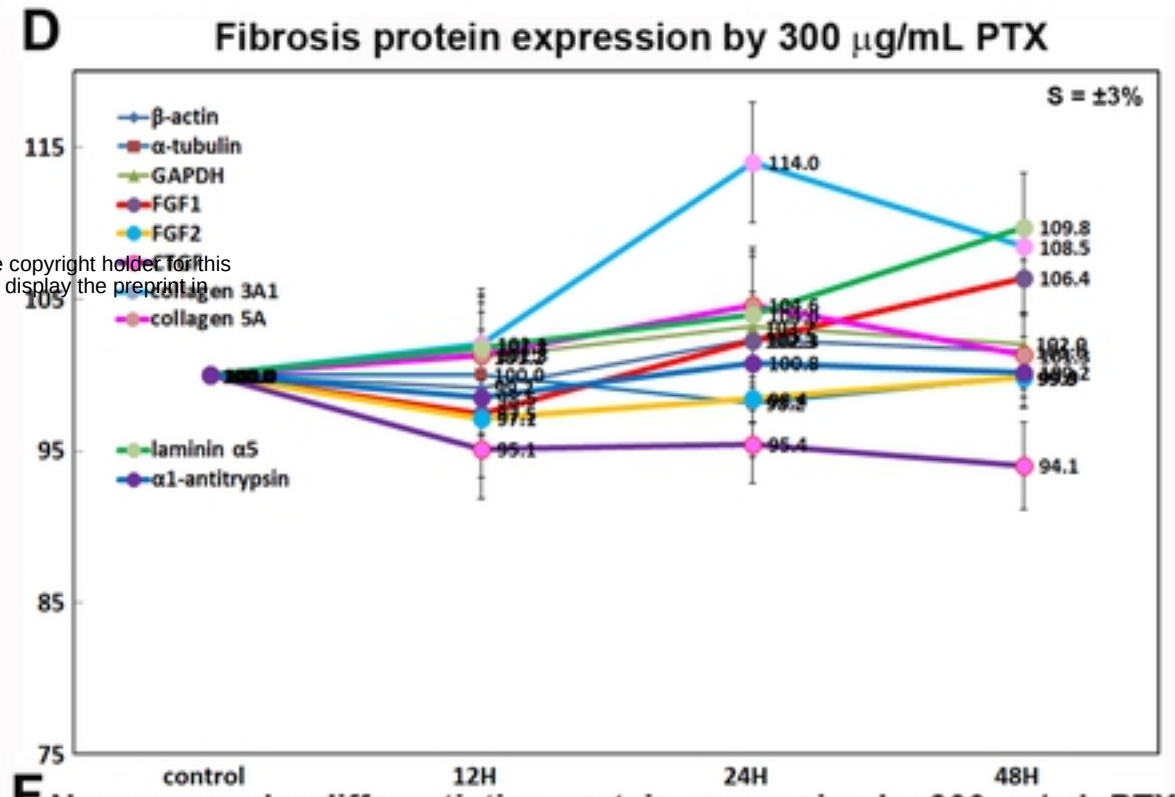

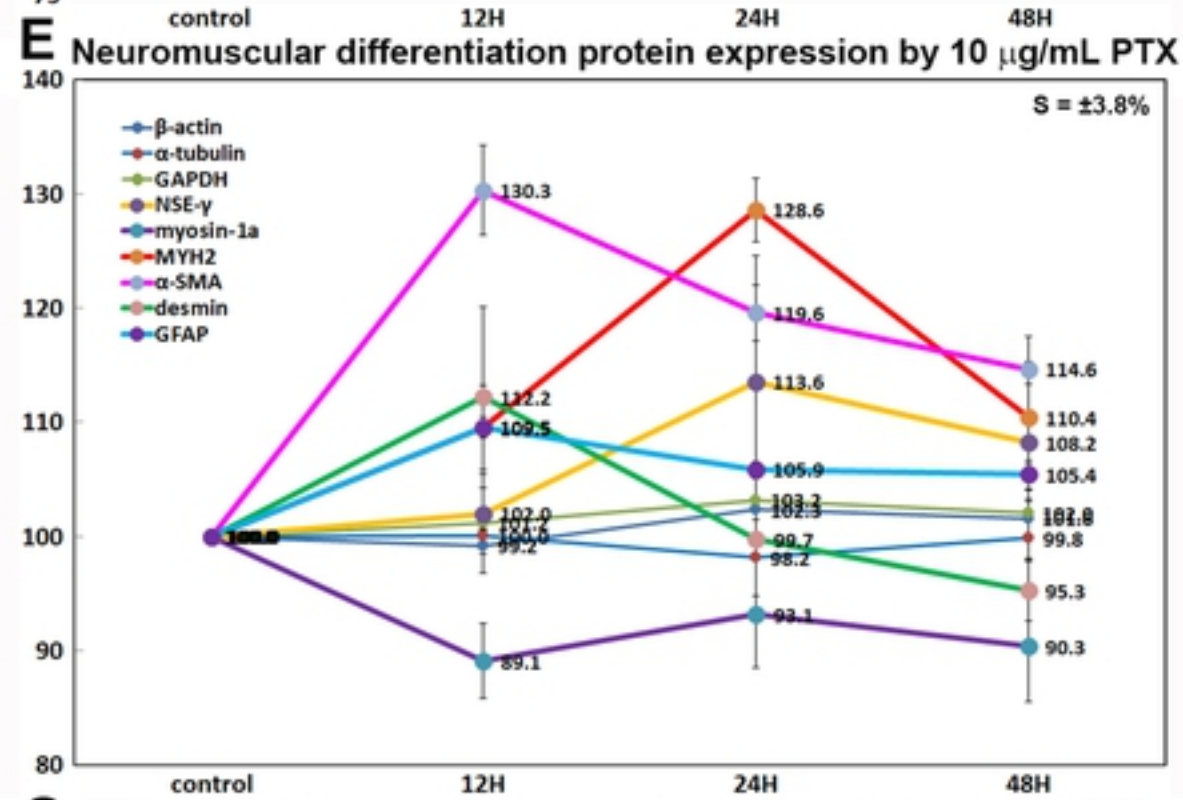

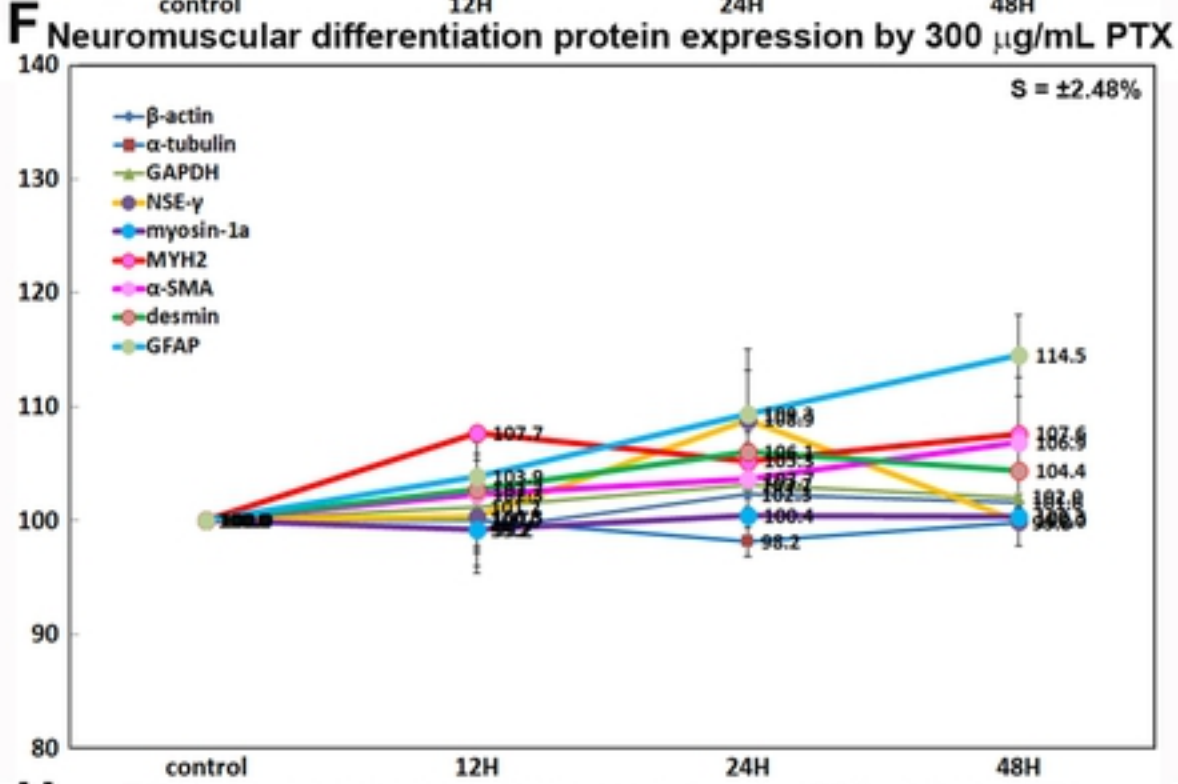

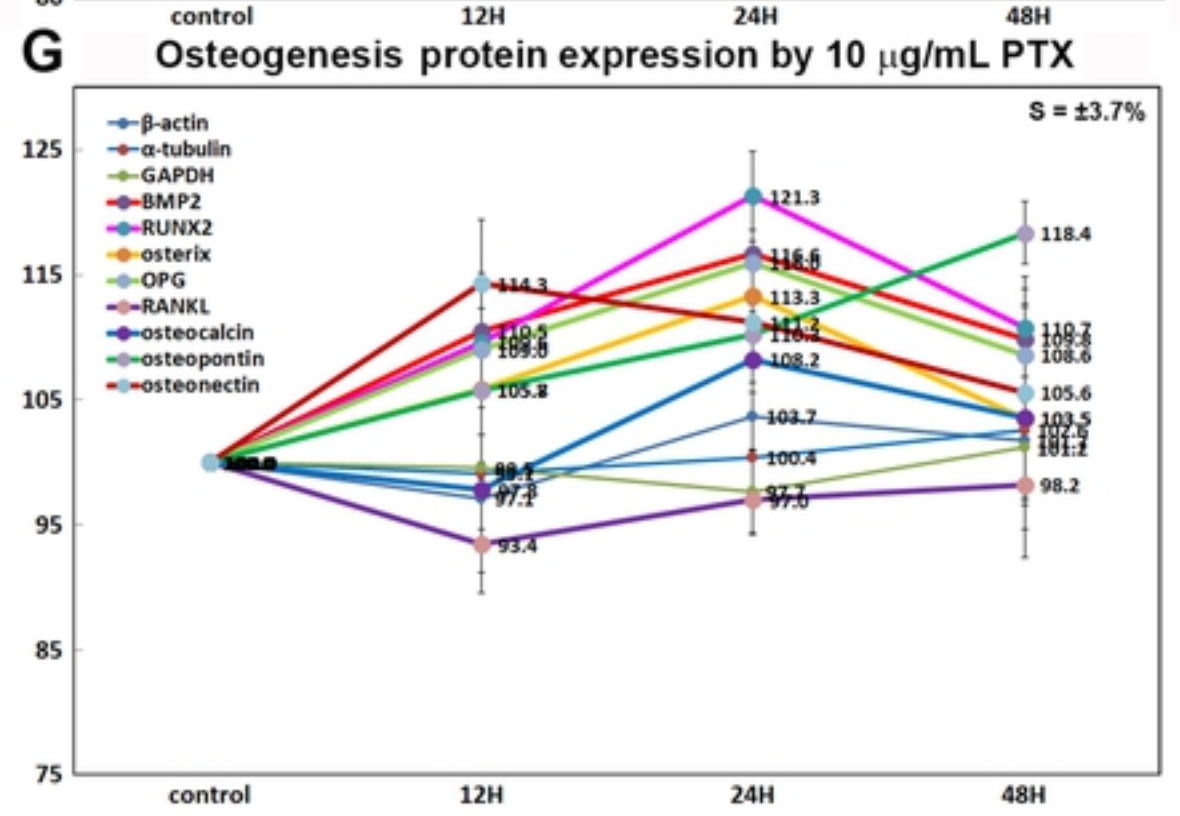

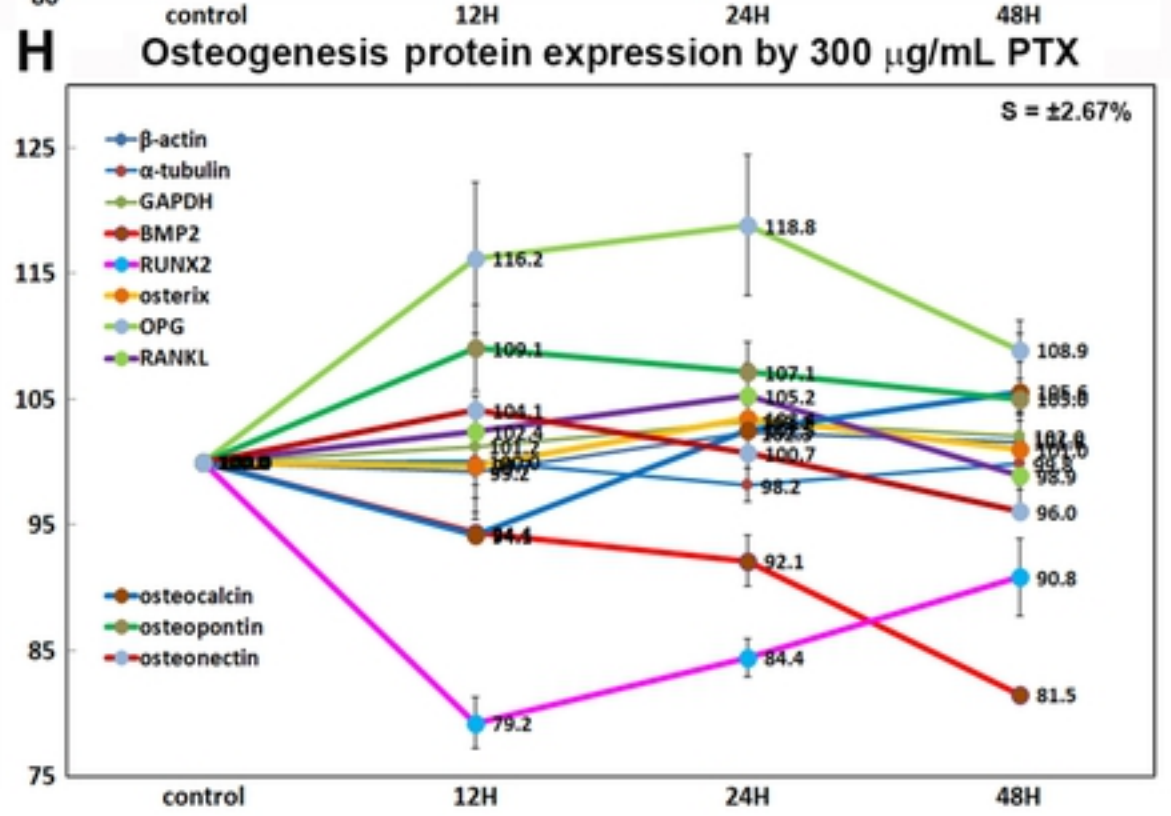

Figure 18

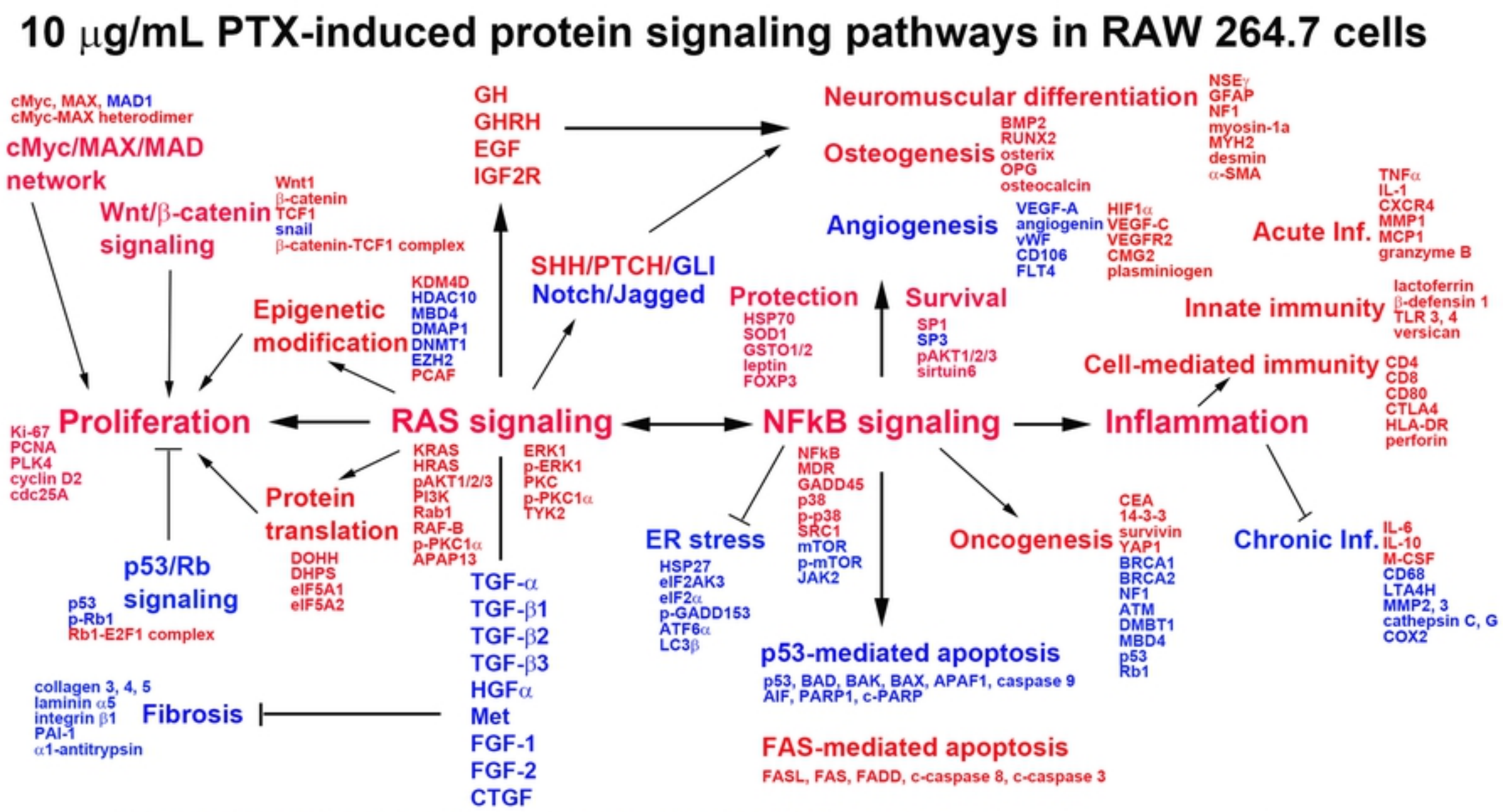
10 μg/mL PTX-induced protein signaling pathways in RAW 264.7 cells
cMyc, MAX, MAD1
cMyc-MAX heterodimer
cMyc/MAX/MAD network
Wnt/β-catenin signaling
Wnt1
β-catenin
TCF1
snail
β-catenin-TCF1 complex
GH
GHRH
EGF
IGF2R
Neuromuscular differentiation
NSEγ
GFAP
NF1
myosin-1a
MYH2
desmin
α-SMA
Osteogenesis
BMP2
RUNX2
osterix
OPG
osteocalcin
Angiogenesis
VEGF-A
angiogenin
vWF
CD106
FLT4
HIF1α
VEGF-C
VEGFR2
CMG2
plasminiogen
Acute Inf.
TNFα
IL-1
CXCR4
MMP1
MCP1
granzyme B
SHH/PTCH/GLI
Notch/Jagged
KDM4D
HDAC10
MBD4
DMAP1
DNMT1
EZH2
PCAF
Epigenetic modification
Protection
HSP70
SOD1
GSTO1/2
leptin
FOXP3
Survival
SP1
SP3
pAKT1/2/3
sirtuin6
Innate immunity
lactoferrin
β-defensin 1
TLR 3, 4
versican
Cell-mediated immunity
CD4
CD8
CD80
CTLA4
HLA-DR
perforin
Proliferation
Ki-67
PCNA
PLK4
cyclin D2
cdc25A
RAS signaling
NFkB signaling
Inflammation
KRAS
HRAS
pAKT1/2/3
PI3K
Rab1
RAF-B
p-PKC1α
APAP13
ERK1
p-ERK1
PKC
p-PKC1α
TYK2
Protein translation
DOHH
DHPS
eIF5A1
eIF5A2
p53/Rb signaling
p53
p-Rb1
Rb1-E2F1 complex
ER stress
HSP27
eIF2AK3
eIF2α
p-GADD153
ATF6α
LC3β
NFkB
MDR
GADD45
p38
p-p38
SRC1
mTOR
p-mTOR
JAK2
Oncogenesis
CEA
14-3-3
survivin
YAP1
BRCA1
BRCA2
NF1
ATM
DMBT1
MBD4
p53
Rb1
Chronic Inf.
IL-6
IL-10
M-CSF
CD68
LTA4H
MMP2, 3
cathepsin C, G
COX2
TGF-α
TGF-β1
TGF-β2
TGF-β3
HGFα
Met
FGF-1
FGF-2
CTGF
Fibrosis
collagen 3, 4, 5
laminin α5
integrin β1
PAI-1
α1-antitrypsin
p53-mediated apoptosis
p53, BAD, BAK, BAX, APAF1, caspase 9
AIF, PARP1, c-PARP
FAS-mediated apoptosis
FASL, FAS, FADD, c-caspase 8, c-caspase 3
Upregulated (red letter) and downregulated (blue letter) signaling and proteins

Figure 19